PHYLOGENETIC INVESTIGATIONS OF SORITID FORAMINIFERA (SUBFAMILY SORITINAE) AND THEIR DINOFLAGELLATE ENDOSYMBIONTS (GENUS *SYMBIODINIUM*)

by

MEGAN E. CEVASCO

A dissertation submitted to the Graduate Faculty in Biology in partial fulfillment of the requirements for the degree of Doctor of Philosophy, The City University of New York

2007

UMI Number: 3284423

ProQuest Information and Learning Company
300 North Zeeb Road
P.O. Box 1346
Ann Arbor, MI 48106-1346

Abstract

PHYLOGENETIC INVESTIGATIONS OF SORITID FORMINIFERA (SUBFAMILY SORITINAE) AND THEIR DINOFLAGELLATE ENDOSYMBIONTS (GENUS SYMBIODINIUM)

by

Megan Cevasco

Advisor: Dr. Mark E. Siddall

The soritinae is a subfamily of endosymbiotic larger foraminifera that inhabit the shallow tropical to subtropical reef habitats. Three genera (*Amphisorus*, *Marginopora,* and *Sorites*) are recognized within this subfamily. Collection of soritine populations from six locations in the Atlantic Ocean, nine locations in the Pacific Ocean and one location in the Red Sea indicates that previously unrecognized morphological and molecular diversity exists within this group. Both small and large subunit ribosomal sequence data, as well as 30 coded morphological characters, were analyzed for 112 soritine taxa using an optimality criterion of parsimony. Within the genus *Amphisorus,* five clades were recovered representing the two existing species *A. hemprichii* and *A. kudakajimaensis*, one species *Amphisorus saurensis* described herein, and potentially two additional species requiring description. Patterns of ribosomal molecular diversity within *Marginopora* and *Sorites* indicate that, although these two genera are morphologically distinct, they are not monophyletic.

Molecular phylogenetic analyses of cultured dinoflagellate endosymbionts (genus *Symbiodinium*) harbored within soritine taxa place the isolates among three clades (A, C, and F). The sequences of four cultures correspond to those recovered through direct amplification of sequences from host taxa. The combination of five separate gene regions from ribosomal, mitochondrial, and plastid DNA produces parsimony solutions (trees) with greater resolution and nodal support than is recovered from any individual gene analysis. Initial observations of chloroplast structure reveal two major morphological types (petal and reticulate). This character, when mapped on the molecular cladograms, was found to be homoplastic. This represents the first molecular characterization of cultured *Symbiodinium* isolates from soritine hosts.

Acknowledgments

Dr. Mark Siddall for his patience and generosity in supporting the entire molecular component of this work, Dr. John Lee for his instruction on electron microscopy and access to specimens and culture facilities, as well as all members of the committee for there time and input. The Learner Gray Grant for Marine Research for funding collection expeditions. Louise Crowely, Pamela Hallock, Wilem Renema, Chris Lobban, and Kasuhiro Fugita for their efforts in collecting specimens for this research. Rebecca Budinoff and Francisca Almeida for helping refining molecular techniques used in this research. And Christopher Cevasco for his ongoing support.

TABLE OF CONTENTS:

LIST OF TABLES:

LIST OF FIGURES:

CHAPTER 1

Introduction

The class Foraminifera (d'Orbigny, 1826) consists of aquatic unicellular eukaryotes distinguished from other protist groups by distinctive bi-directional extensions of the protoplast termed granular reticulopods that form anastomosing networks through an apertured shell (test) (Figure1A). Tests are formed of calcareous, siliceous, or agglutinated organic materials, and the class Foraminifera is further divided into orders based on test composition (Haynes, 1990). Of the twelve ordinal divisions within Foraminifera, the order Miliolida (Delage & Herouard, 1896) first appears in the fossil record in the Carboniferous period (~350 mya) and is characterized by imperforate calcite tests (Loeblich and Tappan, 1987). The construction of the foraminifer's imperforate test walls occurs when calcite needles formed in Golgi vesicles are transported to the site of wall construction where they are deposited (Figure 1B)(Hottinger, 2000b)

Growth in multichambered Miliolid foraminfera occurs by the successive addition of chambers. Each chamber, beginning with the initial test chamber or proloculus, is linked to the adjoining subsequently formed chamber through apertures (foramena). The organism continues to grow and construct new chambers until reproduction, wherein an agamont microspheric (small prolocular chambers) form of the foraminifer asexually divides into multiple embryons. These give rise to either a megalospheric (large prolocular chambers) gamont or schizont form. The schizont megalosphere may continue to asexually reproduce offspring for multiple iterations. In the gamont

Figure 1. Images of Soritine foraminifera and their endosymbionts (genus *Symbiodinium*) : A) Soritne specimens (*Marginopora vertebralis*) from Lizard Island, Australia 15X; B) Calcite crystals of a Hawaiian *Amphisorus* specimen 1.5KX; C) Tests of soritine foraminiferal constituting the "sand" at Coconut Beach, Australia 2X; D) *Symbiodinium* sp. *in symbio* within a chamberlet of a soritine foraminifer— Fuelgen stained chamberlet of *Sorites* fuchsia denotes symbiont chromosomes 1KX; E) Australia soritine foraminifera (*Marginopora vertebralis*) attached to a rocky substrate 1X; F) Australia soritine foraminifera (*Marginopora vertebralis*) attached to a phytal substrate 20X.

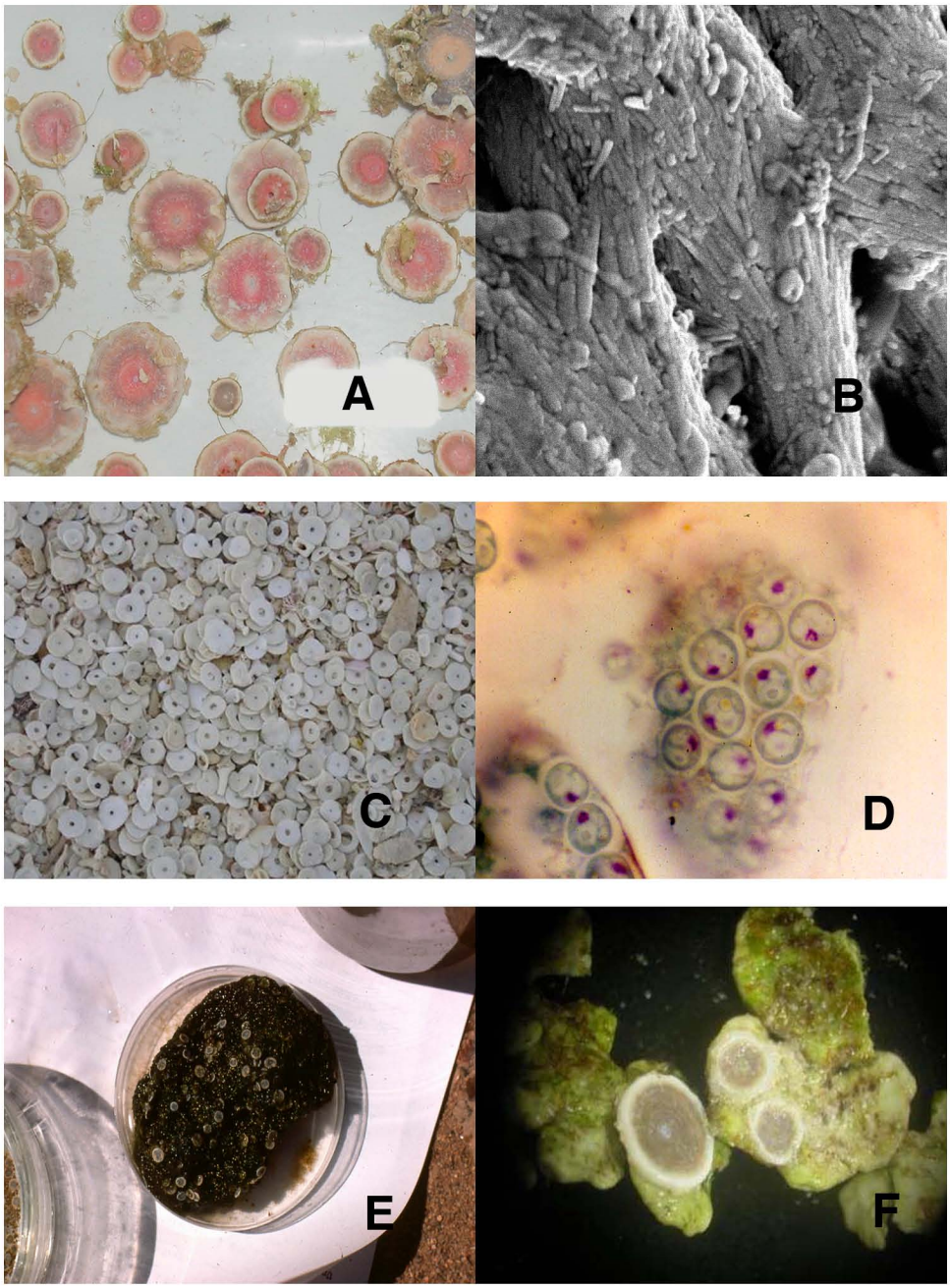
A
B
C
D
E
F

megalosphere, meiotic division forms gametes that will undergo sexual reproduction to generate the microspheric form (Lee et al., 1991).

The importance of foraminifera in both a contemporary and a geological sense arises from their abundance (Figure 1C). In various samples calcareous foraminifera have been observed to occur in densities reaching 4,500/10 cm^2 (Lee, 1995). Due to their contribution to carbonate production, living foraminifera function as an integral component in marine biogeochemical cycles. For example, populations of symbiotic larger foraminifera in Japan were reported to generate carbonate at a rate of 5Kg $CaCO_3$ m^{-2} yr^{-1} (Kasuhiko, 2000). In the fossil record, the chalky deposits of foraminiferal tests, as evident in the exposed white chalky cliff faces at Dover, England, are of stratigraphic, as well as, paleoclimatic, and paleoecological importance.

Since the Pennsylvanian (320 m.y.a.), the fossil record shows periods in which benthic foraminifera typically 60-500μm gave rise to lineages 10-10^2 times larger corresponding to episodes of global warming and expansion of tropical and semitropical habitats (Lee and Hallock, 1987). The collective term "larger foraminifera" refers to foraminferal taxa 0.1-6cm in size that form endosymbiotic associations with microalgae. Larger foraminifera (i.e. fusilinids) were particularly abundant in the late Paleozoic seas, and we associate the abundance of larger foraminifera in the early Cenozoic Thethyean seas with the large mountains and quarries of nummulitic limestone that were used to build the Egyptian pyramids (Lee, 1991). The inference drawn from the fossil record posits that conditions favoring the expansion of clear, oligotrophic,

shallow seas provided ideal conditions for both the establishment of symbiosis and the diversification of larger foraminifera (Hallock, 1986 and Lee and Hallock, 1987)

Among the larger reef-dwelling miliolid foraminifera—subfamily Soritinae (Ehrenberg, 1839)—a particular need to define phylogenetic patterns arises from their potential to serve as sensitive indicators of anthropogenic influences on reef ecosystems. Soritine foraminifera harbor photosynthetic endosymbionts of the dinoflagellate genus *Symbiodinium* (Freudenthal, 1962) within converted vacuoles (symbiosomes) in the foraminifer's protoplasm (Lee et al., 1991) (Figure1D). This association persists in the stable, nutrient-depleted waters characteristic of reef habitats to the benefit of both symbiotic partners (Figure 1 E&F). It enhances calcification in the host foraminfer due to the photosynthetic splitting of bicarbonate while providing usable forms of dissolved nitrogen, phosphorus and other limited nutrients to the dinoflagellate symbionts (ter Kuile and Erez, 1991). The endosymbiotic condition not only characterizes modern reef habitats, but it also appears in the fossil record to have been a similarly successful strategy for surviving in ancient oligotropic marine environments and is generally recognized as a major component in the evolution of larger foraminifera (Lee and Hallock, 1987 and Richardson, 2001).

On a larger ecological scale, the symbiotic condition allows for mixotrophy, which reduces the loss of energy and biomass between trophic levels in the reef ecosystem food web (Hallock, 2000). However, foraminifera, like reef-building corals and other symbiotic reef invertebrate species, are

subject to environmental stresses contributing to symbiont bleaching (loss of zooxanthellate symbionts from host tissue).

The algal cells harbored within marine invertebrate hosts were first recognized by Karl Brandt in the late nineteenth century (Brandt, 1881). To distinguish the intracellular symbionts as separate entities from their hosts Brandt erected the monotypic genus *Zooxanthella* in which he classified all yellow-brown algal endosymbionts as members of the species *Zooxanthella nutricula* (Brandt, 1882).

Prior to their placement within the dinoflagellates, the taxonomic position of zooxanthellae shifted considerably among microalgal groups. Initially regarded as a taxon incerta sedis (Just, 1884), by the mid 1890's zooxanthellae were considered to be ancestral to both the dinoflagellates and the chrysomonads (Klebs,1892). This designation was later revised by Adolf Pascher, who placed them within cryptomonads (Pascher, 1911). Members of the genus *Zooxanthella*, however, were not included in the dinoflagellates until Hovasse (1922), who considered them parasites, proposed that they be placed within the genus *Endodinium*. The identity of zooxanthellae as dinoflagellates was further strenghthened by Doyle and Doyle's (1940) observations and Siro Kawaguti's (1944) recognition that coccoid zooxanthellae cultured from the reef coral *Acropora corymbosa* produced a motile stage of gymnodinioid swarmers and therefore reassigned them to the dinoflagellate genus *Gymnodinium* (Stein, 1878). Yet it was not until 1962 that the exclusively symbiotic genus of *Symbiodinum* was proposed along with the first formal description of the life

cycle and morphology of these zooxanthellate dinoflagellates (Freudenthal, 1962).

Although reef habitats possess the highest biodiversity per unit area of any marine ecosystem, recent changes in light spectral quality (i.e. increased UV), rise in tropical water temperatures, and anthropogenic eutrophication of the seas have contributed to the continual loss of reef habitats on a global scale. In the oligotrophic tropical to semi-tropical waters characteristic of these habitats, the symbiotic association of zooxanthellae with reef invertebrates and protists underpins the diversity of these ecosystems such that removal or “bleaching" of these endosymbionts from the tissue of their host eventuates in reef decline and mortality. Effective conservation measures for reef ecosystems are contingent upon both a comprehensive assessment of the biodiversity contained within each threatened reef area and that of the biological connectivity among areas. An understanding of symbiotic reef foraminifera has promise in playing an integral role in reef conservation measures based on the potential of these protists to serve as indicators of anthropogenic influences on reef ecosystems.

The use of symbiotic foraminifera as bioindicators of reef health first was explored by Hallock (2000) in diatom-bearing reef foraminifera and continues to increase in relevance as the reality of global environmental change brings issues of marine conservation into focus. Requisite to such conservation endeavors, and more fundamentally to the understanding of symbiosis in reef

ecosystems, is the need to define the phylogenetic relationships among both host and endosymbiont taxa.

The research presented herein consists of character-based phylogenetic analyses of soritine foraminfera (Chapters 2 and 3) and their dinoflagellate endosymbionts (genus *Symbiodinium*) (Chapter 4).

CHAPTER 2

A new modern soritid foraminifera, *Amphisorus saurensis* sp. nov., from the Lizard Island group (Great Barrier Reef, Australia)

(Adapted from: Lee, J.J., Burnham, B., and Cevasco, M, 2004.

Micropaleontology. 50(4): 357-368)

2.1 Introduction

The Soritidae (Ehrenberg, 1839) is a family of calcareous benthic foraminifera with three subfamilies classically distinguished by morphological characters relating to growth form, endoskeletal structure, and the arrangement of apertures along the periphery of the tests (Ehrenberg, 1839), (Carpenter, 1883), (Brady, 1881), (Cushman, 1930), (Smout, 1963), (Loeblich and Tappan, 1987), and (Gudmundsson, 1994). In his recent classification of the soritids, Using morphological characters Gudmundsson (1994) delimited the phylogenetic relationships among the genera within the subfamily soritinae in cladistic terms (Table1). The arrangement of the apertures and complexity of internal test architecture are unique characters that distinguish each genus. Through the use of test dissection and internal casts of epoxy resin, Gudmundsson demonstrated an ontogenetic relationship between the endoskeleton and aperture formation and concluded that there is a progression of growth stages that is accompanied by an increase in endoskeleton complexity. In turn, the soritid's internal architecture supports the development of characteristic apertural patterns. The genus *Sorites* is characterized by an endoskeleton of simple transverse partitions (septulae); the genus *Amphisorus* by a duplex skeleton; and the genus *Marginopora* by a complex medial skeleton. The appearance of medial apertures is restricted to the genera *Amphisorus* and *Marginopora* both of which exhibit complex endoskeletons with halved septulate partitions extending from the test wall to singular or multiple annular median canals. The genus *Marginopora* is further

distinguished from *Amphisorus* by the presence of transverse medial partitions that buttress a field of medial apertures bounded by two marginal aperture rows. Consequently, the examination of both characters defining aperture arrangement and internal architecture is a critical component in assigning a generic epithet to new soritid species.

Table 1. Morphological Characters of Gudmundsson (1994)

Character Number & Description[1] modified from (Gudmundsson, 1994)		Soritinae Genera		
		Sorites [2]	***Amphisorus*** [3]	***Marginopora*** [4]
1	Single row of apertures	✓	✓	✓
2	Double displaced, marginal row of apertures	✓	✓	✓
3	Median apertures between marginal aperture rows		✓	✓
12	Flabelliform chambers	✓	✓	✓
13	Cyclic chambers	✓	✓	✓
14	Megalosperic embryo possesses vorhof		✓	✓
18	Internal skeleton with septula	✓	✓	✓
19	Duplex internal skeleton		✓	✓
20	Median internal skeleton			✓
23	Outer wall pits, some fused & form depressions	✓	✓	✓
28	Wavy sutures present	✓	✓	✓

[1]Characters must be present in 1 or more species in a genus to be marked as ✓
[2]Species included in the genus *Sorites*: *S. bradyi*, *S.orbitolitoides*, *S. orbiculus*
[3]Species included in the genus *Amphisorus*: *A. hemprichii*
[4]Species included in the genus *Marginopora*: *M. kudakajimaensis*, *M. vertebralis*

Although patterns in aperture arrangement are used to make distinctions at the generic level, more detailed observations of aperture morphology are informative at the species level. For example, Gudmundsson (1994) distinguished *M. kudakajimensis* from *M. vertebrali*s by the elongate and irregular outline of its median apertures. Moreover, comparison of previous cytological studies on Soritinae taxa (Bacus, 1997), (Lee et al.,1997), (McEnery

and Lee, 1981), (Muller and Lee, 1976) reveal differences in the patterns of both nuclear and symbiont distributions. During a workshop on living foraminifera (1997) (Lee & Hallock, 2000) specimens were collected from Bird Island (Lizard Island Group, Great Barrier Reef) that seemed to one of us (JJL) to be morphologically different from any previously described species. This report is the result of our more detailed study of these newly collected specimens.

2.2 Specimen Collection

The first collection of the new species was made by Dr. Samuel Bowser during the Lizard Island Workshop. Later collections were made by Lance Pearce and Dr. Lyle Vail (Co-Director of the Lizard Island Marine Research Station). The specimens were collected at 24 m off the reef slope to the south of Bird Island. The bottom was relatively barren of macro invertebrates with the main large fauna being some solitary ascidians and a few holothurians. The foraminifera were collected about 8 m below the area of the slope where the isolated coral patches ended. GPS co-ordinates for the collection site were:14' 41" 634 S, 145' 28" 044 E.

2.3 Preparations for the Study of Test Structure

Soritid specimens collected from: Bird Island of the Lizard Island group (Nov., 1997); Eilat, Israel , Gulf of Eilat, Red Sea (1978); and Kudaka jima, Japan (1988). They were prepared for scanning electron microscope (SEM)

examination so that their tests could be compared. The dried tests of specimens were secured on SEM stubs in positions that allowed views of the edges and the disc sides (broad surfaces). SEM compatible silver paint was used as the adhesive for mounting. The specimens were then sputter-coated with 10 nm gold in a Polaron sputter coater.

A subset of the dried specimens were embedded in epoxy resin and ground to expose the internal structure of the tests following the technique introduced by Hottinger (1978). The resin Poly/Bed 812 Embedding Medium was used with DMP-30 as a catalyst. Tests were prepared for embedding by washing them in propylene oxide twice for 30 minutes each wash. Resin was then added to the propylene oxide solution (2 parts propylene oxide : 1 part resin). The percentage of resin was gradually increased to 100% through three serial medium changes. The specimens were placed in a vacuum chamber after each change to draw out any trapped air bubbles. Following infiltration of the 100% resin for 8 hours the specimens were transferred to a new batch of resin to which the DMP-30 hardener had been added. After 4 hours the specimens were placed in a 60° F oven for polymerization.

After the specimens had been cured, they were ground on a geologists grinding wheel, finishing with 600 grit fine sandpaper. The angle and depth of grinding included horizontal (equatorial) and cross-sectional views. The specimens were polished with a micro-polish on a felt wheel and then partially etched with 2 - 5% hydrochloric acid (HCl). The etching digested a small amount of the CaCO3 test on the polished surface, leaving an epoxy cast of the

cytoplasm. The 2 - 5% HCl acid solution was applied to the polished surface for 30 to 60 seconds to partially dissolve the test. These specimens were then mounted on SEM stubs and sputter-coated with 13 nm gold.

Prepared specimens were viewed and photographed using a Zeiss DSM 940 Scanning Electron Microscope. T-Max 100 film was used for the photographs and contact prints were made with Illford Multigrade IV paper. Some digital images were captured using an Orion 23 system and prepared for publication in Adobe Photoshop 5.5.

2.4 Preparations for the Study of Cytology

The Bird Island specimens destined for cytological investigations were fixed in Zenker's solution shortly after their arrival in New York. The tests were decalcified with Poly/No Cal® solution and then dehydrated by passing them through a graded ethyl alcohol series. The were then placed in xylene for two ten minute washes and embedded in Paraplast®.

With the aid of a microtome the embedded specimens were cut into 10µm sections which were adhered to microscope slides with Meyer's albumen. The sections were stained using the modified Feulgen technique outlined in Lee and Pawlowski (1992). Following hydration, specimens underwent hydrolysis in 1N HCL for two minutes at room temperature, for 15 minutes at 60° F and then again for two minutes at room temperature. The sectioned specimens were stained in Schiff's reagent (distilled water 200ml, basic fuchsin 1.0g, $Na_2S_2O_5$ 1.0g and 1 N HCL 20ml) for 2 hours in the dark. They were bleached (distilled

water 100ml, $Na_2S_2O_5$ 0.4g and 12 N HCL 1.0ml) twice for one minute each and then gradually brought up to 95% alcohol for counter-staining with fast green for five minutes. The stained specimens were then dehydrated in a graded alcohol series to 100% ethanol and then placed in toluene twice for 10 minutes, each, before being covered with Permount® and #0 cover slips.

2.5 Preparations for Sequence Analysis

DNA was extracted from the Bird Island specimens using the DNEasy Plant Mini Kit (Qiagen Inc.). The initial PCR amplification of nuclear 18S rDNA was done using the S6r (forward) 5'GGGCAAGTCTGGTGC and S17 (reverse) 5' CGGTCACGTTCGTTGC primer pair of Holzmann et al. (2001). Amplification reaction mixtures for gene fragments used Ready-To-Go PCR Beads (Amersham–Pharmacia Biotech), to which 0.5 μl of each 10 μM primer, 2 μl DNA template, and 22 μl RNase-free H2O was added (total reaction volume, 25 μl). DNA amplification of 35 cycles of 30 s at 94°C, 30 s at 49°C, and 120 s at 72°C followed by 5 min final extension at 72°C was done in an Eppendorf Mastercycler®. The amplification product was then cleaned with the ArrayIt™ PCR Purification Kit (TelChem).

The purified amplification products were prepared for sequencing by adding to reaction tubes 5 μl of the PCR product, 2 μl of 1 μM primer, and 2 μl of Big Dye (Applied Biosystems, Perkin-Elmer Corp.). The sequencing mixture was cycled 35 times at 30 s at 96°C, 60 s at 48°C, and 240 s at 60°C. To remove primers and unincorporated dyes sequences were purified by 70%

isopropanol/70% ethanol precipitation. They were then elecrophoresed in an ABI 3730 sequencer (Applied Biosystems).

Searches were performed for each sequence at the NCBI Experimental BLAST Network Service using the BLASTN program (Altschul, 1990) to indicate to which genus the sequence allied. Selected GenBank sequences of soritids exhibiting sequence similarity to the Bird Island samples were used in molecular phylogenetic analyses. Alignments were done using ClustalW in MacVector 6.53 (Oxford Molecular Group). Parsimony analyses were performed using PAUP* 4.0b10 (Swofford, 2000). Analyses assumed equal weights for all character changes and used the heuristic search option with 100 random addition replicates and tree-bisection-reconnection branch swapping. Nonparametric bootstrap support values for clades were generated using a heuristic bootstrap search of 100 parsimony pseudoreplicates in PAUP*.

2.6 Description of Test Sturcture

The tests of *Amphisorus saurensis* are discoid in shape with an average height of 0.44mm and average diameter of 11.5mm (Figure 2), (Table 2). The surface of the test is not smooth due to indentations that follow the contours of interior chamber and chamberlet partitions. The average number of annular chamber rings recorded was 59 per specimen (Table 2). Additionally, over 80% of the specimens observed exhibited secondary calcification that at least partially obscured the embryonic apparatus (Figure 3).

Figure 2. Positive Correlation between test diameter measurements and the Number of Annular Chambers Observed in *A. saurensis* specimens.

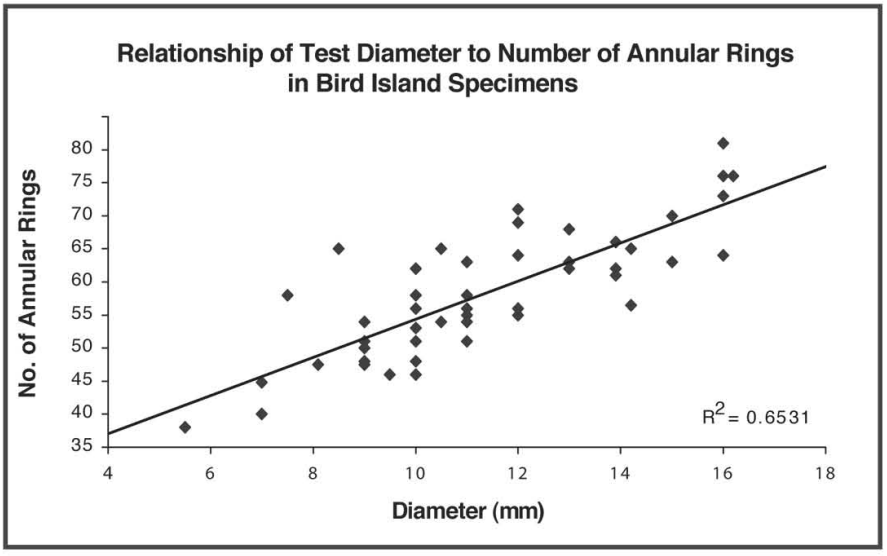
Relationship of Test Diameter to Number of Annular Rings in Bird Island Specimens
No. of Annular Rings
80
75
70
65
60
55
50
45
40
35
4
6
8
10
12
14
16
18
Diameter (mm)
R2 = 0.6531

Figure 3. Embryonic apparatus of *A. saurensis* specimens: A) Interior structure *Amphisorus saurensis*, side view, test has been dissolved away leaving resin filled cytoplasm: (a) proloculus, (b) flexostyle, (c) deuteroloculus (vorhof), (d) foramina between vorhof and adjacent chamberlets, B) Interior structure of embryotic apparatus of *Marginopora kudakajimensis* (Hottinger technique): (a) proloculus, (b) flexostyle, (c) deuteroloculus (vorhof).

A

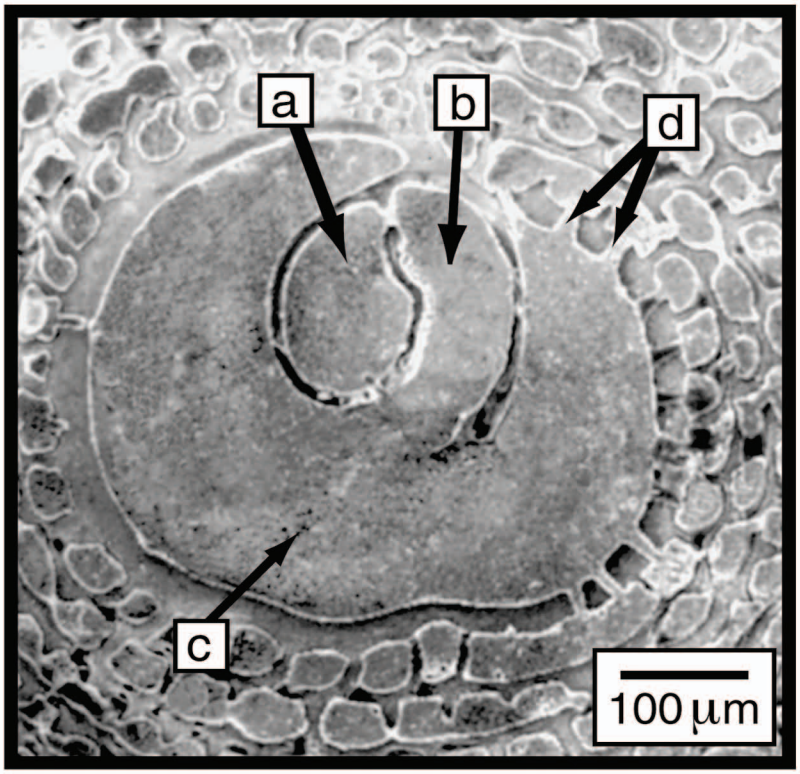

B

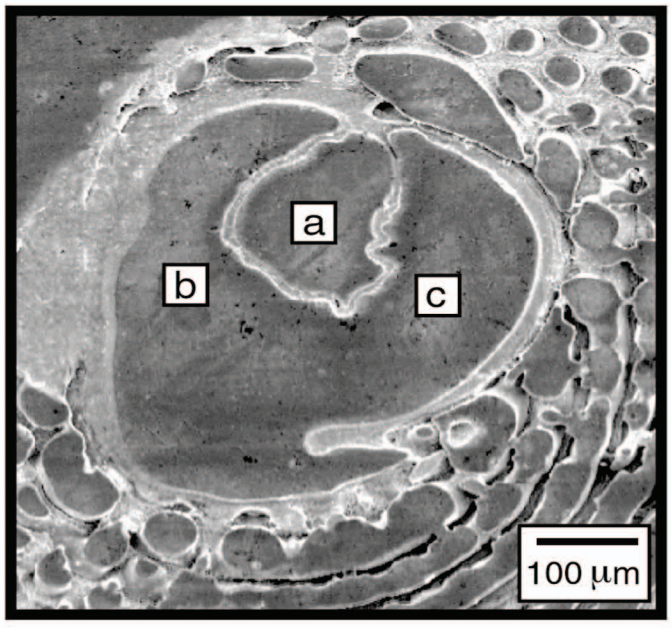

Table 2. Test Dimensions of *Amphisorus saurensis*

Descriptive Statistics						
	Mean	Std. Dev.	Std. Error	Count	Minimum	Maximum
Height (mm)	.440	.053	.007	53	.350	.550
Diameter (mm)	11.538	2.662	.366	53	5.500	16.500
No. of Annular Rings	59.189	9.780	1.343	53	39.000	81.000

The embryonic apparatus of the test is approximately 330µm in diameter and 250µm in height (Figure 3A). It includes the proloculus, flexostyle and deuteroloculus, or vorhof and is similar in aspect to the embryonic apparatus of *M. kudkakajimaensis* (Figure 3). The proloculus is nearly spherical in shape and has one opening to the flexostyle (Figure 3). Encompassing approximately one half of the proloculus, the flexostyle possesses a single opening to the next chamber- the vorhof. The vorhof wraps almost completely around both the proloculus and the flexostyle. It is inflated in size compared to the other two embryonic chambers, representing approximately 75% of the area of the embryonic apparatus. The vorhof has multiple openings or foramina, which connect it to proceeding chambers and chamberlets (Figure 3).

The annular chambers concentrically extending out from the embryonic apparatus are divided by partitions into discreet compartments. The largest compartment consists of a tube-like canal that is situated in the center of the ring. The annular canal is oval in shape and has a maximum diameter of approximately 120µm and runs through the entire length of the ring (Figure 4).

Each annular ring of chambers is divided by internal septulae into two marginal rows of chamberlets situated on each side of the central annular canal. The relative position of chamberlets and septulae is illustrated in Figure 7. Each of the two chamberlets is approximately one third of the height of the chamber ring. The annular canal, sandwiched between the chamberlets, fills in the remaining one third of the height (Figure 4).

Each chamberlet has two or three openings, one of which leads to the median canal of the same annular ring. An aperture of the previous chamber ring forms the other opening and it serves to connect the chamberlet to the prior chamber's annular canal. Each chamberlet, therefore, is connected to its own annular canal and the previous ring's annular canal (Figure 4). Only the chamberlets of the terminal chamber have openings that lead to the exterior environment (Figure 5).

Figure 4. Connections among Chambers: A) Cross-section through center of *Amphisorus saurensis* that was embedded in resin and the test etched away: (a) Embryonic apparatus, B) Cross-section view of *Amphisorus saurensis* that has been embedded in the resin with the test etched away: (a) indicates chamberlets, (b) indicates annular canals, (c) indicates foramina between annular canals.

A

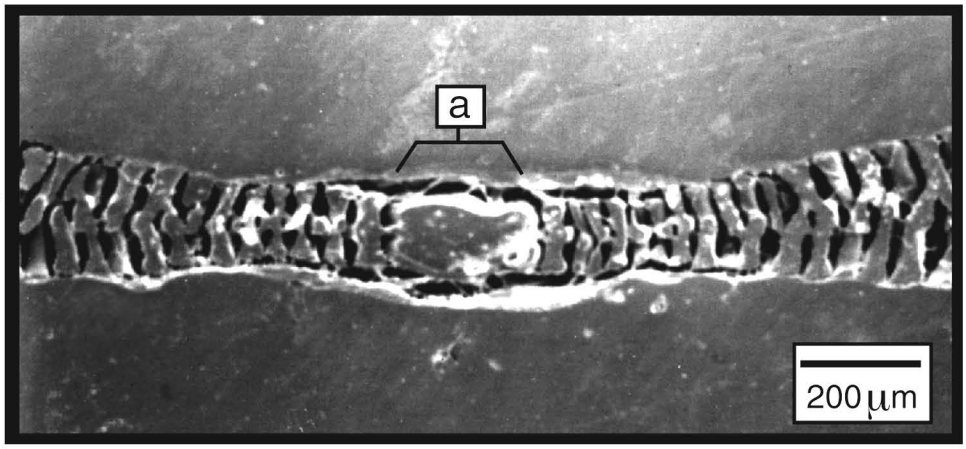

B

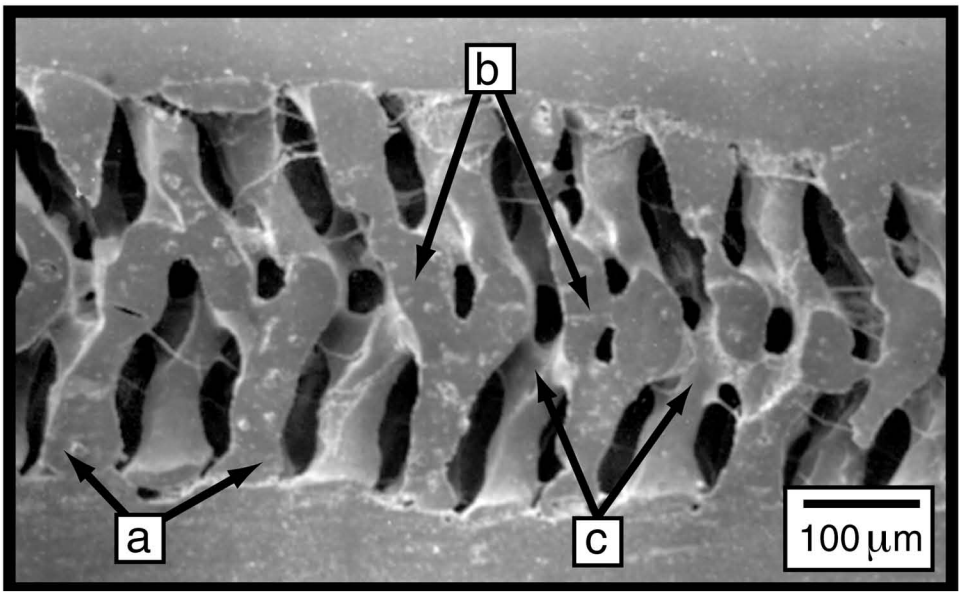

Figure 5. Drawing of *Amphisorus saurensi*s view from edge with outermost test removed to reveal interior of last annular ring: (a) annular canal, (b) chamberlet, (c) septa, (d) previous ring's median aperture, (e) previous ring's marginal aperture**.**

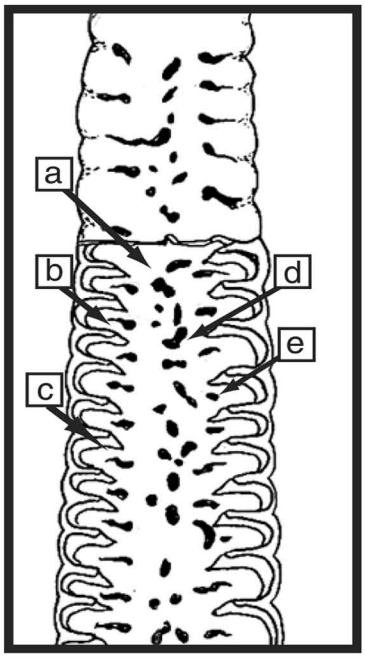
a
b
c
d
e

2.7 Description of Apertures

Amphisorus saurensis has multiple apertures along the test periphery (Figure 6 and Table 3). These apertures, which provide the cytoplasm access to the exterior environment, are characterized by particular patterns of arrangement and shape. Positioned along the middle of the apertural face above the annular canal are median apertures, exhibiting a wide range of shapes from irregular to perfectly round and approximately 30µm in diameter. Some ovate shaped median apertures were observed to be up to 70µm in length. The median apertures may be as close as 25µm from each other or be spaced as far as 75µm from each other (Figure 7). In addition to the median apertures, a row of marginal apertures lines each edge of the apertural face. They are positioned such that they extend from the margin to the median of the edge of the test, towards the median apertures. The marginal apertures vary in shape and size from small and nearly round, 30µm in diameter, to long and sinuous, 25µm in width and 55 to 120µm in length (Figure 10). The edges of the apertures are smooth and without raised rims (lips). Approximately 14 marginal and medial apertures are present in an area of 450µm by 450µm on the apertural face of the test (Figure 6). Around the apertures, multiple pits arranged in irregular patterns often join to form grooves in the apertural surface (Figure 7B).

Table 3. Comparison of Soritine Morphological Features

	Sorites orbiculus Forskal 1775	***Amphisorus hemprichii*** Ehrenberg 1839	***Amphisorus sauronesensis*** (Sp. Nov.)	***Marginopora vertebralis*** Quoi & Gaimard 1830	***Marginopora kudakajimensis*** Gudmundsson 1994
Embryonic Apparatus (Megalosphere)	 50 μm	 100 μm	 100 μm	 100 μm	 100 μm
Periphery Apertures	 100 μm	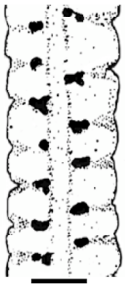 100 μm	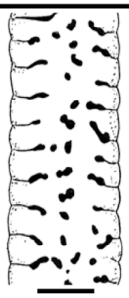 200 μm	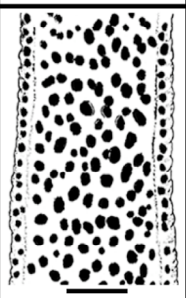 200 μm	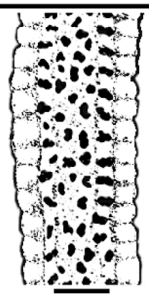 200 μm
Internal structure	 50 μm	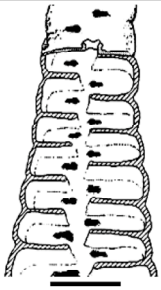 100 μm	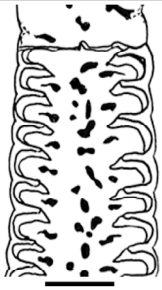 200 μm	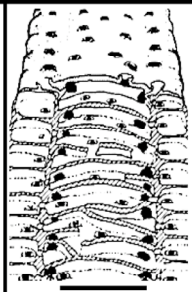 200 μm	 400 μm

Figure 6. Apertures of *Amphisorus saurensis*: A) Edge view of *A. saurensis* specimen test removed to reveal interior of last annular ring: (a) annular canal, (b) chamberlet, (c) septa, (d) previous ring's median aperture, (e) previous ring's marginal aperture, B) Edge view of *A. saurensis*: (a) suture between chamberlet ends in an aperture, (b) 450mm by 450mm square (0.002mm2 area) with 14 apertures (8 marginal apertures & 6 medial apertures).

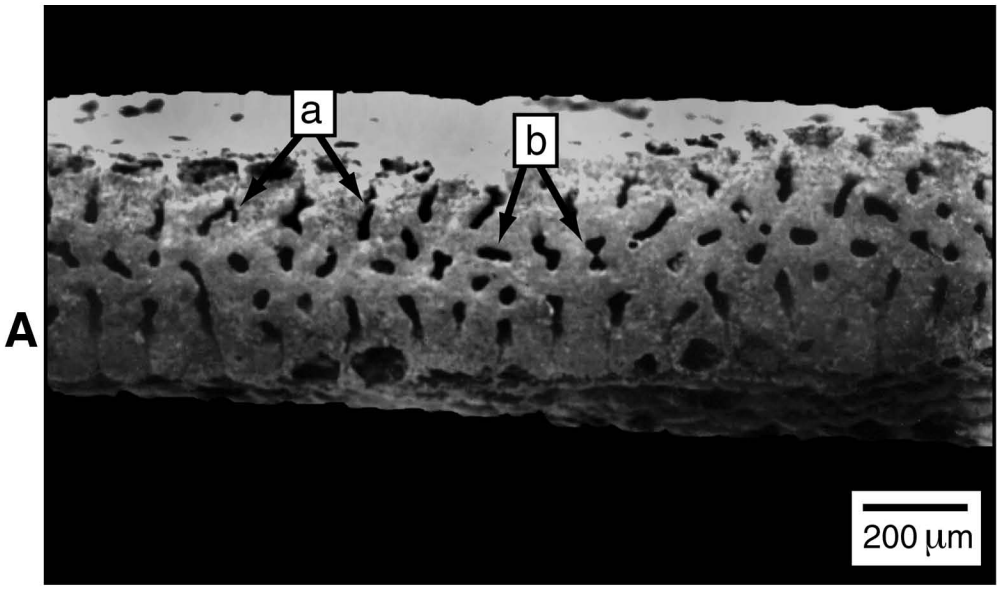
A
a
b
200 μm

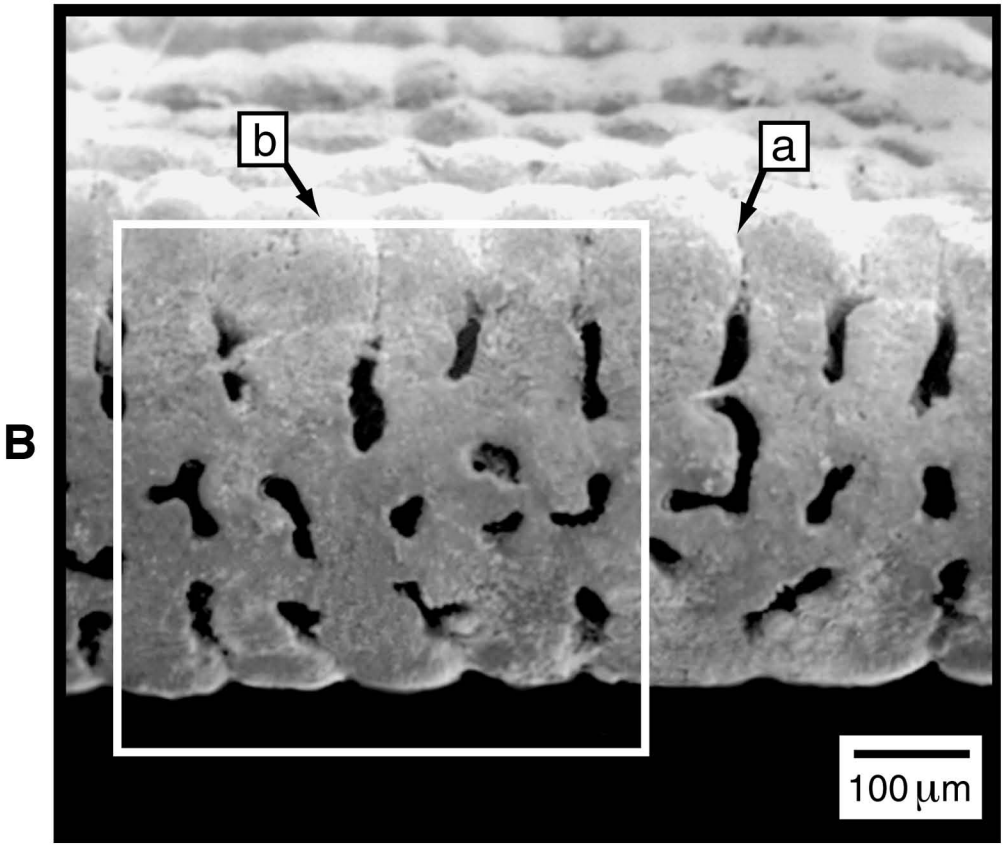
B
b
a
100 μm

Figure 7. Detail of *Amphisorus saurensis* Apertural Face: A) Edge view of *A.saurensis* showing variability in median aperture shapes (a), B) Edge view of *A.saurensis* showing (a) edge of apertures are smooth and without lips, (b) depressions in the calcite are distributed evenly around apertures.

A

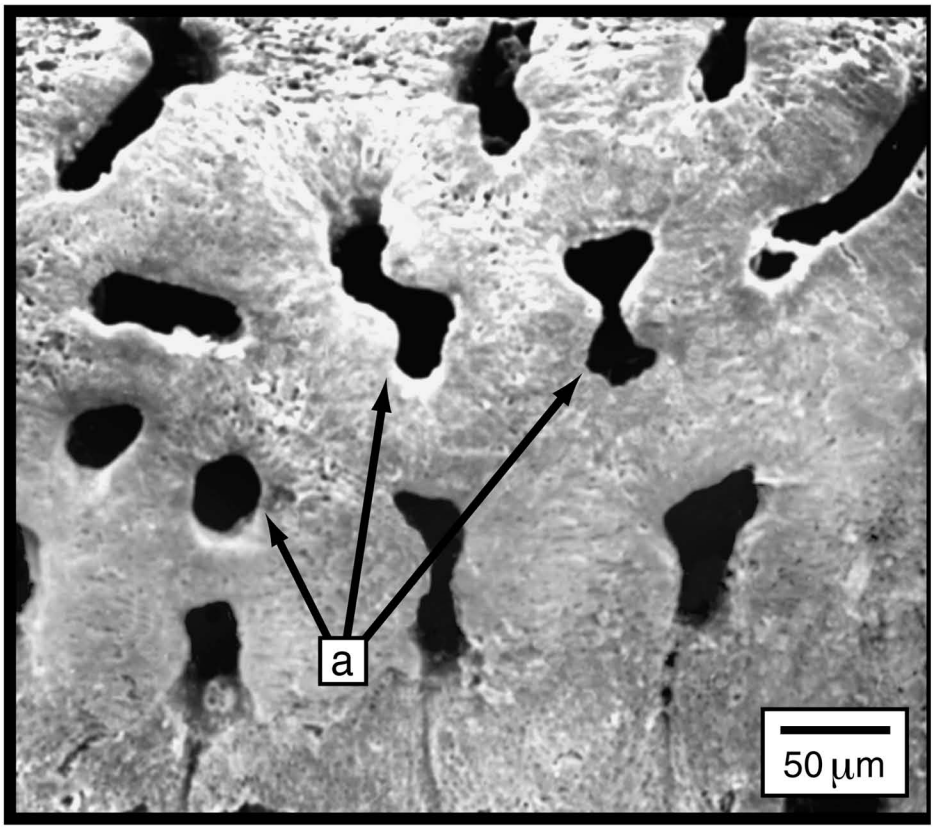

B

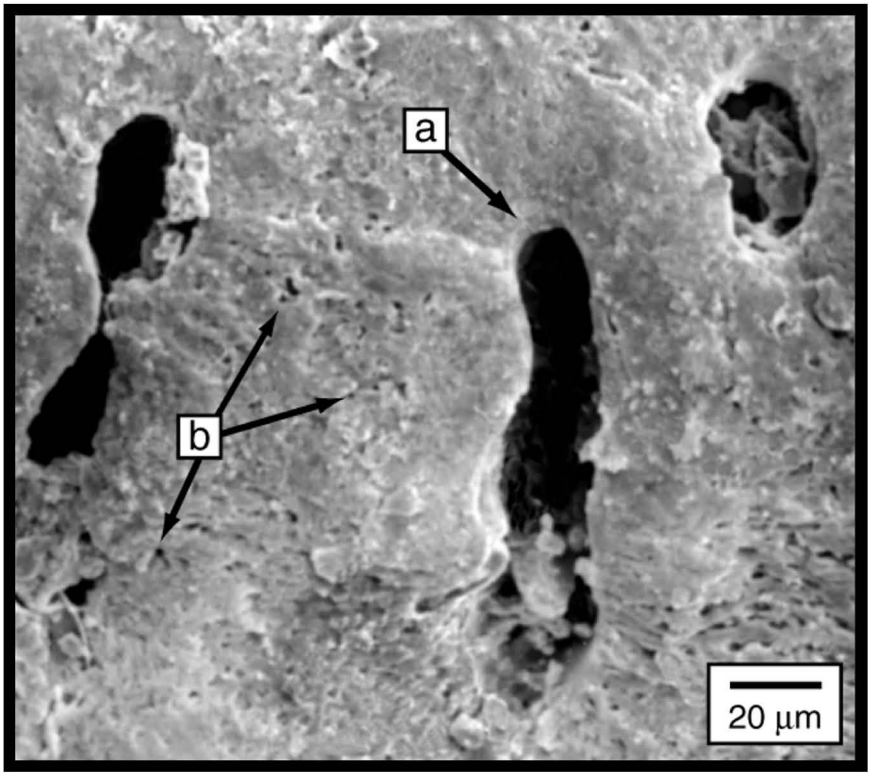

2.8 Description of Cytology

Amphisorus saurensis is dimorphic multinucleate. The somatic nuclei, 18 µm in diameter with an irregular oval shape, were found in the chamberlets, annular canal and near the embryonic apparatus (Figure 8A). The nuclei were spread out and were not in great concentrations in the organism (approximately 6 - 12 per organism). The generative nuclei were smaller (10µm), oval, and confined to the embryonic apparatus (approximately 2-3 per organism).

Symbiotic dinoflagellates (~7.2 µm in diameter) were found in all areas of the test: embryonic apparatus, inner chambers, intermediate chambers, outer chambers and the annular canals. The greatest number were in the intermediate chamberlets (Figure 8B), where the dinoflagellates were concentrated as high as 70 per chamberlet (0.36mm2 area) (Figure 9A). The symbiotic dinoflagellates are not evenly distributed within each chamberlet, they are in higher concentrations near the surface of each (Figure 9B).

Diatoms were also present in the cytoplasm of *Amphisorus saurensis*. The silica shells were oval with lengths of between 14µm and 30µm, and widths of between 7µm and 14µm. The diatoms were not in great concentrations, but they were present in all areas of the foraminifera. Because of the presence of frustules within the symbiosome, which is not commonly noted for symbiotic diatoms, it is believed that the diatoms were not symbionts, but instead captured prey. They may have been cemented to the outer surfaces of the test. Bacteria were also discovered in the foraminifera, although not in great concentrations.

Figure 8. Endosymbiont distribution within *A. saurensis*: A) Longitudinal view of Feulgen stained chamberlets with (a) host nucleus, (b) dinoflagellate nuclei, B) Drawing of *Amphisorus saurensis* showing distribution of symbiotic dinoflagellates in (a) outer chambers, (b) intermediate chambers, (c) inner chambers, (d) embryonic apparatus.

A

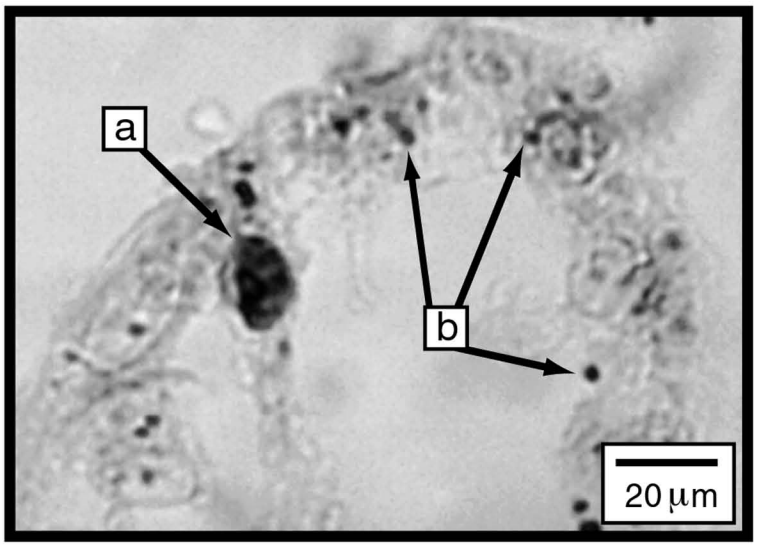

B

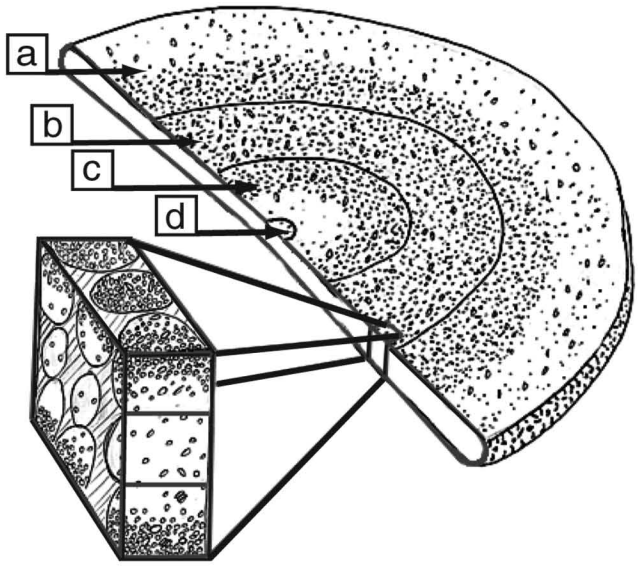

Figure 9. **Endosymbiont concentration within *A. saurensis***: A) Longitudinal view of Feulgen stained chamberlet where (a) indicates symbiotic dinoflagellates, B) Cross-section view of Feulgen stained *Amphisorus saurensis* full height cross-section (a) and single chamberlet (b).

A

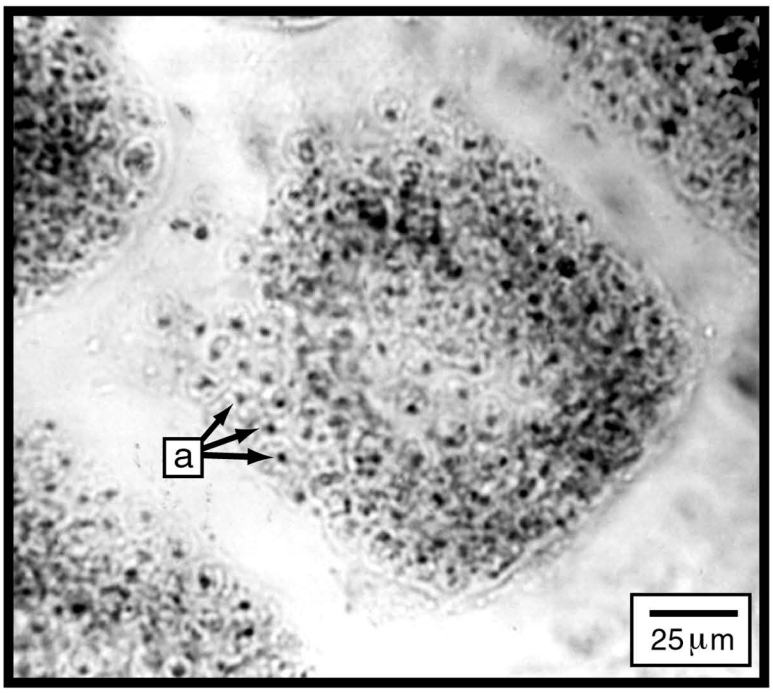

B

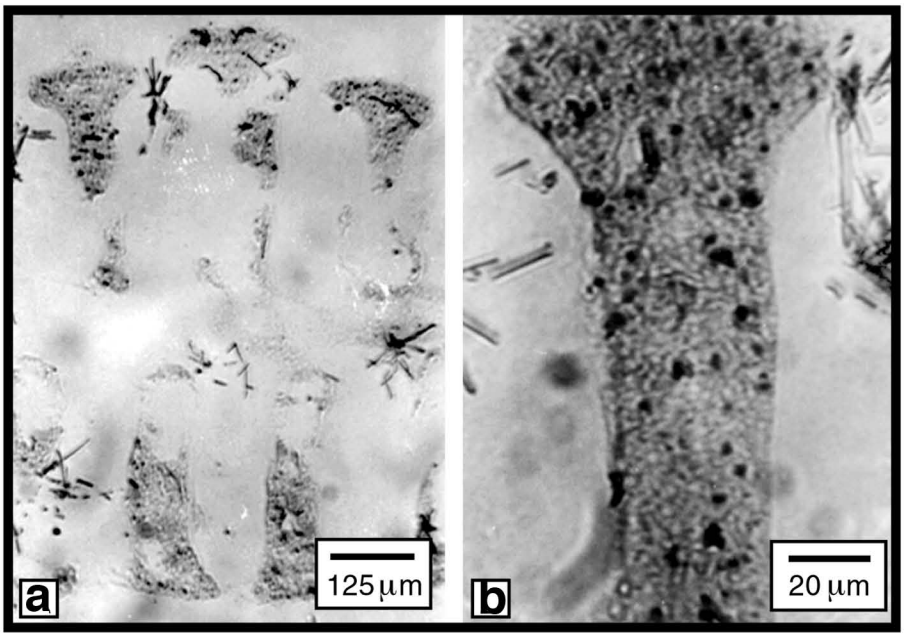

2.9 Molecular Identity

The results from the cladistic molecular analysis of the 18S rDNA fragment (~700bp) of the Bird Island taxa with other soritids (*M. vertebralis*, *A. hemprichii*, and *S. orbiculus*) shows the new specimens as sister taxa to *A. hemprichii* . The strict consensus tree of the two parsimony trees generated in this analysis is shown in Figure 10. Strong bootstrap values of 100 support the Bird island specimens as being most closely related to *A. hemprichii*.

Figure 10. Cladistic analysis of three Bird Island specimens using a fragment of 18S rDNA which identifies the species as belonging to the soritine genus *Amphisorus*. Values above the tree branches indicate the bootstrap support values.

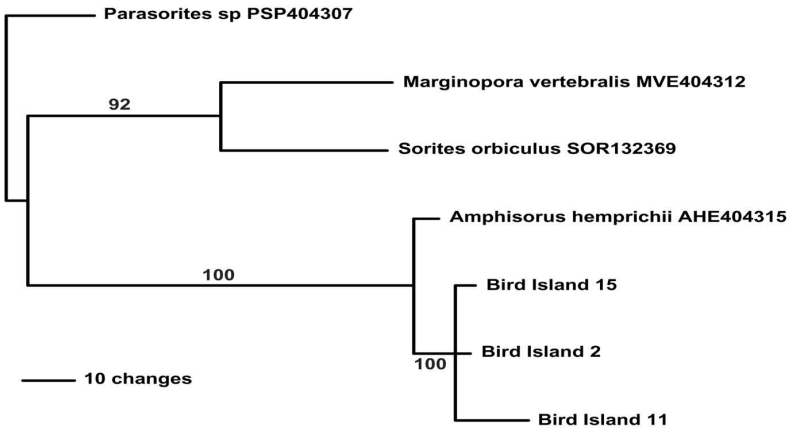
Parasorites sp PSP404307
Marginopora vertebralis MVE404312
92
Sorites orbiculus SOR132369
Amphisorus hemprichii AHE404315
100
Bird Island 15
Bird Island 2
100
10 changes
Bird Island 11

2.10 Shared Characteristics within the subfamily soritinae

Both the internal and external test architecture of the Bird Island specimens support their placement within the subfamily Soritinae. Similar to other foraminifera in this subfamily, *A. saurensis* has a discoid test with planispiral growth of cyclic chambers. The initial chamber growth in *Amphisorus saurensis* follows a pattern characteristic of the Soritinae with an embryonic apparatus in which the proloculus is followed by a flexostyle (Figure 3B). Additionally, the annular chambers that follow the embryonic apparatus are partially divided by septula such that a continuous annular canal runs through each chamber ring (Table 3).

The extension of the apertural face around the peripheral edge of the *A. saurensis* specimens is also a characteristic in common with other members of the Soritinae. Moreover, the placement of each marginal aperture at the terminus of a septula partition observed in *A. saurensis* is a consistent feature of the subfamily (Table 3). The apertures act as a passage for cytoplasm in an annular passage to interact with the outside environment. In their pioneering study of soritid surfaces, Ross and Ross (1978) very beautify illustrated the aperatures of *Marginopora* and *Amphisorus hemprichii*. They clearly illustrate the differences between apertures with smooth calcite linings and outer flanges (lips) and those without them.

Feulgen staining of the foraminifera cytoplasm provides evidence that *A. sauresensis* hosts endosymbiotic dinoflagellates, similar to that of other

members of the subfamily Soritinae. Dinoflagellates were observed in all areas of the foraminifer. Moreover, like the Soritinae genera *Sorites* and *Amphisorus*, the highest concentration of endosymbionts observed in Bird Island specimens occurred in chambers outside the embryonic region (Figure 8).

2.11 Characteristics of the genus *Amphisorus*

Prior to this study, the genus *Amphisorus* was defined by the single species *Amphisorus hemprichii* (Ehrenberg, 1839), found in the Red Sea, Caribbean and Philippine waters, and off the coast of Australia. It is characterized by having a large test that is discoidal and biconcave with thickened rims (a coin shape with the middle compressed). The species is one of a few that were identified as being variants of *Orbitolites* (Carpenter, 1883). Carpenter identified it as *Orbitolites complex*, or *Orbitolites duplex*, it was also named *Orbitolites complanata* (Lamark, 1801). It has occasionally been confused with *Sorites orbiculus* (Forskaål, 1775), due to both having two rows of apertures on the periphery of the test.

The test of *Amphisorus hemprichii* has a series of annular concentric rings of chambers surrounding the embryonic apparatus. The embryonic apparatus consist of a large proloculus, a half-whorl flexostyle and a large deuteroloculus, or vorhof (an extension of the flexostyle). The end of the vorhof is perforated with apertures. The embryonic apparatus is followed by approximately six aseptate flabelliform chambers and up to ten additional spiral chambers subdivided by septulae. Subsequent chambers are annular with a

continuous canal running through the chamber that is not traversed by septulae arising from the chamber walls. The septulae divide the chambers into chamberlets, creating two rows of chamberlets in alternating arrangements (Gudmundsson, 1994).

The vorhof and the first 9 to 15 chambers have a single row of apertures, but the following chambers have two rows of apertures. The apertures on the outside edge of the chamberlets (Figure 11A) follow this pattern of two alternating rows, as well. Some large specimens of *A. hemprichii* have been found to have a third row of apertures on the periphery of the chambers. The exterior ornamentation of the test includes irregularly fused pits and elongate grooves and pits arranged longitudinally around the apertures and by the apertural margin. Specimens can have inflated walls covering the chambers, which can create waviness on the exterior of the test, similar to *Sorites orbiculus* (Gudmundsson, 1994).

In multinucleate specimens, nuclei were located in every chamber but were more concentrated in the older embryonic and intermediate chambers. A large somatic nucleus resides in the proloculus of the embryonic apparatus. Possible generative nuclei have been found in the first 3-4 whorls with some larger somatic nuclei. Dinoflagellates are present in every chamber, but there were more individuals located in the intermediate and outer chambers than in the embryonic chambers (McEnery and Lee, 1981).

Figure 11. Comparison of apertures within the soritinae: A) Edge view of *Amphisorus saurensis* showing (a) marginal apertures, (b) median apertures, (c) absence of lips on marginal and median apertures, B) Edge view of *Amphisorus hemprichii*: (a) marginal apertures, (b) lips on edges of apertures, C) Edge view of *Marginopora kudakajimensis*: (a) marginal apertures, (b) median apertures, (c) lips on edges of apertures, D) Edge view of *Marginopora vertebralis*: (a) marginal apertures, (b) median apertures.

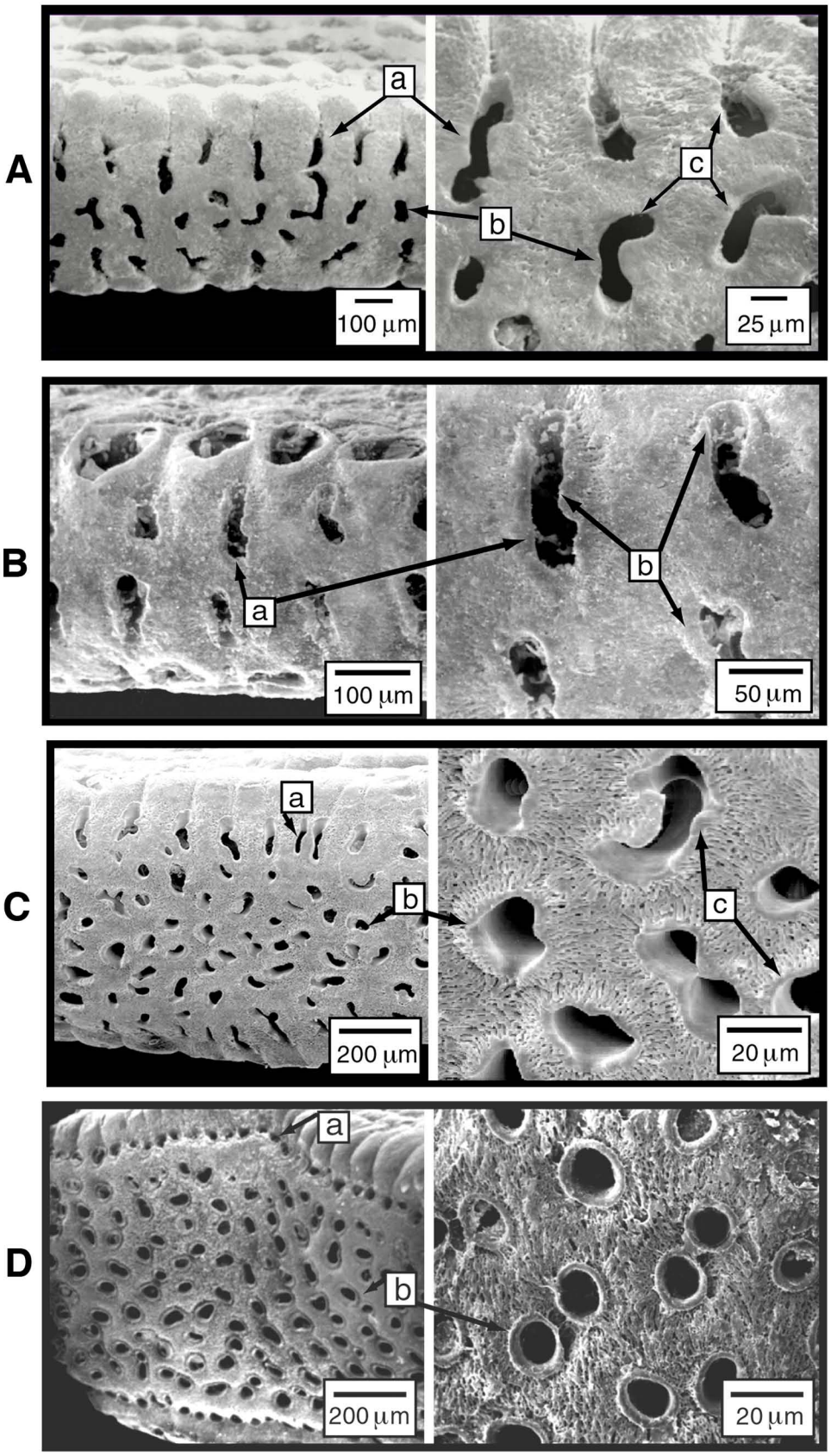
A
a
b
c
100 µm
25 µm
B
a
b
100 µm
50 µm
C
a
b
c
200 µm
20 µm
D
a
b
200 µm
20 µm

2.12 Shared Characteristics with the genus *Amphisorus*

The Bird Island specimens exhibit many character traits in common with *Amphisorus hemprichii*. The embryonic growth and subsequent growth of cyclic chambers closely resembles that of *A. hemprichii*. The megalospheric embryonic apparatus of *Amphisorus saurensis* have a proloculus, flexostyle and vorhof (Figure 3B). Within the subfamily Soritinae, the presence of a vorhof is a characteristic of the genera *Amphisorus* and *Marginopora* (Figure 12, Table 3). Additionally, the annular chambers of both species have chamberlets that are hexagonal and tube-like in shape. The chamberlets of both *A. saurensis* and *A. hemprichii* are arranged in two marginal rows, with each chamberlet extending away from the edge and toward the median. Similarly, the chamberlets of both species possess multiple connections with other sections of the chambers (Table 3). Each chamberlet is positioned atop an aperture of the previous chamber, providing a connection with the previous chamber's median canal. Furthermore, the chamberlets of both species also have connections to its own chamber's median canal (Table 3).

The exterior structure of *A. saurensis* has characteristics similar to that of *A. hemprichii*. The peripheral edges of the Bird Island tests have marginal apertures that are elongate like those of *A. hemprichii* (Figures 11A, B). In both *A. saurensis* and in *A. hemprichii*, the elongate apertures are oriented perpendicular to each marginal edge, thus, forming two parallel rows along the periphery of the test.

2.13 Unique Characteristics

Amphisorus saurensis has characteristics of internal and external test morphology that are unlike those of other soritids. The size of the test of the *A. saurensis* specimens is large. The average diameter of the specimens is 11.5 mm and the average height is 0.44 mm (Table 2). These measurements are larger than those of *A. hemprichii*. The *Amphisorus saurensis* measured had an average diameter that was 60% larger and an average height 30% larger than the average measurements recorded for specimens of *A. hemprichii* from the Red Sea.

The annular canal of *A. saurensis* has a shape and size that is distinct from the canals of *A. hemprichii* and the two species of *Marginopora* (Table 3). In *A. saurensis* the annular canal was observed to change size relative to the height of the test in successive chambers. The diameter of the annular canal of *A. hemprichii* is approximately one fifth of the total height of the internal chambers. In contrast, the annular canal of *A. saurensis* has a relative height that gradually increases with successive chambers, until the annular canal reaches one-third of the height of the test in the outer chambers.

Amphisorus saurensis specimens exhibit a pattern of apertures along the peripheral edge similar but not identical to that of *A. hemprichii*, *M. vertebralis*, and *M. kudakajimaensis* (Figure 11). Like *A. hemprichii* the *A. saurensis* specimens have two rows of elongate marginal apertures along edges of the apertural face (Figure 11A & B). Alternatively, *Amphisorus saurensis* also has median apertures located between the two marginal rows that are similar to the

marginal apertures of *M. vertebralis* (Figure 11D). The median apertures of the *Amphisorus saurensis* are round to teardrop shaped, similar in form and position to those of the two species in the genus *Marginopor*a. However, *A. saurensis* specimens were observed to have fewer median apertures than the two *Marginopora* species (Figure 11).

The results of recent molecular phylogenetic study of the Soritacea (Holzmann et al. 2001) suggest that the molecular evolution of the Soritinae may not reflect progressive morphological complexity from the simpler forms (*Sorites*) through the more complex duplex forms (*Amphisorus*) to the highly differentiated forms represented by *Marginopora*. In that study, *Amphisorus* did not branch between *Sorites* and *Marginopora* as would be expected if there was a linear progression in complexity. This result was treated as preliminary because of uncertainty about the identity of the *Marginopora* cf. *kudakajimaensis* used in that study (Holzmann et al. 2001). They commented that more molecular and genetic studies should be done to clarify the relationships between the two species of *Marginopora*. We agree. For this reason we did not include the sequence of the controversial organism in our comparative analysis. It is clear from our analysis that the new species *Amphisorus saurensis* fits in the clade delineating the genus *Amphisorus*. It is also quite interesting that *Marginopora vertebralis* is sister to a *Sorites orbiculus* GenBank sequence. This suggests that progressive morphological complexity from the simpler forms did not take place with an *Amphisorus* intermediate. Thus, the results of our study are in consonance with those of Holzmann et al.

(2001) and pinpoint the need for continued morphological and genetic work on this foraminiferal group.

2.14 Diagnosis

Amphisorus saurensis sp. nov.

The holotype specimen (Z 6586) has been deposited in the Australian Museum, Sidney along with a paratype specimen (Z 6587). Paratypes have also been deposited in the invertebrate collection at the American Museum of Natural History, New York, and the National Museum of Natural History, D.C. The specific epithet, *saurensis*, reflects the fact that the new species was collected in the reef slope of the Lizard group of islands of the Great Barrier Reef, Australia.

The specimens were collected at about 8 m below the area of the slope where the isolated coral heads ended at 24 m depth off the reef slope to the south of Bird Island. The GPS co-ordinates for the collection site were:14 41 634 S, 145 28 044 E.

The tests of *Amphisorus saurensis* are discoid in shape with an average height of 0.44mm and average diameter of 11.5mm. The average number of annular chamber rings was 59 per specimen. The embryonic apparatus is approximately 330µm in diameter and 250µm in height. The proloculus is nearly spherical and has one opening to the flexostyle. Encompassing half of the proloculus, the flexostyle possesses a single opening to the vorhof. The vorhof wraps almost completely around both the proloculus and the flexostyle.

It is inflated compared to the other two and represents approximately 75% of the area of the embryonic apparatus. The vorhof has multiple foramina which connect it to proceeding chamberlets. Each annular ring of chambers is divided by internal septulae into two marginal rows of chamberlets situated above and below an annular canal. Each of the two chamberlets is approximately one third of the height of the chamber ring. The annular canal, sandwiched between the chamberlets, fills in the remaining one third of the height. Each chamberlet is connected to its own annular canal and the previous ring's annular canal. *Amphisorus saurensis* has multiple apertures along the test periphery. Median apertures ~ 30µm in diameter are positioned along the middle of the apertural face above the annular canal. Their shapes vary from irregular to perfectly round. Some ovate shaped median apertures were up to 70µm. In addition to the median apertures, a row of marginal apertures lines each edge of the apertural face. They extend from the margin towards the median apertures. The marginal apertures vary in shape and size from small and nearly round, 30µm in diameter, to long and sinuous, 25µm in width and 55 to 120µm in length. The edges of the apertures are smooth and without raised rims. The density of apertures along the edge of the test is approximately 14 apertures in an area of 450µm by 450µm Around the apertures multiple pits arranged in irregular patterns often join to form groves in the apertural face.

The annular canal of *A. saurensis* has a shape and size that is distinct from the canals of *A. hemprichii* and the two species of *Marginopora* In *A. saurensis* the annular canal changes size relative to the height of the test in

successive chambers until the annular canal reaches one-third of the height of the test in the outer chambers. The diameter of the annular canal of *A. hemprichii* is approximately one fifth of the total height of the internal chambers. *Amphisorus saurensis* specimens exhibit a pattern of apertures along the peripheral edge similar but not identical to that of *A. hemprichii* and *Marginopora vertebralis*. Like *A. hemprichii*, *A. saurensis* specimens have two rows of elongate marginal apertures along edges of the apertural face, however, *Amphisorus saurensis* also has median apertures located between the two marginal rows that are similar to the marginal apertures of *M. vertebralis*. The median apertures of the *Amphisorus saurensis* are round to teardrop shaped, similar in form and position to those of the two species in the genus *Marginopora*. However, *A. saurensis* has fewer median apertures than the two *Marginopora* species.

CHAPTER 3

Molecular and Morphological Phylogenetic Investigations of Soritine Foraminifera

(ADAPTED FROM: Cevasco, M, Lee, J.J., Siddall, M. Observations of variable test morphologies within the symbiotic foramnifera (genus *Amphisorus*). 2007. *Symbiosis*. in review.)

3.1 Systematics of Soritinae

Contained within the contemporary systematic understanding of foraminifera is a complex history of shifting philosophical and methodological paradigms. Although early accounts of foraminifera date back to the fifth century B.C., ancient Greek writings of Herodotus and later to those of the Roman scholar, Pliny the Elder (23-79 A.D), it was not until the twelfth edition of *Systema Naturae* (Linnaeus, 1766) that foraminifera were systematically described. In this work, Linnaeus broadly defined 15 (non-soritine) foraminiferal species, which he classified as cephalopods in the genus *Nautilus*. The first description of a soritine foraminiferal species, however, was that of *Nautilus orbiculus* put forth by Forskål in 1775. In 1801, Jean Baptiste Lamarck proposed the separate genus *Orbitolites* within the cephalopods, under which he classified all soritine-type foraminifera. It was not until the publication of Alcade d'Orbigny's *Tableau Methodique* in 1826 that foraminifera were reassigned from the molluscs to be recognized as a distinct group of organisms possessing distinctive test (shell) apertures (foramens) (d'Orbigny, 1826).

In the *Tableau Methodique*, d'Orbigny presented the first comprehensive treatment of foraminifera. He subscribed to a far narrower and more empiricist interpretation of variation about a "morphological theme" than did Linnaeus. Consequently, in d'Orbigny's Order Foraminiferés, 87 valid generic names were proposed and 500 species described. But d'Orbigny's classification did retain some of the essentialist underpinnings of the Linnaean classification, in that families were defined by the single character, "plan of growth" (d'Orbigny, 1826).

In 1835, building upon d'Orbigny's work, Felix Dujardin dissolved the tests of foraminifera to better observe the internal morphology. In doing this, Dujardin effectively divorced foraminifera from cephalopods by demonstrating that foraminifera did not possess miniaturized versions of tentacles. Rather, they possess pseudopodia extending from the protoplast sarcode (Dujardin, 1835). The removal of foraminifera from within the cephalopods resulted in C. Ehrenberg's 1839 replacement of the generic name *Nautilus* with *Sorites* such that Forskål 's type species *Nautilus orbiculus* was renamed *Sorites orbiculus*.

In reaction to d'Orbigny's narrow species definitions, the English naturalists of the late 1800's classified foraminifera collected from the global expeditions of the H.M.S. Challenger using a uniformly broad view of variation in which organism diversity was limited to a few central types (Carpenter et al., 1862). The classification used test wall texture and perforation as the sole characters of generic level taxonomy and rejected the use of all other potential characters, contending they were too variable to hold any real taxonomic significance (Carpenter et al., 1862). Therefore, the Carpenter et al.'s (1862) classification of foraminifera collected from the Challenger expedition placed all foraminifera possessing an imperforate wall texture under his suborder Imperforata within Dujardin's order Rhizopoda Reticularia. The classification used Lamarck's genus *Orbitolites* to represent all members of the modern subfamily Soritinae and nested this genus with other calcareous foraminifera in the family Miliolidae. The genus *Orbitolites*, described as a "fundamental type", was based upon test morphology and encompassed all imperforate calcareous discoidal types in which

each chamber communicates with its neighbors by annular passages (Carpenter et al., 1862). Species denominations were not employed; rather the genus *Orbitolites* was roughly divided into three basic varieties of complexity: simple, duplex, and complex. But Carpenter et al. (1862) believed that the varieties represented an intergraded morphological spectrum. It was noted that the simple variety typically showed less extensive internal architecture and a single row of pores along the periphery of the disk. The duplex variety exhibited a uniform double row of apertures, and the complex variety exhibited a non-uniform double row of apertures along the periphery and had the most extensive internal structure of the three varieties. Generally, these "varieties" correspond to modern genera as follows: simple = *Sorites* (Ehrenberg, 1839); duplex = *Amphisorus* (Ehrenberg, 1839); complex = *Marginopora* (Quoi & Gaimard in Blainville, 1830).

Another influential classification of the Challenger fm oraminifera was produced in 1881 by the English naturalist H. B. Brady. Brady, similar to Carpenter et al. (1862), had a broad view of variation but also adhered to Linnaean taxonomic practice to achieve what he termed the ultimate systematic goal of reducing anomalies in existing groups (Brady, 1881). Although he "fairly doubted whether 'species'…can be said to exist among the lower protozoa" (Brady, 1881, p. 34), Brady noted the excess of variate and sub-variate descriptive names that can result from strictly adhering to a central types concept. Additionally, Brady did not select single characters as definitive of a specific classification level, but rather he looked for consistency among all characters. Brady (1881) recognized the soritid foraminifera of the Challenger as the genus *Orbitolites* and nested the genus within

the subfamily Orbitolitinae, which is defined as having an initial planispiral growth followed by cyclic test growth.

The first comprehensive classification of foraminifera to incorporate observations made using methodological advances in microscopy (e.g., SEM imaging) was published by Alfred Loeblich and Helen Tappan in 1987. This classification recognizes the priority of the subfamily Soritinae (Ehrenberg, 1839) over its junior synonym subfamily Orbitolitinae (Brady, 1881). Loeblich and Tappan (1987) placed three extant genera within the Soritinae: *Sorites*, *Amphisorus*, and *Marginopora*. Each genus is diagnosed on a composite of characters reflecting plan of growth and internal complexity as well as information available from a variety of sources such as life cycle observations. For example, the genus *Marginopora* is described as having a discoid test up to 30 mm in diameter, harboring endosymbiotic dinoflagellates, and forming a multi-chambered juvenarium before release of embryos from the microspheric test (Loeblich and Tappan, 1987).

This classification also recognizes the two extinct soritine genera, *Orbitolites* (Lamarck, 1801) and *Yaberinella* (Vaughan, 1928), which are both based on fossil (Eocene) specimens. The absence of connections between adjacent chamberlets is used to distinguish the fossil genus *Orbitolites* from that of the extant genus *Marginopora*. In the case of the genus *Yaberinella*, poor preservation obscuring character data in the fossils casts doubt on the assignment of this monotypic genus to the Soritinae such that the genus has been excluded from phylogenetic treatments (Gudmundsson, 1994), or if included, has been placed

outside the family Soritidae (Hottinger, 2000a). Loeblich and Tappan (1987) noted the tenuous position of this genus pending the discovery of better-preserved *Yaberinella* specimens.

A systematic treatment of the subfamily Soritinae using morphological character data was published in 1994 by Gudmundar Gudmundsson. His analysis employed both light and scanning electron imaging techniques to construct a 28-character matrix from which a single cladogram was manually constructed (Figure 12A). Similar to the generic (*Orbitolites*) designation of Carpenter et al. (1862), Gudmundsson's (1994) tree construction highlights the phylogenetic contribution of character ontogeny inferred from the complexity of internal skeleton architecture as well as from the pattern of initial chamber growth. The three genera comprising the subfamily Soritinae in this classification roughly parallel the Carpenters et al. (1862) "types" and are distinguished from each other by the following morphological characters: *Sorites* = presence of a simple internal skeleton consisting of septula, absence of an embryonic third chamber (vorhof), and absence of median apertures; *Amphisorus* = presence of a duplex (but absence of a median) internal skeleton; and *Marginopora* = presence of a median internal skeleton. Although Gudmundsson's 1994 classification does not add genera to the Soritinae, it does reassign two species to the genus *Sorites*; *S. bradyi = Peneroplis bradyi* (Cushman, 1930) and *S. orbitolitoides = Parasorites orbitolitoides* (Hofker, 1930). Additionally, a new species was described within the genus *Marginopora*: *M. kudakajimaensis* (Gudmundsson, 1994) (Table 4).

Figure 12. **Existing phylogenetic hypotheses of relationships among the soritinae**: A) The manually constructed phylogenetic tree of the Soritnae from Gudmundsson (1994), B) Extract from the neighbor-joining tree (1644 nucleotide ssu rDNA) from Holzmann, (2001), C) Extract from the parsimony tree generated from the morphological character analysis of Richardson (2001).

A

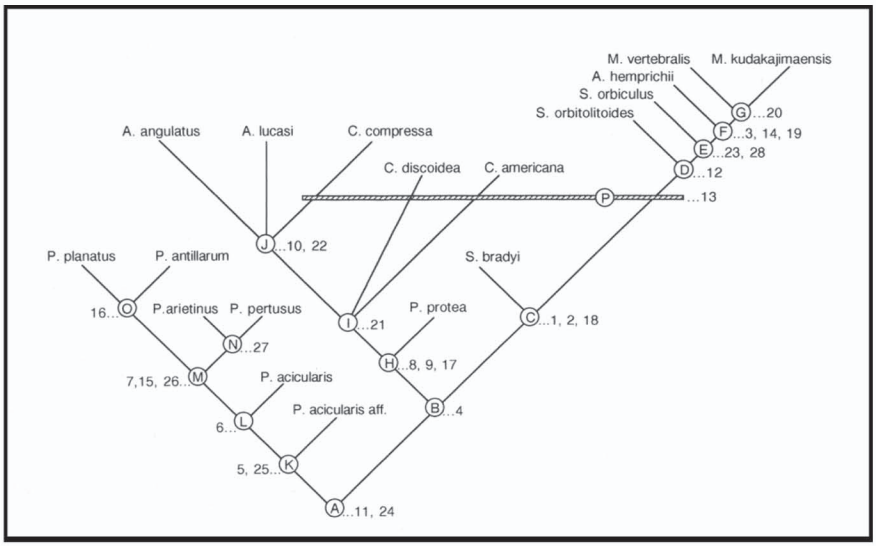
M. vertebralis
M. kudakajimaensis
A. hemprichii
S. orbiculus
S. orbitolitoides
G ...20
F ...3, 14, 19
E ...23, 28
D ...12
P ...13
A. angulatus
A. lucasi
C. compressa
C. discoidea
C. americana
J ...10, 22
P. planatus
P. antillarum
S. bradyi
16... O
P.arietinus
P. pertusus
P. protea
I ...21
C ...1, 2, 18
N ...27
H ...8, 9, 17
7,15, 26... M
P. acicularis
P. acicularis aff.
6... L
B ...4
5, 25... K
A ...11, 24

B

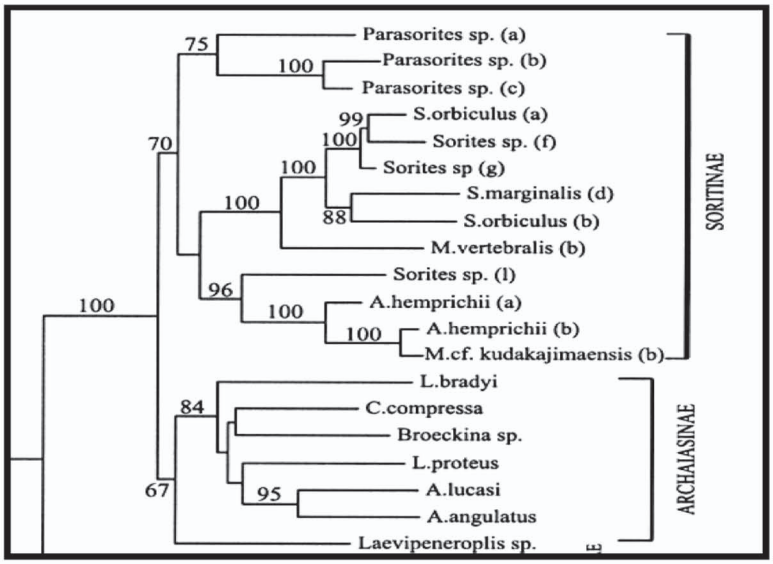
Parasorites sp. (a)
Parasorites sp. (b)
Parasorites sp. (c)
S.orbiculus (a)
Sorites sp. (f)
Sorites sp (g)
S.marginalis (d)
S.orbiculus (b)
M.vertebralis (b)
Sorites sp. (l)
A.hemprichii (a)
A.hemprichii (b)
M.cf. kudakajimaensis (b)
L.bradyi
C.compressa
Broeckina sp.
L.proteus
A.lucasi
A.angulatus
Laevipeneroplis sp.
SORITINAE
ARCHAIASINAE

C

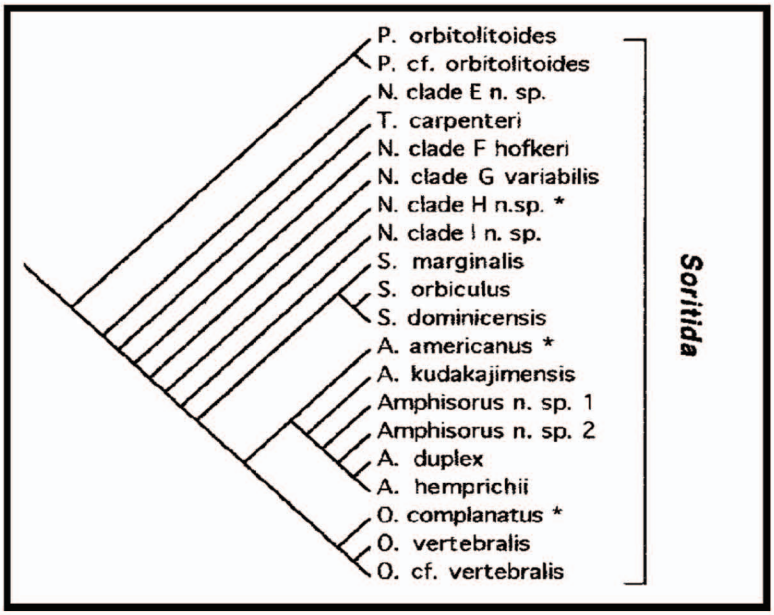
P. orbitolitoides
P. cf. orbitolitoides
N. clade E n. sp.
T. carpenteri
N. clade F hofkeri
N. clade G variabilis
N. clade H n.sp. *
N. clade I n. sp.
S. marginalis
S. orbiculus
S. dominicensis
A. americanus *
A. kudakajimensis
Amphisorus n. sp. 1
Amphisorus n. sp. 2
A. duplex
A. hemprichii
O. complanatus *
O. vertebralis
O. cf. vertebralis
Soritida

Table 4. Classification of the Subfamily Soritinae (Gudmundsson, 1994)

Kingdom Protozoa

Phylum Granulorecticulosa

Class Foraminifera

Order Miliolida

Family Soritidae

SUBFAMILY SORITINAE (Ehrenberg, 1839)

Genus *Sorites* (Ehrenberg, 1839)

Sorites bradyi (Cushman, 1930)

Sorites orbiculus (Forskål, 1775)

Sorites orbitolitoides (Hofker, 1930)

Genus *Amphisorus* (Ehrenberg, 1839)

Amphisorus hemprichii (Ehrenberg, 1839)

Genus Marginopora (Quoi & Gaimard in Blainville, 1830)

Marginopora kudakajimaensis (Gudmundsson, 1994)

Marginopora vertebralis (Quoi & Gaimard, 1830)

The first molecular phylogeny including the subfamily Soritinae was published by Holzmann et al. in 2001 (Figure 12B). This study analyzed partial SSU rDNA (778 bp) sequences of 13 soritine specimens using neighbor joining algorithms, and subsets of this dataset were also analyzed using maximum likelihood and parsimony (Holzmann et al., 2001).

One major result of this work was reassignment of Gudmundsson's 1994 *Sorites orbitolitoides* to the genus *Parasorites* (Seiglie et al., 1977). The Holzmann et al. (2001) analyses place *Parasorites* as the sister group to *Sorites*, and as such it was designated as the basal soritine genus. Of the remaining soritine genera, both *Marginopora* and *Sorites* were shown to be polyphyletic, and the genus *Amphisorus* was paraphyletic. Holzmann et al. (2001) posit their results to be the product of convergent evolution. However, it is also possible that much of the apparent polyphyly and paraphyly within the Soritinae is reflective of specimen misidentification and/or the need for additional data to better resolve relationships below the generic level.

In contrast to the findings of Holzmann et al. (2001), the morphological character-based parsimony analysis of soritid foramifera of Richardson (2001) shows an alternate relationship scheme among the soritine genera (Figure 12C). Richardson's 2001 analysis converts the clade containing soritine taxa to Soritida using PhyloCode conventions of nomenclature (Cantino and de Queiroz, 2000). This clade includes *Parasorites*, *Taramellina* (Munier-Chalmas, 1902), five new clades (E-I), *Sorites*, *Amphisorus*, and *Orbitolites* (Lamarck, 1801). Unlike Holzmann (2001), the Richardson (2001) analysis shows each of the genera

Sorities, *Amphisorus*, and *Orbitolites* (coverted from *Marginopora*) form monophyletic clades.

The monotypic genus of *Taramellina* was proposed by Munier-Chalmas (1902) with the type species *Sorites dominicensis* (Ehrenberg, 1839) and is generally recognized as synonymous with the genus *Sorites* (e.g., Cushman, 1933; Loebilch and Tappan, 1987; Gudmundsson, 1994). Richardson resurrects this genus, which forms a polytomy with the five additionally proposed genera based on the presence of the following two characters: pits of 1-2 μm in diameter in the chamber walls and haphazardly distributed pits on the apertural face.

Richardson also overturns Gudmundson's synonymy of *S. marginalis* as variant of *S. orbiculus* by distinguishing *S. marginalis* based on the presence of 2-3 μm pits in the chamber walls. Additionally, *Sorites dominicensis* is resurrected, although it does not have any character diagnosably distinct from the other named *Sorites* species.

Five extant terminal taxa are included in the *Amphisorus* clade (*A. hemprichii*, *A. duplex* (Carpenter, 1883), *A. kudakajimensis*, *A*. n. sp. 1, *A*. n. sp. 2). The species *kudakajimensis* falls within the *Amphisorus* clade as it does in the molecular analysis of Holzmann et al. (2001). The terminal *A*. n. sp. 1 is similar to *A. kudakajimensis* but has a distinct prolocular morphology and possesses four rather than five rows of apertures. The second proposed *Amphisorus* species *A*. n. sp. 2 is distinguished from *A. hemprichii* by the presence of partial transverse furrows on its apertural face. Although Carpenter's 1883 *duplex* taxon has been synonymized with *A. hemprichii* (Loeblich and Tappan, 1987), Richardson

distinguishes *A. dulplex* as a separate species characterized by apertural rims which are both "fluted" and raised as opposed to the raised apertural rims of *A. hemprichii*.

Conflict among these most recent analyses of Soritine foramifera (i.e., Gudmundsson, 1994; Holzmann et al., 2001; and Richardson, 2001) indicates the need for additional data and/or taxa to better resolve soritine relationships. Specifically within the genus *Sorites*, Gudmundsson's 1994 inclusion of *Parasorites orbitolitoides* merits re-evaluation, as it is the only soritine taxon to possess chlorophyte symbionts and lack a septulate endoskeleton. The placement of these species within the genus *Sorites*, however, may be a product of the character matrix used; coding character complexes as either present or absent (i.e., circular, crescentic, or elongate apertures forming a double, displaced marginal row) could obfuscate character state information. This reassignment is also at odds with both the molecular phylogeny of Holzmann et al. (2001) and the morphological phylogeny of Richardson (2001).

Gudmundsson also designates *Sorites marginalis* (Lamarck, 1816) as a variant of *Sorites orbiculus* (Forskål, 1775) based on significant overlap in test morphology such that 37% of the specimens examined were indistinguishable to either species (Gudmundsson, 1994). In contrast, both Holzmann et al. (2001) and Richardson (2001) consider *S. marginalis* and *S. orbiculus* distinct species. Holzmann et al. (2001) also refers to a set of specimens they were unable to definitively assign as either *S. marginalis* or *S. orbiculus*. The molecular analyses

of these ambiguous *Sorites* specimens, however, place one of these specimens within the genus *Amphisorus* while another forms the sister group to *S. orbiculus*.

Within the genus *Amphisorus*, further investigation is merited to resolve the differences among the recent phylogenetic treatments. This formerly monotypic genus recently has been expanded with newly described Australian species *Amphisorus sauronesensis* (Lee et al., 2004), and Richardson's (2001) analysis indicates that additional species diversity may also characterize this genus (e.g. *A. duplex*, *A*. n. sp. 1, and *A*. n. sp. 2). Moreover, both Holzmann et al. (2001) and Richardson (2001) concur that the genus *Marginopora* may be monotypic and that *kudakajimensis* specimens should be reassigned to the genus *Amphisorus*.

3.2 Specimen Collection

Foraminifera included in this research were obtained from 15 distinct Atlantic, Pacific, and Red Sea foraminiferal populations. A majority of specimens analyzed were collected during field expeditions in 2001-2005 using SCUBA at ≤ 25 meters depth from phytal substrates (e.g., *Halophyla* sp. , *Halimeada* sp.) and non-phytal (e.g. sand, rock, coral) substrates located adjacent to coral reefs. Additional soritine specimens were collected and contributed to this work by colleagues. Specimen collection locations are provided in Table 5. Subsequent to collection, a portion of the foraminifer test was removed and dried for scanning electron microscopy, while the remainder of the specimen was stored in 95 -100% ethanol for DNA extraction

Table 5. Specimen Collection Information

Location	GPS	Taxa Genera	Depth	Collection Date
Red Sea:				
Eilat (Israel)	29°30'N 34°55'E	*Amphisorus* *Sorites*	3-4 m	Jan 2001
Atlantic:				
Puerto Rico				
Culebra Island	17°57'N 67°03'W	*Sorites*	6 m	July 2003
La Parguera	17°58'N 67°01'W	*Sorites*	1-2 m	July 2003
Antigua				
Made Island	17°15'N 61°77'W	*Sorites*	1-2 m	July 2003
Florida Keys				
Key Largo	25°7'N 80°17'W	*Sorites*	1-5 m	May/June 2006 (P. Hallock)
Key West	24°32'N 81°48'W	*Sorites*	1-5 m	May/June 2006 (P. Hallock)
Sand Key	24°27'N 81°52'W	*Sorites*	1-5 m	May/June 2006 (P. Hallock)
Pacific:				
Indonesia				
East Kalimantan	02°08'N 118°30'E	*Amphisorus*	10 m	Feb 2003 (W. Renema)
Australia				
Bird Island	14°41'S 145°28'E	*Amphisorus* *Marginopora*	23 m	Feb 2003 (L. Pearce)
Lizard Island	14°39'S 145°26'E	*Marginopora*	2-9 m	Feb 2004
Japan				
Kudaka-Jima	26°9'N 127°53'E	*Amphisorus*	1-4 m	May 2004 (K. Fujito)
Zampa, Okinawa	26°26'N 127°42'E	*Amphisorus*	1-4 m	
Philippines				
Cebu	10°4'N 124°5'E	*Amphisours*	6-10 m	Oct 2004 (W. Renema)

continued

Hawaii				Jan 2005
Kailua, Oahu	21°30'N 157°50'W	*Amphisorus Marginopora*	2-4 m	Jan 2005
Poipu, Kauai	21°52'N 159°27'W	*Amphisorus*	2-6 m	Jan 2005
Guam				
Ritidian Point	13°39'N 144°51'E	*Amphisorus Marginopora*	4-10 m	May 2006 (C. Lobban)

3.3 Preparation for Morphological Examination

A minimum of 10 specimens from each population of foraminifera obtained were prepared for scanning electron microscope (SEM) examination by first washing each test in distilled water and removing as much surface debris as possible with a red sable brush (#1). The foraminifera then were either scalpel dissected or subjected to a casting technique modified from Hottinger (1979). Both dissected tests and specimen casts were sputter-coated with approximately 10 nm of gold prior to SEM observation. Specimens were observed and imaged in either the Zeiss DSM 940 scanning electron microscope at City College (CUNY) or the Hitachi S-4700 cold-field emission scanning electron microscope at the American Museum of Natural History.

The casting technique required that specimens be prepared for embedding by twice washing each foraminiferal specimen for 30 minutes in propylene oxide. The resin Poly/Bed 812 Embedding Medium then was added to specimens in a 1:2 ratio to the propylene oxide in which they were immersed. The percentage of resin was gradually increased to 100% through three serial medium changes. Specimens were placed in a vacuum chamber after each change to remove air bubbles.

Following overnight infiltration of the resin, the specimens were transferred into resin to which the hardener DMP-30 had been added and placed in a 60° C oven for polymerization.

After the specimens were cured, they were ground on a geologist's wheel using 600 grit fine sandpaper and then micro-polished on a felt-wheel. Specimens were ground at transverse angles and in cross-section. The carbonate test exposed through grinding was etched with 1% acetic acid ($C_2H_4O_2$) to create an epoxy cast of the foraminifera to elucidate patterns of connectivity among chamberlets and chambers (Figure 13).

3.4 Preparation for Molecular Examination

Qiagen DNeasy® kits were used to extract DNA from each foraminferal specimen. The extracted DNA was then subjected to PCR amplification using 2 µl of template in 25 µl reaction tubes of PuReTaq Ready-To-Go™ PCR Beads (GE Healthcare). Although the PCR profile varied depending on the primer set used and the population being amplified, in general the conditions that proved the most successful in amplifying the foraminferal template required at least 30 cycles of 94° for 30-45 seconds, 49°-52° annealing for 30-40 seconds and a 72° extension for 45-60 seconds. Successful amplification products were sequenced in both directions with ABI PRISM BigDye Terminator (Applied Biosystems) and electrophoresed in ABI Prism™ 3730 sequencer (Applied Biosystems). PCR amplification and cycle sequence products were cleaned using the Agencourt® solutions AMPure® and CleanSeq® respectively.

To develop additional primer sets specific to soritine foraminifera, a cDNA library was generated in which the dinoflagellate endosymbiont cDNA was subtracted from that of the soritine foraminiferal hosts.

Construction of this subtracted cDNA library required that both foraminiferal specimens and dinoflagellates isolated and cultured from foraminferal hosts were preserved in RNAlater® solution (Ambion™). These specimens were then pulverized on ice with a tissue grinder in a Knotes glass tissue homogenizer. In the foraminiferal specimens, the protoplasm was then separated from the carbonate test remnants by refrigerated centrifugation at 5ºC at 6,000 g. The supernatant was then subjected to mRNA extraction following the protocols outlined in the Roche™ mRNA isolation kit. Once ≥ 2 ng of foraminiferal RNA was obtained, the Clontech SuperSMART™ PCR cDNA Synthesis Kit was used to generate cDNA transcripts. This kit generates cDNA transcripts using an oligo dT primer at the 3' end of the nucleotide string such that the reverse transcriptase enzyme moves from the 3' to the 5' end where the enzymes terminal transferase adds a string of cytosine bases. The kit then attaches an oligo with a guanine (G) sting at the 3' end, thereby allowing for the synthesis of full-length cDNA transcripts.

Subsequent to foraminiferal and dinoflagellate cDNA synthesis, the Clontech PCR-Select™ cDNA Subtraction Kit was used to perform the subtraction of symbiont transcripts from those of host origin. This protocol consisted of an initial restriction enzyme digestion (*Rsa*-1), followed by the ligation of two adaptor oligos to the tester (foraminiferal cDNA). The tester and driver (symbiont cDNA)

Figure 13. Hottinger technique: Soritine specimen (40X) embedded in a resin block and ground to create lateral section through the embryonic apparatus. Calcite has been lightly etched with weak acid.

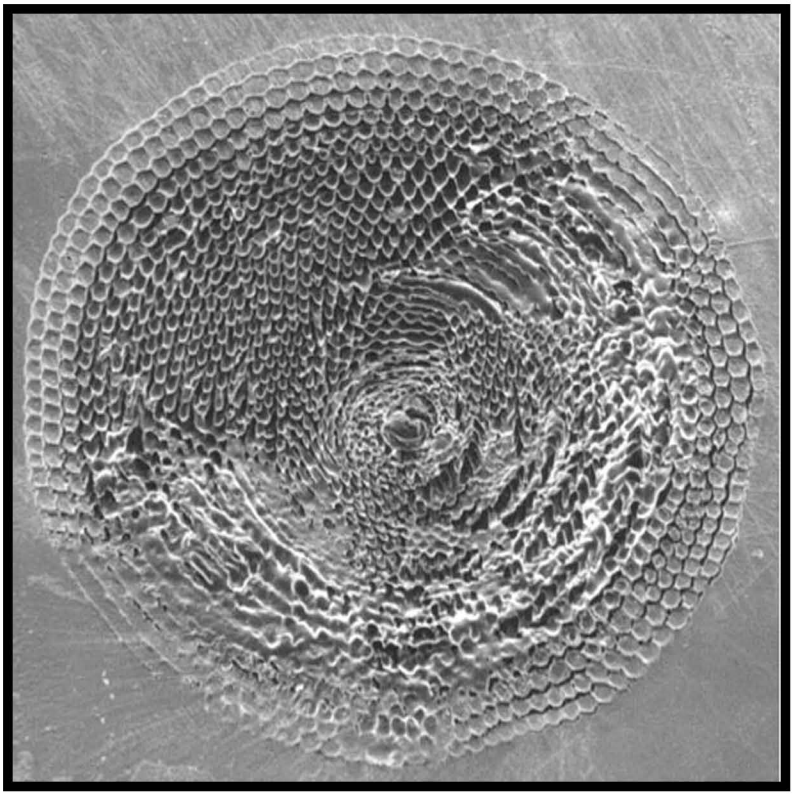

were then hybridized and incubated together to allow for the driver transcripts to anneal to each other. A PCR step with nested primers was then performed that amplified only the adaptor-linked tester transcripts that are not of driver origin (i.e. hybridized to the driver cDNA transcripts).

The foraminiferal transcript enriched PCR product was electrophoresed in a low melting point agarose gel such that the transcripts > 500 nt were gel extracted. This population of cDNA was then cloned into a bacterial vector using the protocol provided in the TOPO™ TA cloning kit. Cloned transcripts were then amplified and sequenced with the provided M13 primers.

3.5 Morphological Character Exploration

Below the ordinal level, foraminiferal taxonomy reflects the distribution of designated "key" characters primarily associated with test growth, chamber form, and aperture morphology. Appendix A contains both the matrix of 30 morphological characters constructed from light and electron microscopic observations of soritine populations and the coding conventions employed in this study. Selected characters from Gudmundsson (1994) and Richardson (2001) that have been incorporated in the current character matrix are indicated in Appendix A. As the soritine groupings corresponding to "key" character distributions vary throughout the literature (see 3.1), the geographic location of specimens rather than a presumed taxanomic identity is used in the discussion of soritine characters that follows.

Five matrix characters are present in all sampled soritine populations but absent in the three outgroup taxa included in this study: *Laevipeneroplis proteus* (d'Orbigny, 1839), *Parasorites orbitolitoides* (Hofker, 1930), and *Peneroplis pertusus* (Forskal, 1775). One character observed in living soritine specimens is the presence of dinoflagellate endosymbionts distributed throughout the foraminifer's annular chambers (character 8) (see Chapter 2, Figures 8 and 9). Although the outgroup taxa also retain algal symbionts (*Parasorites orbitolitoides* and *Laevipeneroplis proteus* retain chlorophytes; *Peneroplis pertusus* retains rhodophytes), dinoflagellate are only known to form an endosymbiosis in benthic foraminifera within the genera *Amphisorus*, *Marginopora*, and *Sorites*. Another character found in all of the soritine specimens is that of wavy sutures (character 15) between successive chambers corresponding to the chamberlet boundaries (Figure 14A). This character was first proposed by Gudmundsson (1994) and distinguishes soritine morphology from that of other discoid benthic foraminfera. The presence of an endoskeleton (character 16) formed on the inner surface of the chamber wall and consisting of plate-like elements (septula) and/or interseptal pillars was also observed in all observed populations (Figure 14B and C). The endoskeleton of all the sampled populations creates distinct chamberlets (chamber subdivisions) within each the annular chambers (character 17) (Figure 14B and C). Finally, connecting each chamberlet to successive chambers is a tubular opening (stolon) in the chamber wall forming an intercameral aperture that allows for a crosswise-oblique flow of protoplasm (character 22) (Figure 15) radiating outward from the initial embryonic chambers.

Observations of the endoskeletal morphology of specimens yielded four characters that varied among but not within sampled populations. Septular formation (character 18) was found to exist in three discreet states. Septula spanning across the chamber diameter were found in all of the Caribbean populations and in the Ritidian Bay:2 (Guam) specimens (Figure 16B and D). Septula that extend from the wall (septum) to the chamber median in an alternating pattern were observed in both the Red Sea and Bird Is.:1(Australia) populations (Figure 17B). All other Pacific populations— Ritidian Bay:1 and Ritidian Bay:3 (Guam), Kalimantan (Indonesia), Kudaka Is. and Zampa Beach (Japan), Cebu (Philippines), Lizard Is., Pidgeon Point, and Bird Is.:2 (Australia), and all Hawaiian locations—possess septula that span a distance ≤ one-fourth of the chamber diameter. A canal connecting the protoplasm of one chamberlet to the next within each annular chamber characterizes all sampled populations. The Caribbean, Red Sea, Ritidian Bay:2 and Bird Is.:1 populations have a single canal running through each annular chamber (Figure 18B). Six Pacific populations—Kalimantan, Cebu, Kauai and Oahu:1(Hawaii) , Zampa beach and Ritidian Bay:1—possess a canal that is divided by pillars into two parallel channels (Figure 19B and Figure 20C, E, and F). Irregular partitioning of the annular canal that creates multiple channels was observed in the remaining sampled Pacific populations: Bird Island:2, Lizard Island, and Pigeon Point, Ritidian Bay:3, Oahu:2, and Japan (Figure 16G and Figure19D). In addition to canal partitioning, observations of the growth pattern of the canal area concomitant with test growth (character 20) indicate that the Kalimantan, Cebu, Kudaka Is., Ritidian Bay:3, and all of the Australian populations

Figure 14. Endoskeletal Characters: A) Wavy sutures (character 15) between chamber whorls indicated by arrows on Hawaiian (Oahu:1) specimen (200X), B) Guam specimen (180X) with partial test removed to expose endoskeltal calcite (character 16) dividing chamber whorls into chamberlets (character 17), C) Hawaiian (Poipu) specimen (800X) in cross-section showing endoskelatal structure.

A

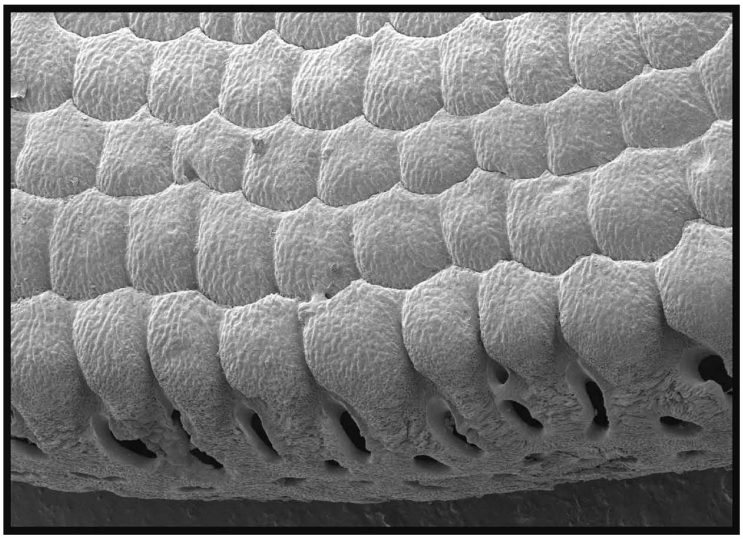

B

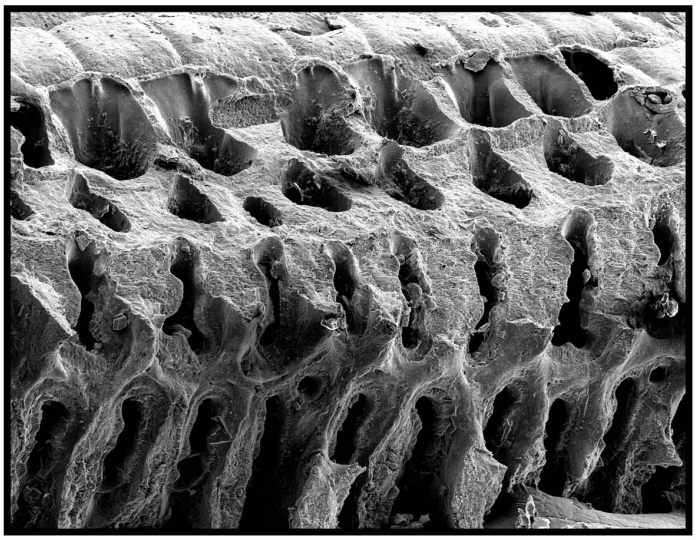

C

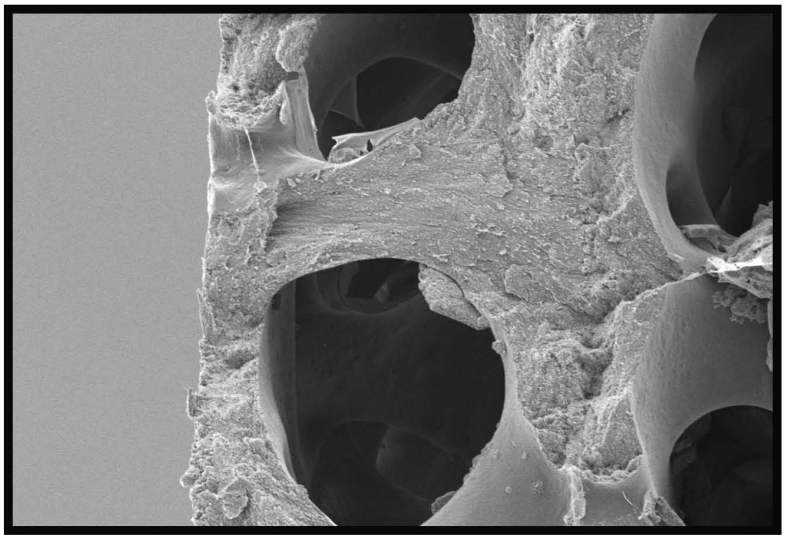

Figure 15. Connections Among Chamber Whorls: A) Resin cast of Australia (Lizard Island) specimen (400X) where red and yellow bars indicate crosswise-oblique connections (Character 22) between chamber whorls, B) Guam specimen (140X) with partial test removed to expose cytoplasmic pathways between chamber whorls (Character 22) as highlighted by red and yellow bars.

A

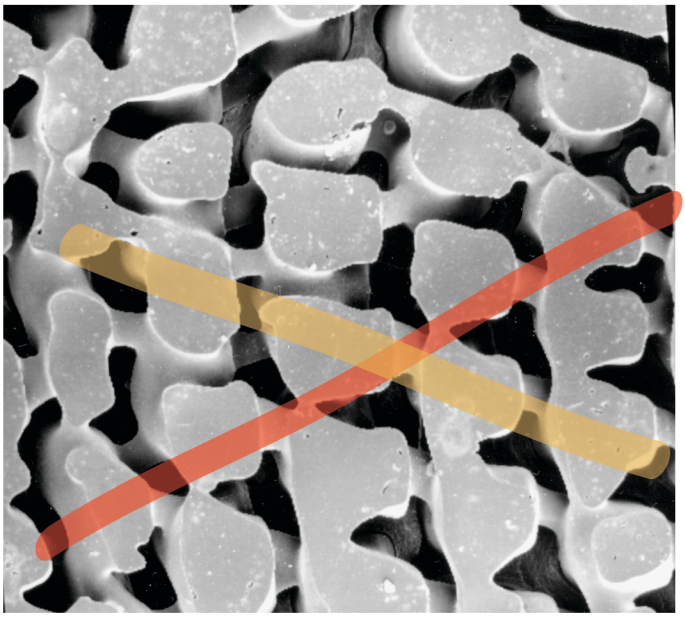

B

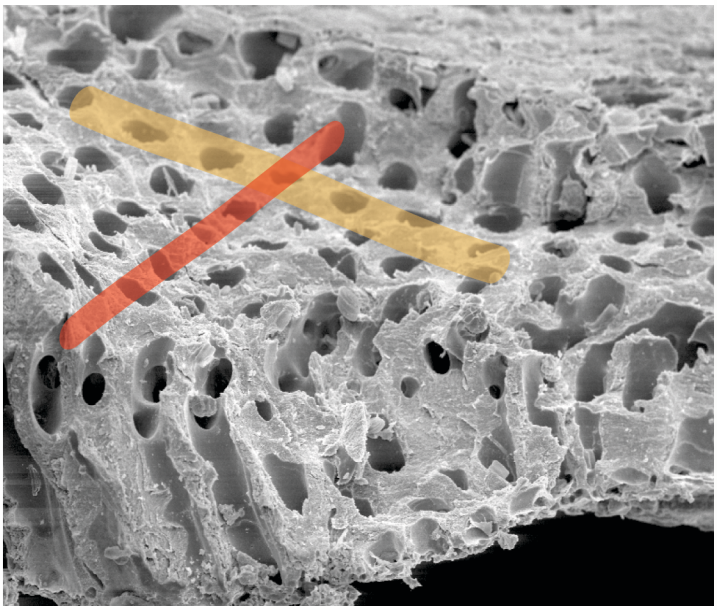

have canals that expand with test growth (Figure17E).

Apertural morphology often provides "key" characters in foraminiferal taxonomy. Seven characters are included in this study relating to the placement, shape, arrangement, and number of apertures observed in the sampled soritine populations. Classically, the presence of marginal apertures has been used to distinguish the genera *Amphisorus* and *Marginopora* from the genus *Sorites* (e.g. Brady, 1881; Loeblich and Tappan, 1987; Gudmundsson, 1994). A double row of marginal apertures (character 23) (Figure 16H, Figure 17A and D, Figure19A and C) was observed in all but the Ritidian Bay:2 and Caribbean populations, which possess lateral apertures (character 25) (Figure 16A). Lying between the two rows of marginal apertures, medial apertures (character 24) are found in all the populations that possessed marginal apertures, albeit infrequently in the Red Sea specimens (Figure 16E, Figure 17A and D, Figure 18D, Figure 19A and C, and Figure 20B and G).

Aperture shape (character 27) consisted of three primary forms: round to ovate (Figure 16F), elongate (Figure 17D), and irregular (Figure19C). It was also necessary to code for combinations of the three observed aperture shapes to account for differences in the shape of multiple apertures along a specimen's test periphery. The Ritidian Bay:2, Ritidian Bay:3, Bird Is.:2, Lizard Is., Pigeon Point, Oahu:2, and Caribbean populations have round to ovate apertures (Figure 16E). The Bird Is.:1 population's apertures are irregular (Figure 18A). Bird Is.:1 was the only population to possess only irregular apertures. The Ritidian Bay:1, Kauai, Oahu:1,

Figure 16. Scanning electron microscope images of morphological characteristics noted in Ritidian Bay:2, Caribbean populations [A-D] and Ritidian Bay:3 Bird Is.:2, Lizard Is., and Oahu:2 populations [E-H]: A) Arrangement of lateral apertures top image = double apertural row (300X), bottom image =single aperture row (376X), B) Chamber morphology from above with the top layer of calcite removed (800X), C) Whole test showing the general discoid test shape common to all genera within the soritinae (50X), D) Cross-section showing chamber morphology and the annular canals (as indicated by the arrows) (700X), E) Peripheral (apertural) view showing he shape, number, and placement of marginal apertures (90X), F) A single peripheral aperture exhibiting a pronounced lip and generally circular shape (2,000X), G) Resin cast cross-section showing the presence of a well developed median skeleton (black areas) within the chambers (100X), H) Peripheral view of an abnormally formed specimen illustrating distinct patterning of marginal vs. median apertures (50X) (Figure 18). These same Pacific populations were also found to have interseptal pillars (character 19) located throughout chamber medial sections (Figure.19E).

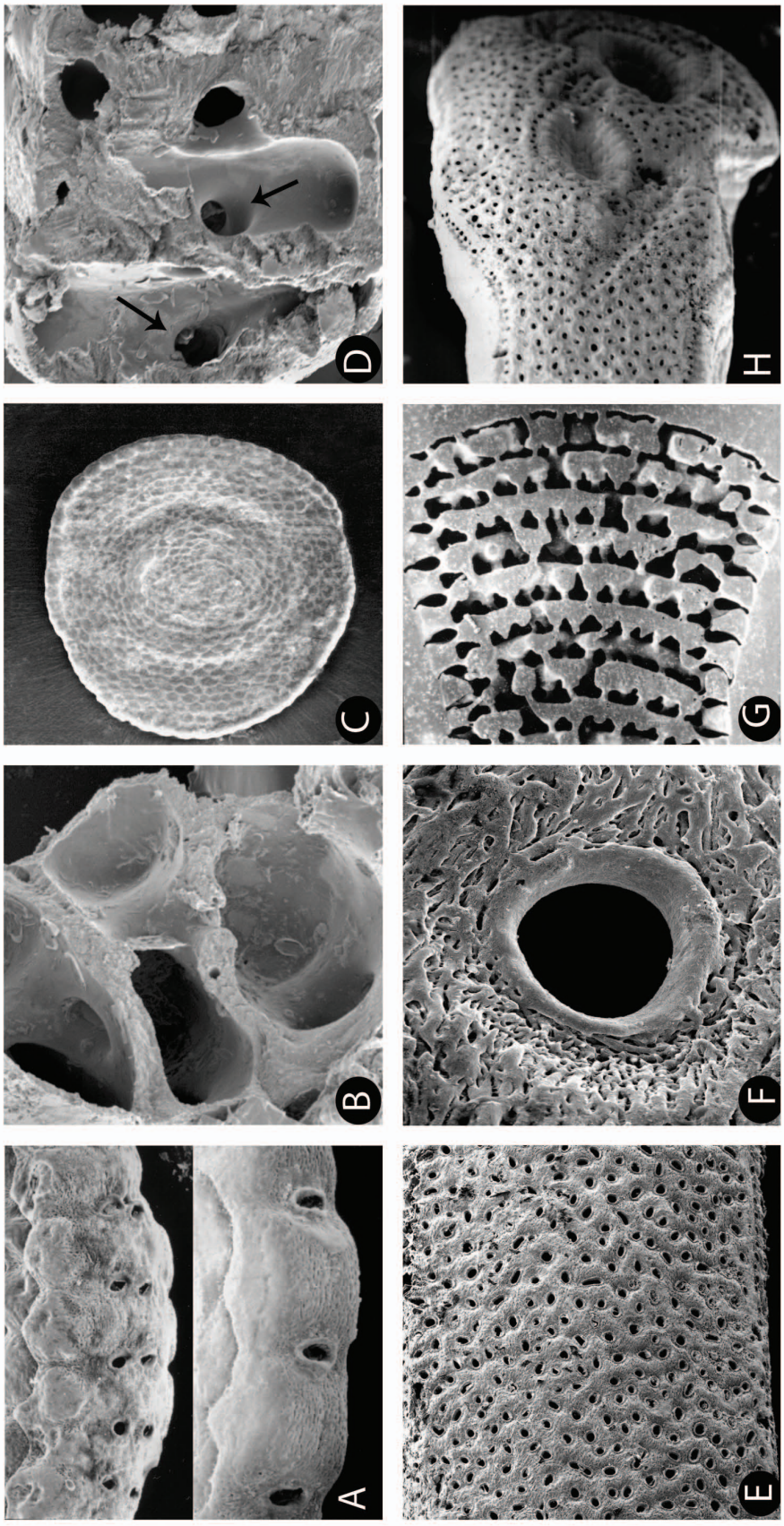
A
B
C
D
E
F
G
H

Figure 17. Scanning Electron Microscope images of soritines from the Red Sea [A- C] and Guam , Ritidian Bay:1 [D-F] populations: A) Apertural view of an Eilat specimen showing a double row of elongate marginal apertures as well as a median aperture (200X), B) Test fracture cross-section of an Eilat specimen showing the annular canals dividing upper and lower offset chamberlets (300X), C) Resin cast cross-section showing the cytoplasmic connection between chambers (yellow arrow) (300X), D) Apertural view of a Guam specimen showing the double row of elongate marginal apertures and circular median apertures (160X), E) Test fracture of a specimen with a portion of chamber tops removed with some annular canals visible (black arrows) (160X), F) Resin cast cross-section with the calcite only partially etched to reveal a two-dimensional slice of to illustrate the cytoplasmic connections between chambers (yellow arrow) (300X).

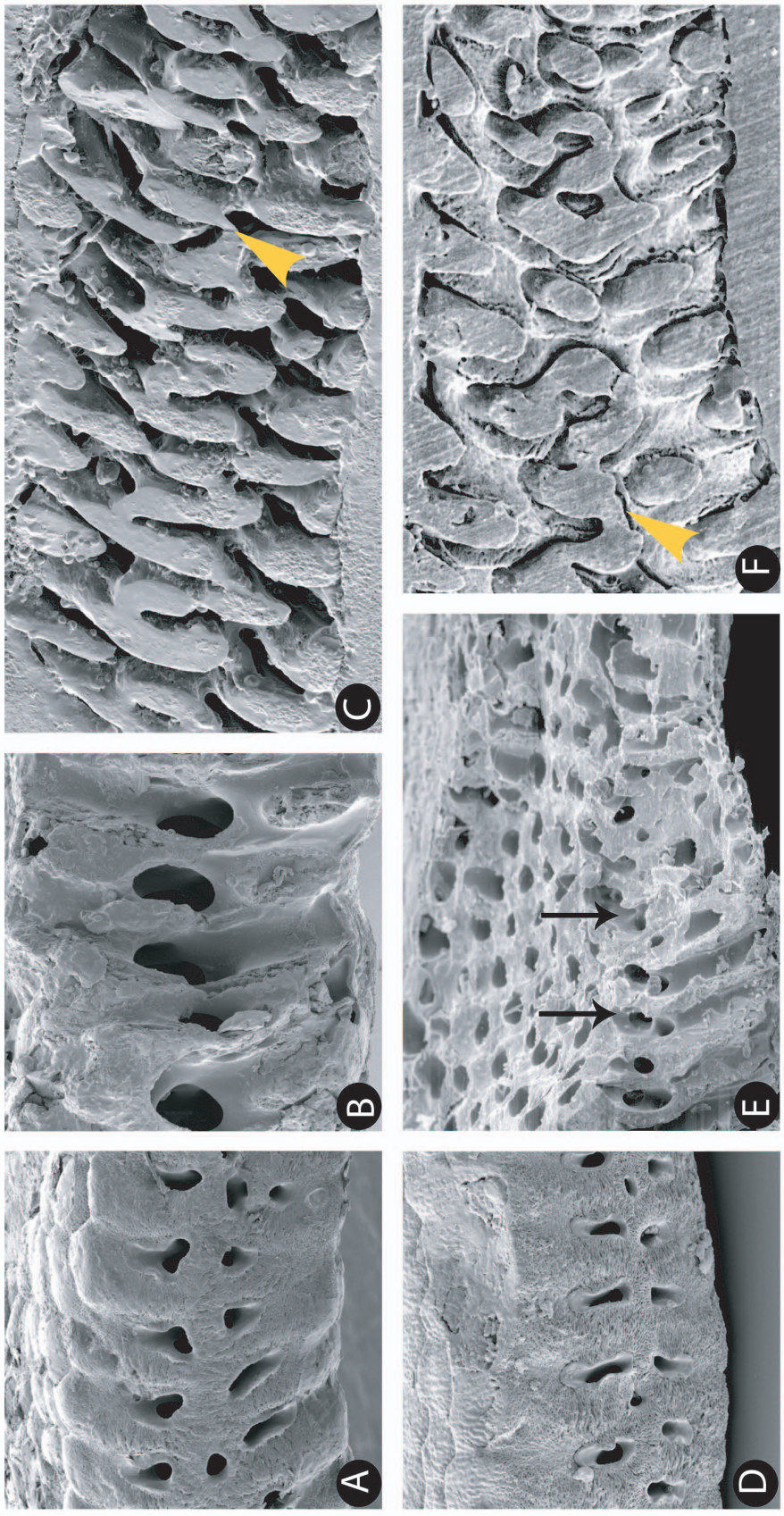
A
B
C
D
E
F

Figure 18. Scanning electron microscope images of specimens from Australia (Bird Island:1)[A-C] and Hawaii (Oahu:1 and Poipu) [D-G]: A) Test fracture with outer chamber removed to expose the aperatural face of the penultimate chamber (200X), B) Test fracture cross-section of the outer chambers showing the expansion of the annular canal (110X), C) Test fracture cross-section exposing an early chamber apertural face and showing chamber expansion (110X), D) Peripheral view of the elongated marginal and irregular medial apertures (200X), E) Test fracture of specimen with outer chamber removed showing the presence of simple median calcite structure (arrow) (180X), F) Test fracture cross-section specimen showing two annular canals running parallel through chambers (200X), G) Test fracture cross-section of the outer chamber whorls showing annular canals and aperture outlets (800X).

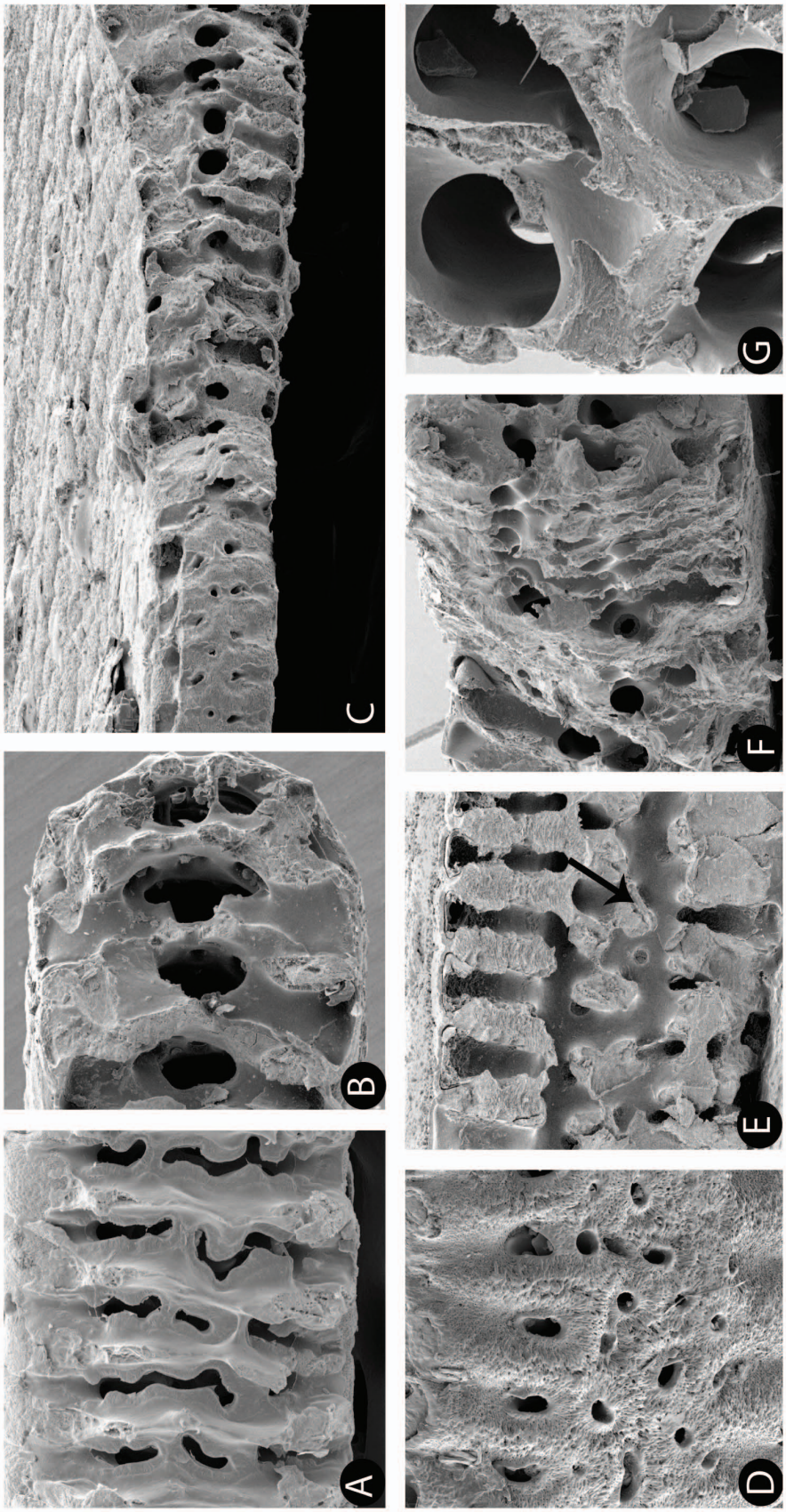
A
B
C
D
E
F
G

Figure 19. Scanning electron microscope images of specimens from Zampa Point [A-B] and Kudaka Island [C-E] (Japan): A) Peripheral apertures showing two elongate marginal rows and irregular median aperture rows (150X), B) Resin cast cross-section of a specimen showing the proloculus (P) and the development of complexity in the median skeleton (yellow, arrow = example of apertural connection between successive chambers) (180X), C) Peripheral apertures of a specimen showing two elongate marginal rows and multiple irregular median apertures (150X), D) Test fracture cross-section of a specimen showing the complexity in annular canals (green circles) (180X), E) Test fracture cross-section of a specimen showing at the test periphery showing the extent of median skeletal development (130X).

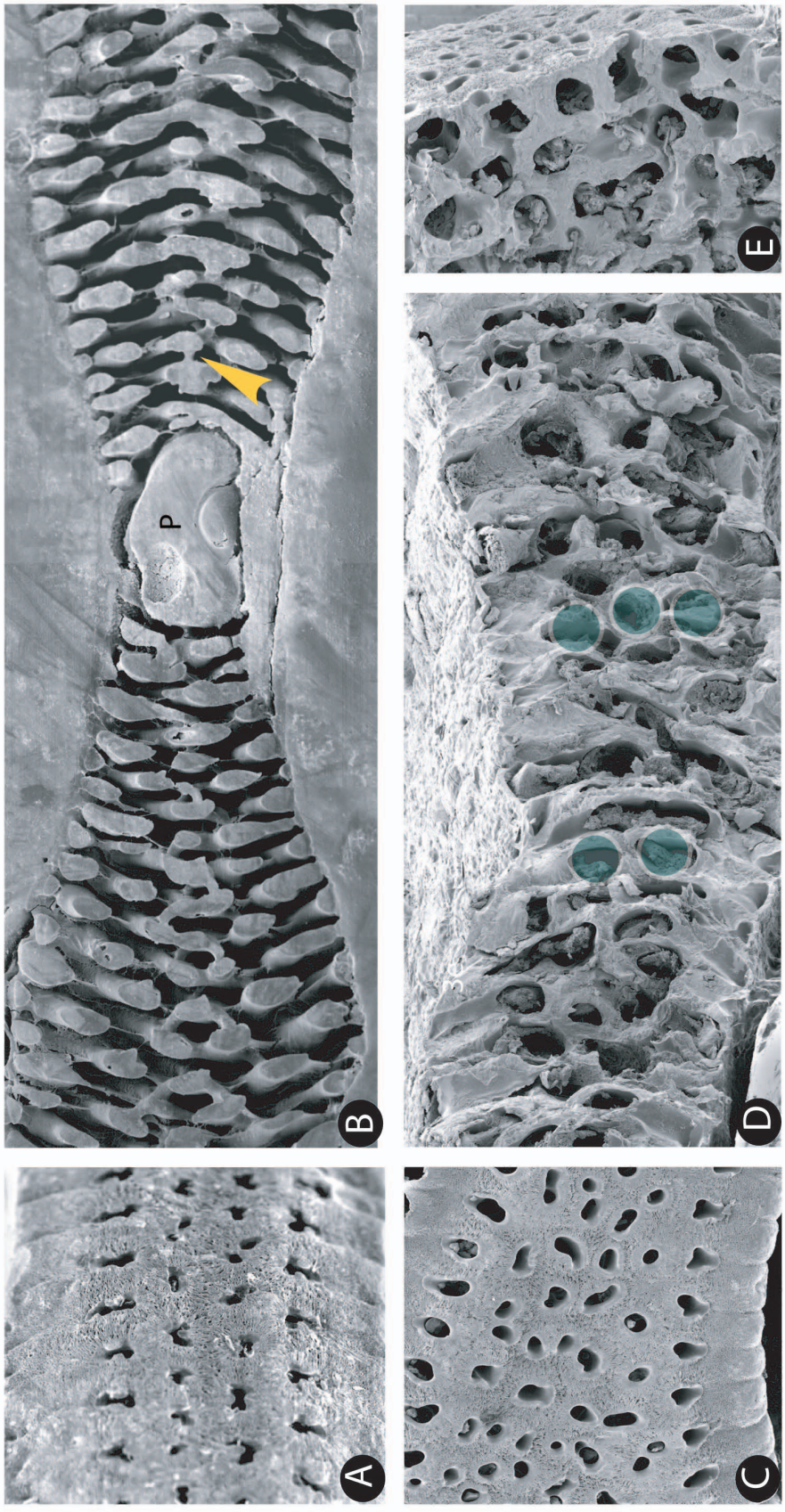
A
B
P
C
D
E

Figure 20. Scanning electron microscope images specimens from East Kalimantan [A-D], and Cebu, Philippines[E-G]: A) Test fracture of a specimen with the outer chamber face removed to apertures in detail (450X), B) Peripheral view of a specimen which shows a double row of elongate apertures and multiple irregular median apertures (150X), C) Test fracture partial cross-section of a specimen exhibiting a duplex internal skeleton (130X), D) Test fracture cross-section of a specimen showing the presence of a double annular canal (150X), E) Test fracture cross-section of a specimen exhibiting a series of parallel annular canals (180X), F) Test fracture cross-section of a specimen showing the progression from a single to double annular canals (green circles) (180X), G) Peripheral view showing a double row of elongate apertures and multiple irregular median apertures (100X).

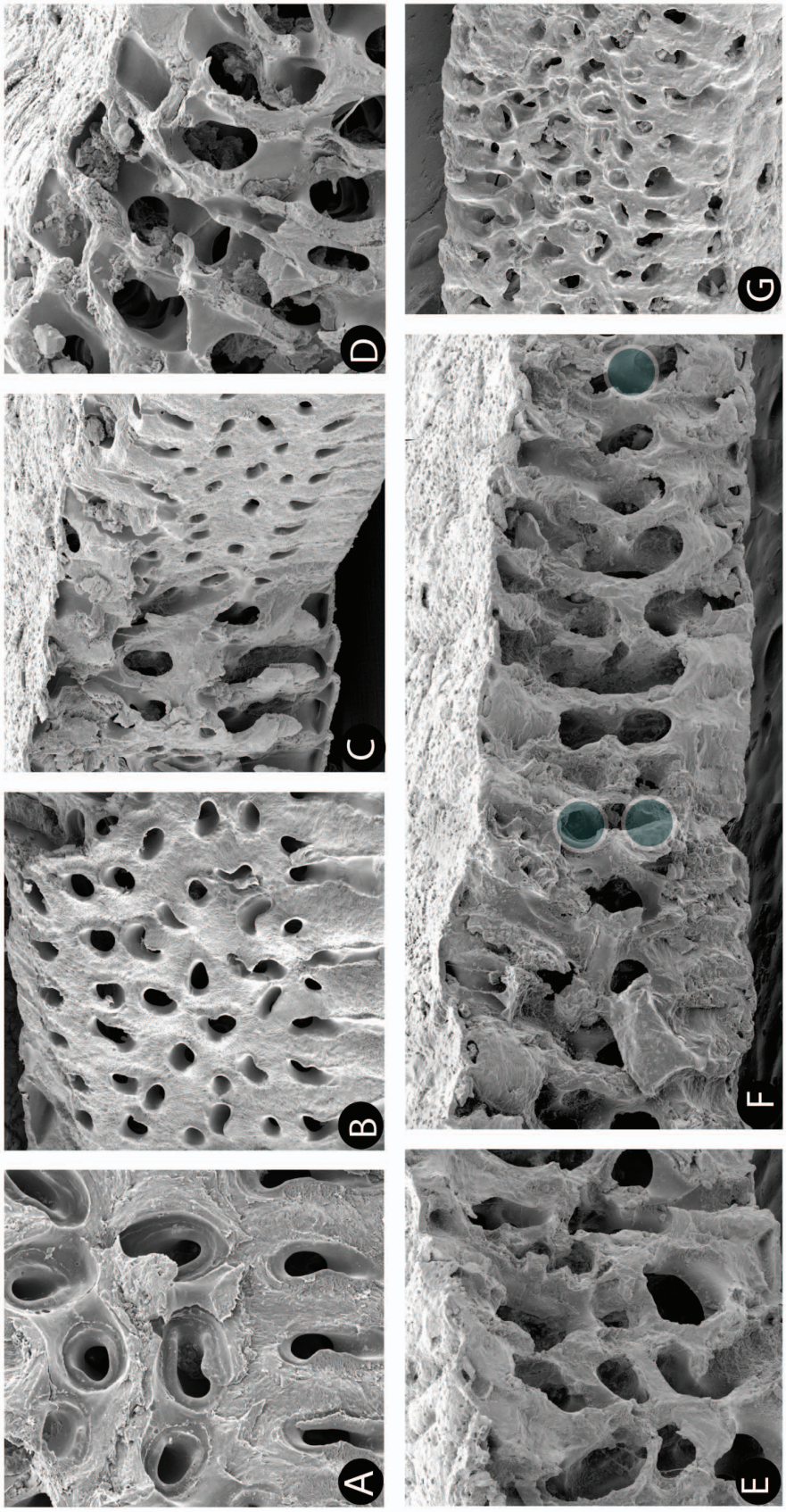
A
B
C
D
E
F
G

Oahu:1, and Red Sea populations were observed to have both round/ovate and elongate shaped apertures (Figure 18D and Figure 17A and D). The Zampa Beach population was characterized by both elongate and irregularly shaped apertures (Figure 19A). However the apertures of the other Japanese population (Kudaka Is.), as well as those from Kalimantan and Cebu show all three primary forms (Figure 19C and Figure 20B and G).

To normalize the data, the size (i.e., maximum dimension) of apertures was coded relative to chamber height (character 28) rather than by actual dimension. In the Bird Is.:2, Lizard Is., Pigeon Point, Oahu:2, Ritidian Bay:3, Kudaka Is., Kalimantan, Zampa Beach, and Cebu populations, apertures are < 1/4 of the height of the final chamber (Figure 16E and Figure 20C). Apertures ranging in size between 1/4 to 1/2 of chamber height characterize the following populations: Ritidian Bay:1, Red Sea, Bird Is.:1, Kauai, and Oahu:1 (Figure 17D). The remaining populations of the Ritidian Bay:2 and Caribbean specimens were observed to have apertures generally greater than 1/2 the height of the chamber's apertural face (Figure 16A)

Although aperture density (character 29) is necessarily influenced by apertural size, its distribution only partially overlaps that of character 28. With the exception of Zampa Beach, in all other populations where the aperture size was < 1/4 chamber height the density of apertures exceeded three per chamberlet (Figure 19C). The Zampa Beach specimens, however, showed 2-3 apertures per chamberlet, akin to those of the larger apertured Bird Is.:1, Kauai, and Oahu:1

populations. Ritidian Bay:1 and Red Sea specimens possess apertures measuring 1/4-1/2 chamber height and have an apertural density of 1-2 apertures per chamberlet. This apertural density was also found to characterize the Ritidian Bay:2 and Caribbean populations, in which apertural size exceeds 1/2 of the chamber height (Figure 16D).

Only the Bird Is.:1 and Zampa Beach specimens were found to have apertures in which a calcite rim or lip (character 30) was absent (Figure 19A).

The patterns of character distribution across the specimens examined approximate those of the soritine genera *Sorites*, *Amphisorus*, and *Marginopora*. Among the Caribbean and Ritidian Bay:2 populations, which correspond to the genus *Sorites*, no consistent morphological differences were noted. This distribution agrees with Gudmundsson (1994) in the lack of a diagnosable difference between *S. orbiculus* and *S. marginalis*. In contrast to the findings of Richardson (2001), pits were not observed in the chamber walls of any of the Caribbean or Ritidian Bay specimens (Figure 16C) and so could not be used to distinguish *S. marginalis*.

An identical character distribution also occurs among the Lizard Is., Pigeon Point, and Oahu:2 specimens, which correspond to the genus *Marginopora*. Bird Is.:2 and Ritidian Bay:3 specimens exhibit a similar pattern of character states and differ only in that they are slightly larger and in that the Bird Is.:2 population exhibits the autapomorphic trait of loss of its embryonic chambers in the later stages of growth.

The two Red Sea populations—Eilat:stones collected from hard substrates at a depth of 15 m and Eilat:*Halophyla* collected from phytal substrates at a depth of 5 m—show identical character distributions that correspond to the genus *Amphisorus*. Although distinguished from the Eilat populations by annular canals that are divided by interseptal pillars, Hawaiian specimens (Kauai and Oahu:1) also were found to share an "*Amphisorus*-like" character distribution. Similarly the patterns of both the Zampa Beach and Ritidian Bay:1 specimens resemble those of the Hawaiian "*Amphisorus*-like" specimens. The characters observed in the Bird Is.:1 specimens are unique among the populations examined and match those described for the species *Amphisorus sauronensis* (Lee et al., 2004)

The Cebu and Kalimantan populations show identical character distribution patterns, although it was not clear prior to phylogenetic anlaysis to which genus they most closely align. Similarly, this pattern found in the Kudaka Is. specimens lacks an obvious generic affinity and could explain the ambiguity of the placement of Kudaka soritines first within *Marginopora* by Gudmundsson (1994) and then within *Amphisorus* (Holzmann et al., 2001 and Richardson, 2001).

3.6 Molecular Character Exploration

This research aimed to expand the extant molecular data set to resolve the phylogenetic relationships among soritine taxa. Multiple approaches were attempted to find additional molecular markers beyond the ribosomal small subunit (SSU rDNA) used by Holzmann et al., (2001) appropriate to resolving relationships in lower level taxa. Although many of the attempts were unsuccessful, one

approach, in which the soritine sequences generated from a subtracted DNA library were found by a BLAST query to be similar to the large subunit sequences of other foraminiferan groups, was used to design ribosomal large subunit (LSU rDNA) primers for the Soritinae.

The small 450nt section of LSU rDNA contains a short variable region (~50 nt) that likely corresponds a to loop structure in the molecule. However, the most notable variability in the sequence is specific to the Zampa Beach specimens. Each of the three Zampa Beach sequences contains multiple unique sections of 4-100 nt found between conserved regions shared with the other taxa. The structural affinity of these sections has not been determined.

In addition to the LSU sequences, SSU rDNA sequences were recovered using the primers of Holzmann et al. (2001) and Garcia-Cuetos et al. (2005). Table 6. contains a list of the primers used in this study.

Table 6. Sequence primers for soritine foraminifera used in this work

Primer	Sequence 5'→3'	Reference
SSUrDNA		
SA10 (f)	CTCAAAGATTAAGCCATGCAAGTGG	Holzmann et al., 2001
S6R (f)	GGGCAAGTCTGGTGC	Holzmann et al., 2001
S12 (f)	CTACCAAAAGCGAAAGC	Holzmann et al., 2001
S14F3 (f)	ACGCAMGTGTAAACTTG	Holzmann et al., 2001
S13 (r)	GCAACAATGATTGTATAGGC	Holzmann et al., 2001
S17 (r)	CGGTCACGTTCGTTGC	Holzmann et al., 2001
LYS1 (r)	CTCCAACTATCTCCATCGA	Garcia-Cuetos et al., 2005
LSUrDNA		
F5LSU (f)	CTGACGTGCAAATCGTTRCCGCCT	Cevasco et al., in review
R4LSU (r)	CTTCCATGGCCACCGTCCTGCTGTC	Cevasco et al., in review

When concatenated, these primer sets cover the majority of the small subunit genes. Successful amplification using these primers varied depending on population and specimen preservation. Often, slight adjustments in the PCR profile implemented (e.g., changing the annealing temperature) improved results for one set of samples, while worsening the yield in another set. Amplifying shorter fragments within longer read primer sets was another fairly successful tactic to improve yields. For example, fragments of about 700 nt in length that were unable to be amplified in some populations using the primer pair S12 (forward) and S17 (reverse) often would amplify a shorter fragment of 400 nt using the primer pair S14F3 and S17. This approach maximized the number of taxa for which sequence data was collected but also created pockets of missing data.

To avoid discarding data, three molecular data sets were constructed: a complete 48 taxa data set of partial SSU and LSU sequences (1762 nt), a complete 122 taxa data set of a short (377 nt) variable region of SSU and an 112 taxa data set of partial SSU and LSU sequences (2717 nt) and morphology which is approximately 80% complete.

3.7 Phylogenetic Analyses

Sequences were edited using CodonCode Aligner (CodonCode Corporation) and Geneious© 3.4 (Biomatters Ltd.). When required for analysis, sequence aligments were preformed using the Clustal W software as implemented in Geneious© 3.4 (Biomatters Ltd.) under multiple gap cost regimes. The alignment parameter combination of gap opening cost 15 and gap extension cost 5

produced the most parsimonious solutions in the phylogenetic reconstructions requiring aligned datasets.

The parsimony optimality criterion was implemented in all phylogenetic analyses conducted. Analyses using aligned data (static homology statements) were performed using T.N.T. Version 1.1 (Goloboff, Farris, and Nixon, 2001). All characters were treated as non-additive and equally weighted with gaps treated as missing data. For each dataset analyzed, 100 replicates of random taxon addition were performed by way of the Wagner tree-building algorithm (Kluge and Farris, 1969). The search strategy implemented used both tree bisection-reconnection (tbr) branch swapping and "new technology" search options of tree drifting and sectorial searches (20 replicates each) to find a globally optimal solution for a given dataset. The tree drifting algorithm implement in TNT aids in finding a globally optimal tree by a process of simulated annealing wherein suboptimal solutions are temporarily accepted with a certain probability (dependant upon both the relative fit and length difference calculations) to help the tree search escape local optima (Goloboff, 1999). Likewise, sectorial searches are heuristic aids for reaching a globally optimal solution wherein selected portions of the tree are subjected to reanalysis and then replaced when a better solution is found (Goloboff, 1999).

Parsimony analyses were also conducted using a dynamic homology approach as implemented in the program POY 4 Beta (Varón et al., 2007). The use of a dynamic homology approach in which homology statements are tree specific (generated during tree building) rather than pre-defined, allowed for the direct optimization of unaligned sequences. The gap cost parameters used in direct

optimization were as follows: two for gap opening and one for gap extension. As in the TNT analyses, all characters directly optimized in POY with the optimality criterion of parsimony were treated as non-additive and equally weighted.

Unlike static approaches in which matrix (i.e. alignment) columns are fixed forming statements of primary homology, dynamic programming optimizes characters on a tree as it is being constructed (Wheeler, 1996). The dynamic homology property, while allowing for greater flexibility in tree construction, requires numerous initial Wagner tree builds to provide enough swappable branch arrangements to escape suboptimal solutions. The unaligned *Symbiodinium* datasets analyzed in this study were used to build 200 initial Wagner trees. These trees were then subjected to tbr swapping followed by a round of tree fusing. Tree fusing as it implemented in POY refers to a heuristic algorithm in which clades with identical composition of terminals are exchanged between pairs of trees to escape the local optimum (Goloboff, 1999).

In analyses of the larger datasets with greater than 80 taxa and 2000 total characters (nucleotide and morphology), the parsimony ratchet was implemented to improve the efficiency of searches in finding globally optimal solutions. To augment hill-climbing search strategies (e.g. tbr), the parsimony ratchet escapes local optima by implementing partial changes to a tree based on character conflict without altering the structure of the tree as a whole, (Nixon, 1999). In both static and dynamic homology analyses of larger datasets, 50 ratchet iterations were performed subsequent to tbr branch swapping.

Parsimony jackknife support values were calculated for the lowest cost trees generated from both static homology (TNT) and direct optimization (POY) analyses. In the POY analyses, dynamic homology characters were converted to static matrices that could be subjected to jackknife resampling by generating an implied alignment specific to the lowest cost tree. In both programs (TNT and POY) jackknife frequencies were calculated from 1000 pseudoreplicates of matrix resampling without replacement (36% deletion) using random taxon addition and tree bisection-reconnection swapping (Farris, 1999).

3.8 Results

The static homology parsimony analysis of 47 taxa with complete sequence coverage of 1762 nt spanning portions of both the small and the large ribosomal subunits yielded five equally parsimonious solutions (trees) 1917 in length (Figure 21). Dynamic homology analyses resulted in two minimum cost trees 2092 in length (Appendix B) that were topologically similar to the static homology trees. The strict consensus of the static homology trees provided in Figure 21 shows two major groupings of soritine foraminifera with high support (jac = 89). The first major soritine clade is divided further into separate *Marginopor*a and *Sorites* specimen clades. The other clade contains all of the *Amphisorus* specimens from the Red Sea and Pacific Ocean basins. Within the *Amphisorus* clade, Hawaiian specimens form a sister group to the Australian (Bird Island) specimens with high support (jac = 100). Strong support (jac = 100) was also recovered for the sister relationship between *Amphisorus* specimens from Kudaka Island, Japan and Eilat,

Israel. This analysis also places the South East Asian *Amphisorus* populations in separate clades often not sister to each other (e.g. Kudaka-Island's non-sister relationship with a population of geographically close Japanese *Amphisorus* specimens from Zampa point.

Analysis of a short (377 nt) fragment covering a variable region of the ribosomal small subunit for 122 taxa, analogous to that reported in Garcia-Cuetos et al. (2005), produced the most parsimonious solution of 436 steps using a static homology approach, while the direct optimization analysis yielded minimum length trees of 508 steps. A strict consensus tree of 30 equally parsimonious trees generated in TNT is depicted in Figure 22. The analyzed fragment was apparently unable to distinguish the outgroup peneroplid taxa as two outgroup taxa were placed within the soritine in-group with high support. The consensus tree consists of two major clades. The first clade is defined by low jackknife support and contains both Pacific and Atlantic *Sorites* specimens interspersed among populations of Pacific *Marginopora* specimens. The other clade also places multiple genera (*Marginopora* and *Sorites*) from geographically disparate locations (i.e. Australia and Florida) as sister taxa. However, high support values (jac > 80) distinguish a partition between a grouping of all the *Amphisorus* specimes and the *Marginopora/Sorites* taxa.

The combined analysis using direct optimization of ssu and lsu rDNA sequences with the morphological data set yielded a single tree of 4431 steps (Figure 23). The static homology parsimony analysis in TNT recovered three

Figure 21. Strict Consensus Parsimony Tree (1917 steps): Generated from five equally parsimonious solutions resulting from TNT analyses of ribosomal DNA (1762 nucleotides) for 47 taxa. Jackknife support values > 50 are indicated at the nodes. Color shading denotes major clade divisions (blue = *Sorites* morphological type, green = *Marinopora* morphological type, red = *Amphisorus* morphological type, *A. hemprichii* = maroon, *A. kudakajimaensis* = rose, *A. saurensis* = yellow).

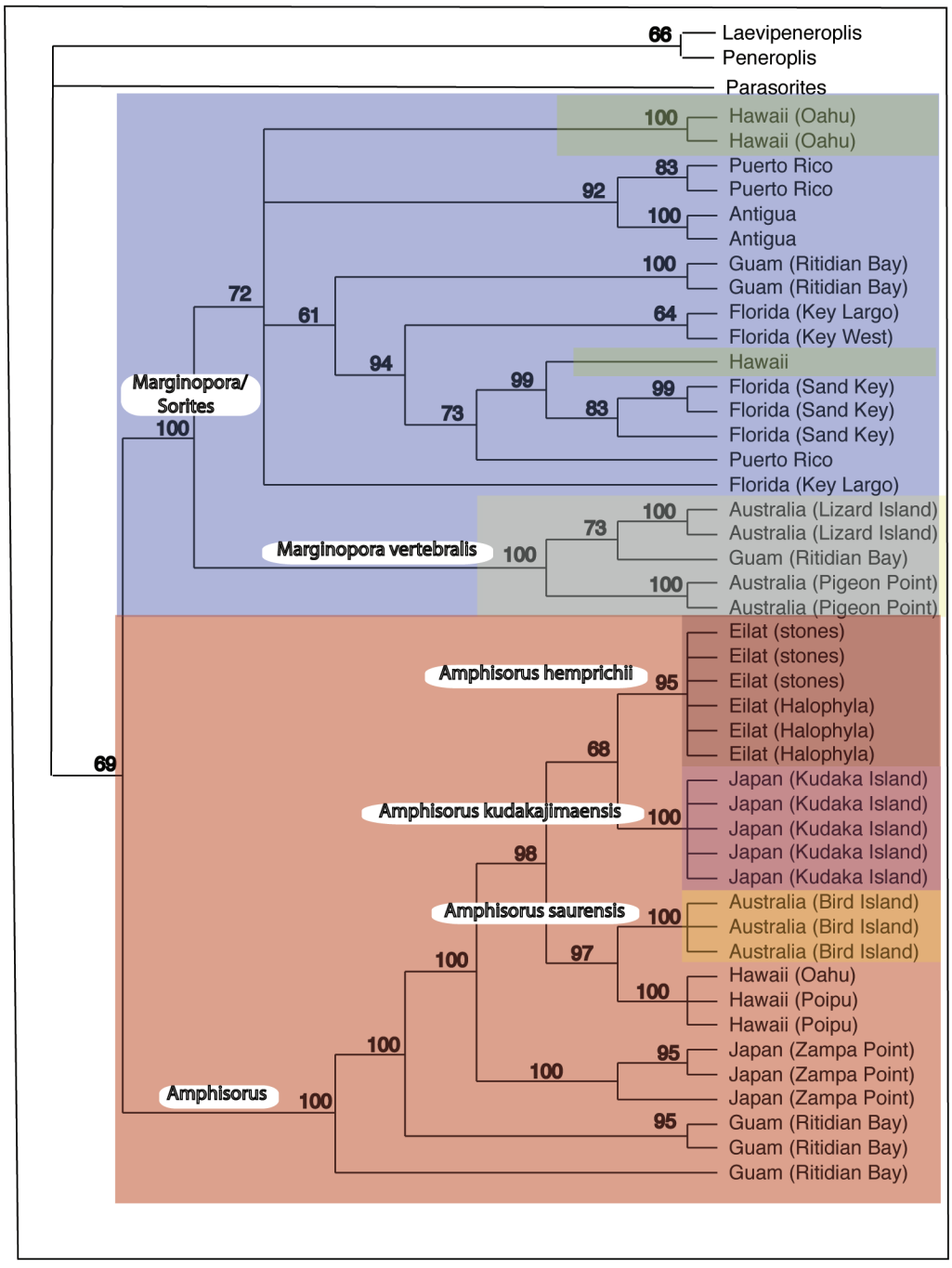
66
Laevipeneroplis
Peneroplis
Parasorites
100
Hawaii (Oahu)
Hawaii (Oahu)
83
Puerto Rico
92
Puerto Rico
100
Antigua
Antigua
100
Guam (Ritidian Bay)
72
Guam (Ritidian Bay)
61
64
Florida (Key Largo)
Florida (Key West)
94
Hawaii
Marginopora/
Sorites
99
Florida (Sand Key)
99
73
83
Florida (Sand Key)
100
Florida (Sand Key)
Puerto Rico
Florida (Key Largo)
100
Australia (Lizard Island)
73
Australia (Lizard Island)
Marginopora vertebralis
100
Guam (Ritidian Bay)
100
Australia (Pigeon Point)
Australia (Pigeon Point)
Eilat (stones)
Eilat (stones)
Amphisorus hemprichii
95
Eilat (stones)
Eilat (Halophyla)
68
Eilat (Halophyla)
Eilat (Halophyla)
69
Japan (Kudaka Island)
Japan (Kudaka Island)
Amphisorus kudakajimaensis
100
Japan (Kudaka Island)
Japan (Kudaka Island)
98
Japan (Kudaka Island)
Amphisorus saurensis
100
Australia (Bird Island)
Australia (Bird Island)
97
Australia (Bird Island)
100
Hawaii (Oahu)
100
Hawaii (Poipu)
Hawaii (Poipu)
100
95
Japan (Zampa Point)
100
Japan (Zampa Point)
Amphisorus
100
Japan (Zampa Point)
95
Guam (Ritidian Bay)
Guam (Ritidian Bay)
Guam (Ritidian Bay)

Figure 22. Strict Consensus Parsimony Tree (436 steps): Generated from 30 equally parsimonious solutions resulting from TNT analyses of small subunit ribosomal DNA fragment (377 nucleotides) for 122 taxa. Jackknife support values > 50 are indicated at the nodes. A) Clade containing *Marginopora* (blue) and *Sorites* (green) type morphologies; B) Clade (red) containing *Amphisorus* (red) type morphologies.

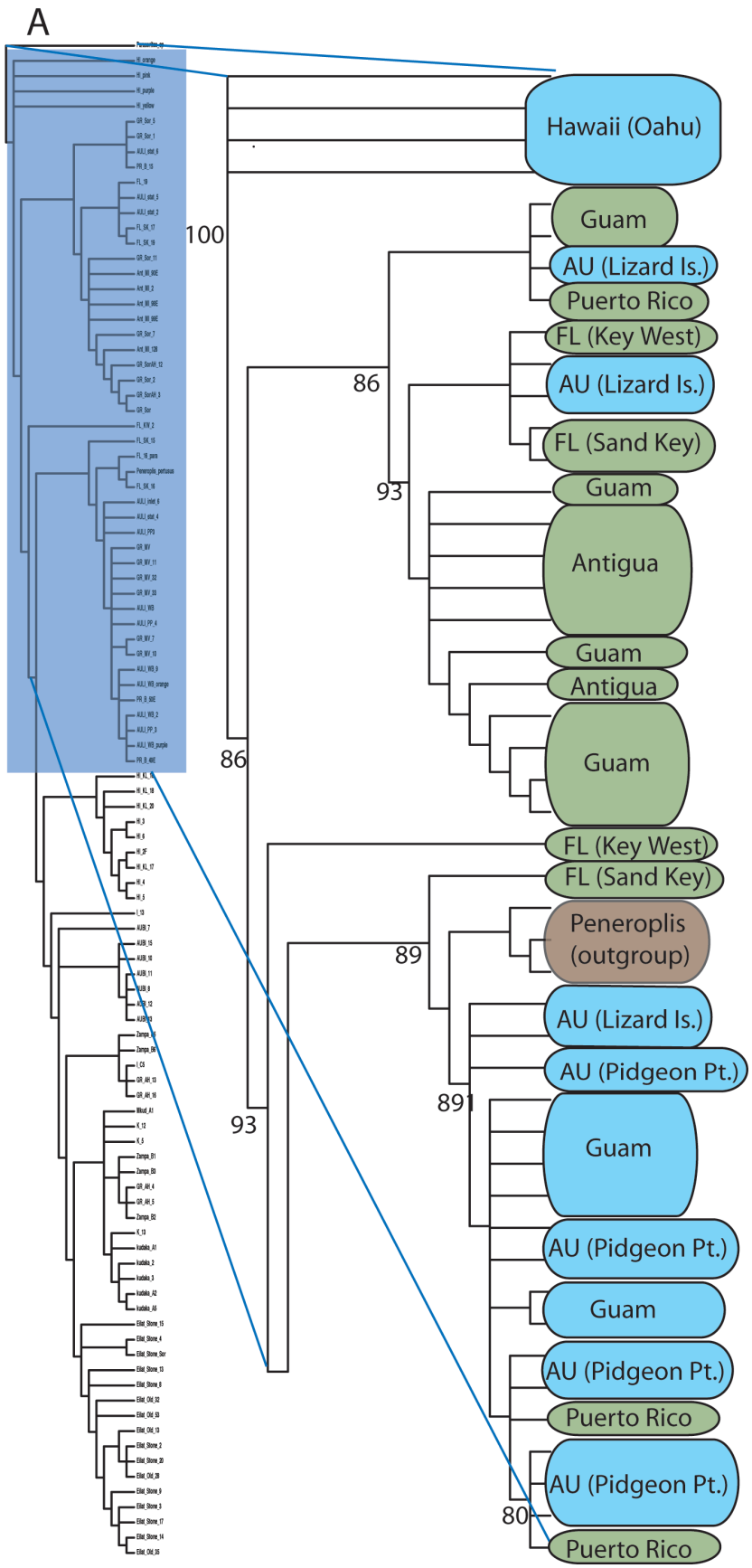
A
Hawaii (Oahu)
Guam
AU (Lizard Is.)
Puerto Rico
FL (Key West)
AU (Lizard Is.)
FL (Sand Key)
Guam
Antigua
Guam
Antigua
Guam
FL (Key West)
FL (Sand Key)
Peneroplis (outgroup)
AU (Lizard Is.)
AU (Pidgeon Pt.)
Guam
AU (Pidgeon Pt.)
Guam
AU (Pidgeon Pt.)
Puerto Rico
AU (Pidgeon Pt.)
Puerto Rico
100
86
93
86
89
91
93
80

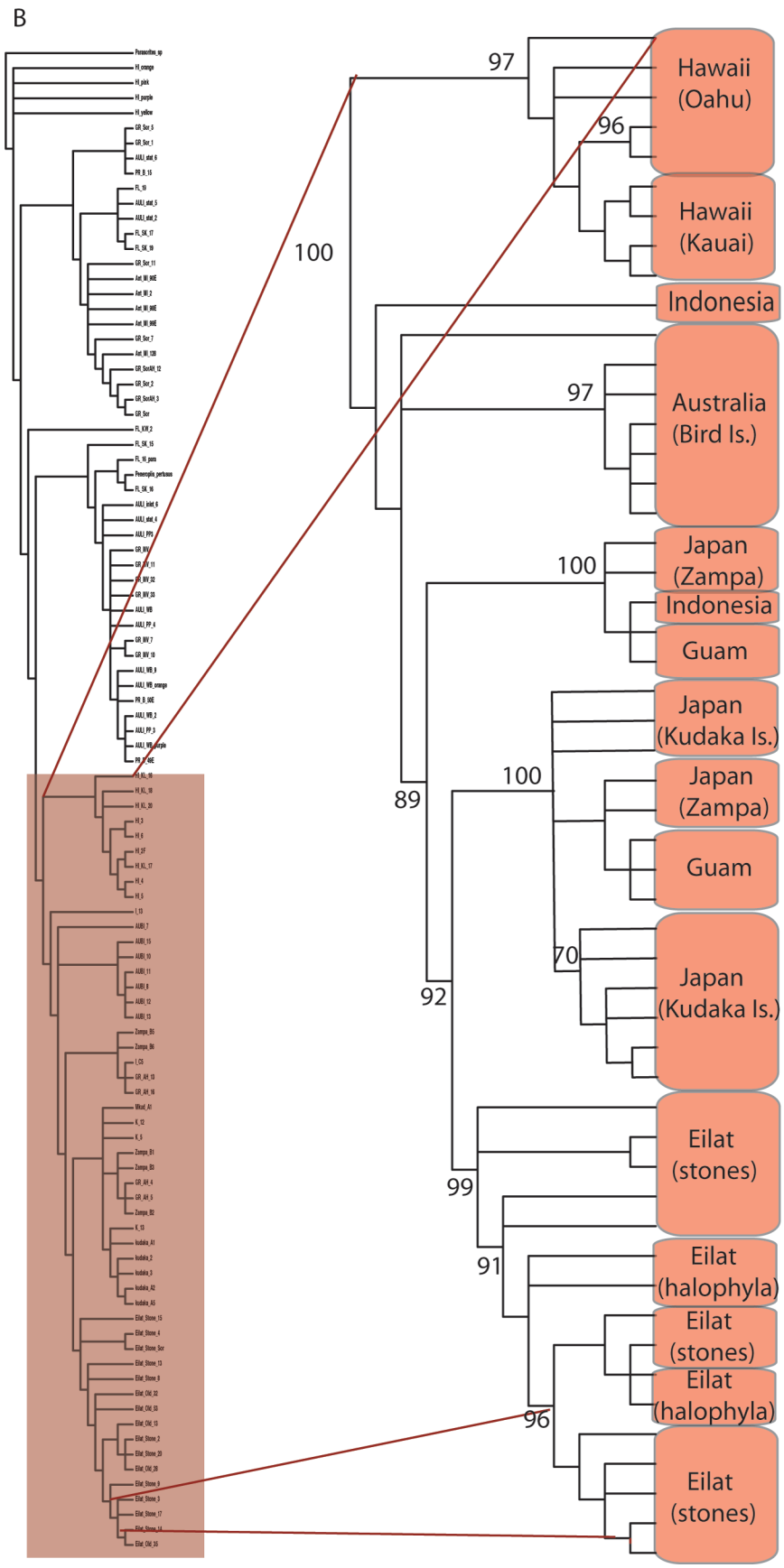
B
97
96
100
Hawaii (Oahu)
Hawaii (Kauai)
Indonesia
97
Australia (Bird Is.)
100
Japan (Zampa)
Indonesia
Guam
Japan (Kudaka Is.)
100
89
Japan (Zampa)
Guam
70
Japan (Kudaka Is.)
92
Eilat (stones)
99
91
Eilat (halophyla)
Eilat (stones)
Eilat (halophyla)
96
Eilat (stones)

minimum length trees of 4477 steps (Appendix B). As in the ssu rDNA analysis, two major clades were recovered. One major clade containing the *Marginopora* and *Sorites* genera is further divided such that *Sorites* populations from Antigua group together in a well-supported clade, while Guam, Sand Key (FL), as well as some of the Puerto Rican and Key West (FL) specimens, group together in a well supported (jac =1 00) clade. Another division within the larger *Sorites / Marginopora* clade groups *Sorite*s specimens from Key West (FL), Key Largo (FL), and Puerto Rico with *Marginopora* populations collected from Australia and Guam (jac = 100).

The second major division among the soritines consists of a well-supported (jac= 100) Hawaiian *Marginopora* clade as sister to the clade containing all *Amphisorus* populations. This placement renders the genus *Marginopora* paraphyletic. The well supported (jac = 100) *Amphisorus* clade is divided into five major groups consisting of the following populations: 1) Okinawa (JP) and Guam,2) Australia, 3) Hawaii, 4) Kudaka- Island (JP), and 5) Eilat (IS). The two Indonesian specimens included in the analysis placed separately within the *Amphisorus* group, one placed inside the Australian/Hawaiian clade as sister to the Hawaiian specimens and the other as sister to the *Amphisorus* specimens collected in Kudaka Island, Japan.

The phylogenetic analyses conducted in this work reveal biogeographic partitioning at both the generic and population levels in terms of morphological types. Despite the polyphyly of *Sorites* and *Marginopora* populations, only the *Sorites* morphological type was recovered from Atlantic

populations. All morphological variants (spanning all genera), however, were recovered from Pacific sampling locations.

At the population level the analyses revealed discreet morphologies within the genus *Amphisorus* in Indo-Pacific populations. Distinct *Amphisorus* morphologies were recovered which correspond to five clades (Guam\Okinawa, Kudaka Island, Australia, Hawaii, and Red Sea). Interestingly, this pattern distinguishes the Okinawa (Zampa Point) population as separate from the neighboring Kudaka Island population.

Figure 23. Parsimony Tree (4431 steps): Generated from directly optimizing dynamic homology characters using POY. Partial large and small subunit ribosomal DNA as well as morphological data were included in this analysis (2687 characters) for 114 taxa. Jackknife support values > 50 are indicated at the nodes. A) Includes *Marginopora* (blue) and *Sorites* (green) clades; B) Depicts *Amphisorus* (red) clades.

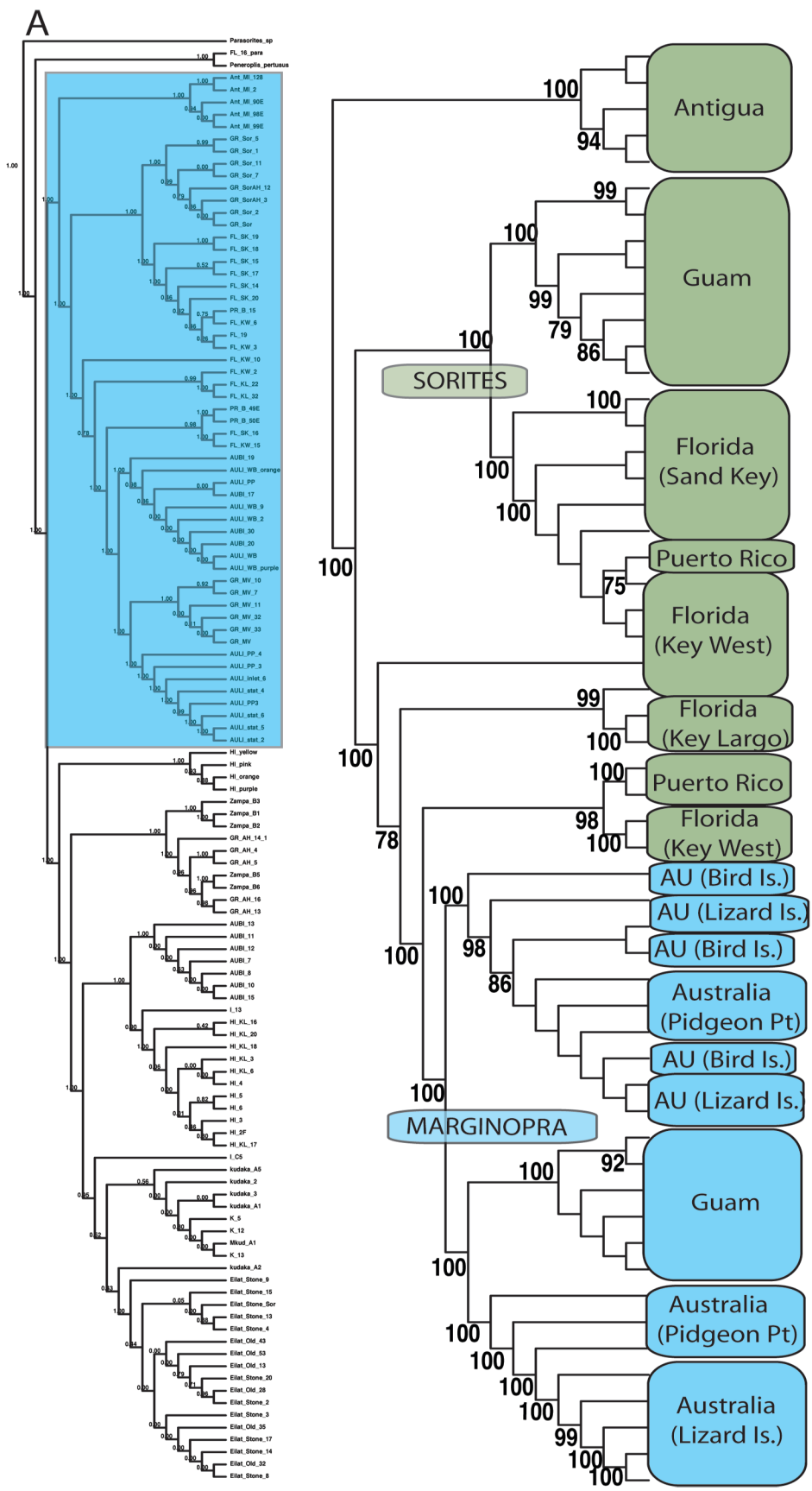
A
Parasorites_sp
FL_16_para
Peneroplis_pertusus
Ant_MI_128
Ant_MI_2
Ant_MI_90E
Ant_MI_98E
Ant_MI_99E
GR_Sor_5
GR_Sor_1
GR_Sor_11
GR_Sor_7
GR_SorAH_12
GR_SorAH_3
GR_Sor_2
GR_Sor
FL_SK_19
FL_SK_18
FL_SK_15
FL_SK_17
FL_SK_14
FL_SK_20
PR_B_15
FL_KW_6
FL_19
FL_KW_3
FL_KW_10
FL_KW_2
FL_KL_22
FL_KL_32
PR_B_49E
PR_B_50E
FL_SK_16
FL_KW_15
AUBI_19
AUU_WB_orange
AUU_PP
AUBI_17
AUU_WB_9
AUU_WB_2
AUBI_30
AUBI_20
AUU_WB
AUU_WB_purple
GR_MV_10
GR_MV_7
GR_MV_11
GR_MV_32
GR_MV_33
GR_MV
AUU_PP_4
AUU_PP_3
AUU_inlet_6
AUU_stat_4
AUU_PP3
AUU_stat_6
AUU_stat_5
AUU_stat_2
HI_yellow
HI_pink
HI_orange
HI_purple
Zampa_B3
Zampa_B1
Zampa_B2
GR_AH_14_1
GR_AH_4
GR_AH_5
Zampa_B5
Zampa_B6
GR_AH_16
GR_AH_13
AUBI_13
AUBI_11
AUBI_12
AUBI_7
AUBI_8
AUBI_10
AUBI_15
I_13
HI_KL_16
HI_KL_20
HI_KL_18
HI_KL_3
HI_KL_6
HI_4
HI_5
HI_6
HI_3
HI_2F
HI_KL_17
I_C5
kudaka_A5
kudaka_2
kudaka_3
kudaka_A1
K_5
K_12
Mkud_A1
K_13
kudaka_A2
Eilat_Stone_9
Eilat_Stone_15
Eilat_Stone_Sor
Eilat_Stone_13
Eilat_Stone_4
Eilat_Old_43
Eilat_Old_53
Eilat_Old_13
Eilat_Stone_20
Eilat_Old_28
Eilat_Stone_2
Eilat_Stone_3
Eilat_Old_35
Eilat_Stone_17
Eilat_Stone_14
Eilat_Old_32
Eilat_Stone_8
Antigua
Guam
SORITES
Florida (Sand Key)
Puerto Rico
Florida (Key West)
Florida (Key Largo)
Puerto Rico
Florida (Key West)
AU (Bird Is.)
AU (Lizard Is.)
AU (Bird Is.)
Australia (Pidgeon Pt)
AU (Bird Is.)
AU (Lizard Is.)
MARGINOPRA
Guam
Australia (Pidgeon Pt)
Australia (Lizard Is.)

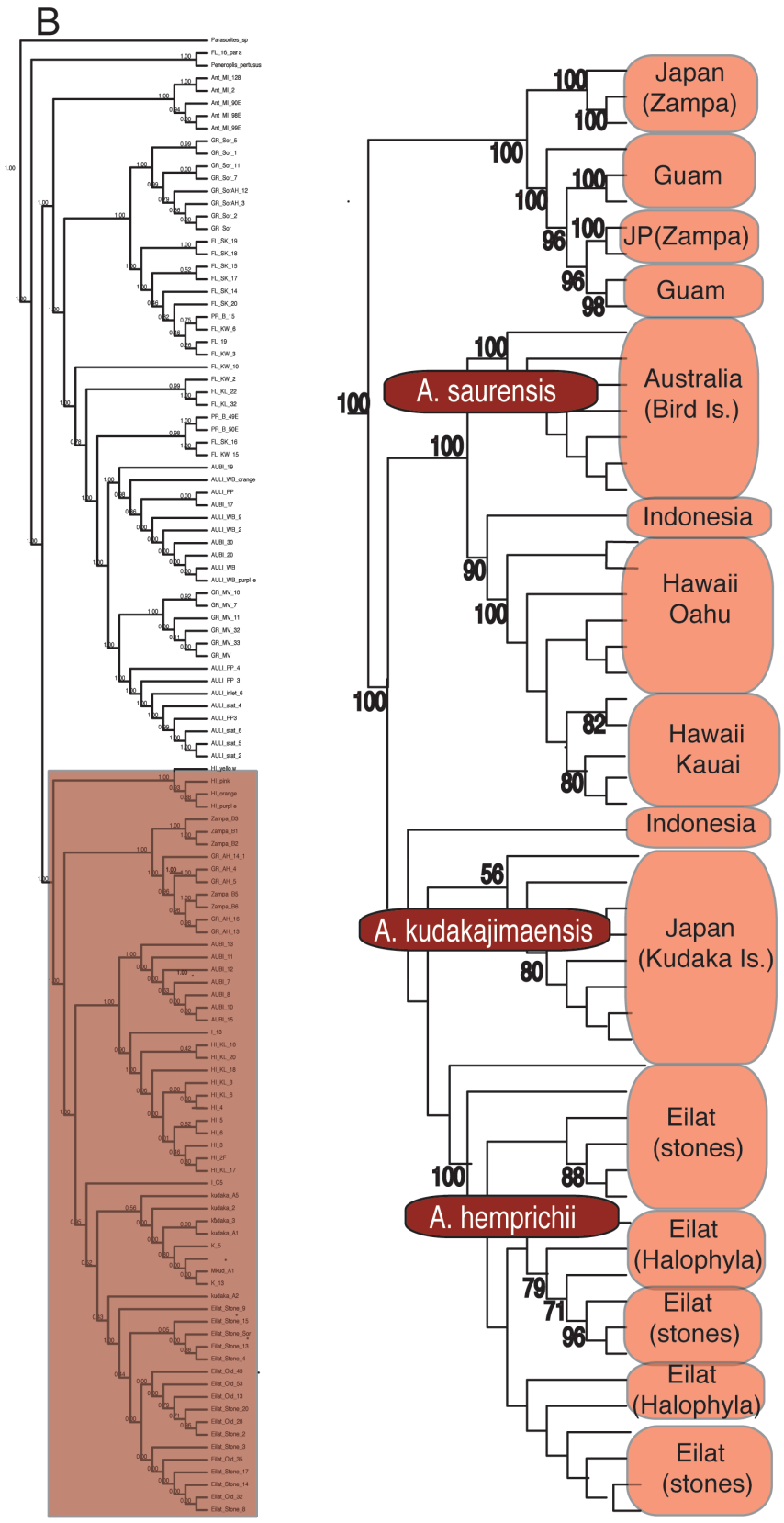
B
Japan (Zampa)
Guam
JP(Zampa)
Guam
A. saurensis
Australia (Bird Is.)
Indonesia
Hawaii Oahu
Hawaii Kauai
Indonesia
A. kudakajimaensis
Japan (Kudaka Is.)
Eilat (stones)
A. hemprichii
Eilat (Halophyla)
Eilat (stones)
Eilat (Halophyla)
Eilat (stones)

3.9 Discussion

This work presents the first analyses of soritine foraminifera to include both nucleotide and morphological characters. Previously, the most comprehensive analysis of this foraminiferal subfamily to include over 1000 base pairs was that presented in Garcia-Cuetos et al. (2005) wherein small subunit rDNA genes were analyzed for 33 members of the soritinae. This study demonstrates that analysis of the ssu rDNA variable region alone was not sufficient to resolving soritine relationships and was unable to differentiate outgroup taxa (see Figure 22). The inclusion of additional ssu rDNA data, as well as that of the large subunit rDNA variable region sequences and morphological characters to the analyses improved phylogenetic resolution and to contribute to a better understanding of the diversity contained within this subfamily.

The results obtained in this study concur with Holzmann et al. (2001) in the placement of the genus *Marginopora* within the clade containing the genus *Sorites*. This result may seem counterintuitive to the apparent trend toward increased complexity of test architecture, whereby *Sorites* has the least complex and *Marginopora* the most complex as depicted in Gudmundsson (1994) and Richardson (2001). This placement, however, remained well supported (jac = 100) after the inclusion of morphological characters. Alternately the placement of a separate Hawaiian *Marginopora* clade outside the *Sorites / Marginopora* clade indicates the need for further investigation (i.e. development of additional molecular markers and increased taxonomic sampling) of this genus.

A second important result of these analyses is that previously unrecognized patterns of diversity were revealed within the genus *Amphisorus*. Three species that correspond to distinctive phenotypes are currently recognized within the genus: *Amphisorus hemprichii* with an annular canal having a constant diameter throughout chamber whorls, (*Amphisorus*) *kudakajimaensis* with an irregularly partitioned annular canal that is expanded in outer whorls, and *Amphisorus saurensis* whith a large diameter (>15 mm) and large irregularly shaped medial apertures. Each of these taxa is recovered molecularly as a separate clade. Moreover, even specimens collected from different substrates (phytal vs. stone) and depths (1 m vs.16 m) in the Red Sea still grouped as a single *Amphisorus hemprichii* clade.

In addition to the named species, a well-supported clade was recovered that contained the Hawaiian (Oahu and Kauai) morphologically indistinguishable *Amphisorus* specimens. Although the Hawaiian specimens are morphologically similar to the *A. hemprichii* except in that Hawaiian populations possess a double row of annular canals rather than a single canal and exhibit truncated septular heights less than a quarter of the total chamber height, molecularly they consistently form a sister clade to *A. saurensis*. Distinct morphological differences between *A. saurensis* and the Hawaiian populations including the double row of annular canals and exhibiting elongate rather than irregularly shaped apertures, however, indicate these populations may constitute a distinct Hawaiian species.

The populations collected off of Zampa Point, Okinawa, Japan and from Ritidian Bay, Guam, were also found to form a well-supported clade,

notwithstanding their morphological differences (e.g. the presence lipped apertures and lower apertural density in the Guam population). It is notable that the support for this Guam and Okinawan clade was high (jac = 100) despite large (20-50 nt) insertions in the lsu rDNA of the Okinawan specimens. The conflation of the Okinawan population with the Guam population rather than its nearest geographic neighbor (Kudaka Island population) was unexpected and merits further fine-scale biogeographic investigation. The variable placement of the two Indonesian *Amphisorus* specimens is likely a product of missing data as only partial sequences were recovered from them due to poor specimen preservation.

In contrast to the assumption often made that South East Asian soritine populations with "*Amphisorus*-like" morphologies are *A. kudkajimaensis* (e.g. Holzmann et al., 2001), the analyses conducted in this study indicate that *A. kudakajimaensis* is distinct both morphologically and molecularly from other Pacific *Amphisorus* populations, even those collected from nearby sites (i.e. Zampa beach, Okinawa, Japan). *A. kudakajimaensis* Moreover, these analyses indicate that *A. hemprichii* may have a range limited to the Red Sea and may not be the globally distributed species encompassing all other observed *Amphisoru*s-like morphologies as was previously believed (see Loblich and Tappan, 1987). The previously unrecognized diversity in the genus *Amphisorus* both molecularly and morphologically that was revealed in these analyses indicates the need for possible taxonomic revision of this genus.

CHAPTER 4

Molecular Identities of Endosymbiotic Dinoflagellates Cultured from Soritine Foraminifera

4.1 Diversity of *Symbiodinium*

When first proposed, the type species *Symbiodinium microadriaticum* (Freudenthal, 1962), isolated from the jellyfish host *Cassiopeia xamachana*, represented the total diversity within the genus recognized at that time. Despite the prior observations of Doyle and Doyle (1940) who noted variability among zooxanthellae under experimental conditions, the idea of a single pandemic *Symbiodinium* species was supported initially by morphological observations that interpreted *Symbiodinium microadriaticum* to be structurally identical to the zooxanthellae found in both sea amenones and tridacnid clams (Kevin et al., 1969; Taylor, 1968). The uniform appearance of these dinoflagellates *in symbio* as yellow-brown cocciod cells 5-15 μm in diameter, solidified the perception that *Symbiodinium microadriaticum*, alternately referred to as *Gymnodinium microadriaticum* (Kawaguti, 1944), was pandemic among invertebrate host species distributed through the Caribbean, Indo-Pacific and Mediterranean (Taylor, 1974).

This paradigm of uniformity among zooxanthellae, however, was soon challenged by significant variation noted in characteristics among *Symbiodinium* isolates including isoenzyme profiles (Schoenberg and Trench, 1980a, b, c), karyotypes (Blank and Trench, 1985a; Trench and Blank, 1987), plastid number (Blank and Trench 1985b), and mycosporine-like amino acid production (Banaszak et al., 2000). To date, detailed observation of *Symbiodinium* cultured from a range of host taxa have produced 11 “named" species. Five of the named *Symbiodinum* taxa are formally described: *S. microadriaticum* (Freudenthal,

1962), *S. pilosum* (Trench and Blank, 1987), *S. kawagutii* (Trench and Blank, 1987), *S. goreaui* (Trench and Blank, 1987), and *S.* (*Gymnodinium*) *linucheae* (Trench and Thinh, 1995). The other six *Symbiodinium* species lack formal descriptions: *S. californium* (Banaszak et al., 1993), *S. corculorum, S. meadrinae*, *S. pulchrorum*, *S. bermudense*, *S. cariborum*, and *S. muscatinei* (LaJeunesse and Trench, 2000, and LaJeunesse, 2001). A detailed discussion of the taxonomic validity of these species names is found in Trench (2000).

In addition to described species, molecular analyses have revealed unexpectedly high diversity among *Symbiodinium* taxa (Baker, 2003; Baker and Rowan, 1997; Carlos et al., 1999; LaJeunesse and Trench, 2000; Pochon et al., 2001; Pochon et al., 2004; Rowan and Powers, 1991; Santos et al., 2002; Takabayashi et al., 2004). Using restriction fragment length polymorphism (RFLP) data and sequences derived from nuclear small subunit ribosomal DNA (ssu rDNA), Rowan and Powers (1991) divided the genus *Symbiodinium* into three major clades (A, B, and C). Currently molecular rDNA phylogenies now recognize eight clades of *Symbiodinium* (A – H) (Pochon and Pawlowski, 2006). The clade D was recognized in the Palauan sponge (*Haliclona koremella*) by Carlos et al. (1999). Clades E and F were discovered by LaJeunesse and Trench (2000) and LaJeunesse (2001), respectively. The final two clades, G (Pochon et al., 2001) and H (Pochon, 2006), were identified using *Symbiodinium* sequences recovered from foraminiferal hosts. These *Symbiodinium* clades also have been recovered in phylogenies inferred from both plastid (cpDNA) (Santos et al., 2002) and mitochondrial (Takabayashi et al., 2004) genes. The schematic

diagram in Figure 24, drawn from Coffroth and Santos (2005), provides a general consensus of the relationships among *Symbiodinium* clades. The positioning of clades B, C, F and H in Figure 24, however, is variable depending on the method of analysis and genetic markers used (Pochon and Pawlowski, 2006; Coffroth and Santos, 2005).

Within any given clade, the detection of additional genetic diversity has fostered a departure from Linnean classification in favor of recognizing *Symbiodinium* subclade "types" (LaJeunesse, 2001; Santos, 2001; van Oppen et al., 2001). These types are based on unique sequence patterns in the ribosomal internal transcribed spacer (ITS) regions (LaJeunesse, 2001, 2002) or differences in the electrophoretic mobility of ITS amplicons subjected to denaturing gradient gel electrophoresis (DGGE) (LaJeunesse, 2003). High levels of diversity noted in studies employing ITS typing support the possibility that hundreds of *Symbiodinium* types currently exist, although the number of *Symbiodinium* types recovered varies among clades (e.g. 22 types in Clade B vs. 76 types in Clade A) (LaJeunesse, 2001).

The distribution of *Symbiodinium* "types" is non-random with respect to host taxa and is the result of a complex set of interactions and varying degrees of specificity between the symbiotic partners (Coffroth and Santos, 2005). To show the range of host participants in endosymbiotic association with *Symbiodinium* Table 7, from Trench (1997) and (Lobban et al., 2002), provides a partial list of the invertebrate and protistan host taxa.

Figure 24. Generalized consensus schematic depicting the phylogenetic relationships among the major clades of *Symbiodinium* inferred from 28S ribosomal DNA sequences from Coffroth and Santos (2005)

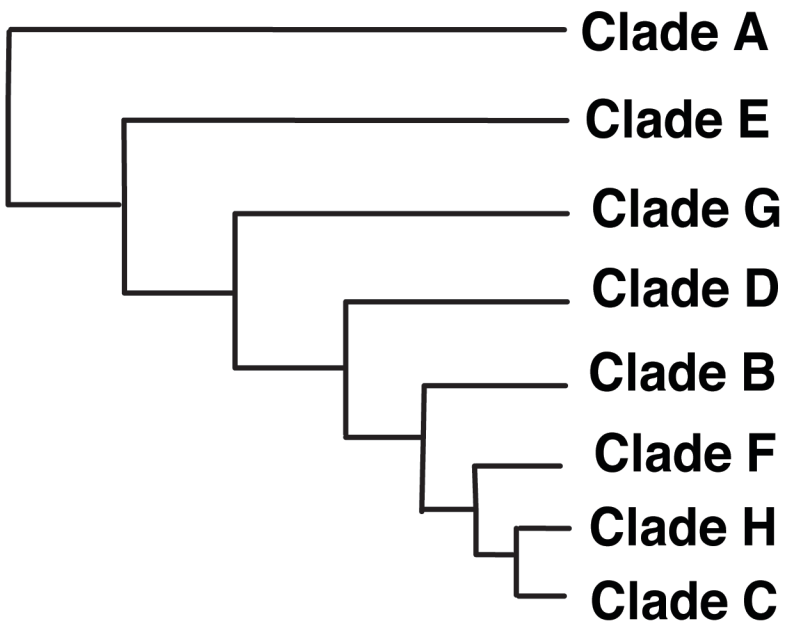
Clade A
Clade E
Clade G
Clade D
Clade B
Clade F
Clade H
Clade C

Table 7. *Symbiodinium* & host taxa (Trench, 1997 & Lobban, et al., 2002)

***Symbiodinium* taxon**	**Host taxon**
Symbiodinium sp.	*Amphisorus hemprichii* (Foraminifera)
Symbiodinium sp.	*Amphisorus kudakaejimensis* (Foraminifera)
Symbiodinium sp.	*Marginopora vertebralis* (Foraminifera)
Symbiodinium sp.	*Sorites orbiculus* (Foraminifera)
Symbiodinium sp.	*Oculina diffusa* (Scleractinia)
Symbiodinium sp.	*Maristentor dinoferus* (Spiritrichea)
Symbiodinium sp.	*Millepora dichotoma* (Hydrozoa)
S. microadriaticum	*Cassiopoeia xamachana* (Rhizostomae)
S. goreauii	*Ragactis ludida* (Actiniaria)
S. kawagutii	*Montipora verrucosa* (Scleractinia)
S. pilosum	*Zoanthus sociatus* (Zoanthidae)
S. corculorum	*Corculum cardissa* (Bivalvia)
S. bermudense	*Aiptasia pulchella* (Actiniaria)
S. californium	*Anthopleura elegantissima* (Acitiniaria)

Initially, isozyme data suggested that each *Symbiodinium* type tracked a particular host taxon across its geographic range (Schoenberg and Trench, 1980 a, b, c). Later analyses of molecular sequence data, however, revealed that while some *Symbiodinium* lineages are host specific (e.g. type C21 with *Montipora* spp.), others are found in multiple host species (e.g. types C1, C2,

and C3 with invertebrate hosts from multiple phyla (LaJeunesse et al., 2003)). Conversely, multiple *Symbiodinium* types have been recovered from a single host (LaJeunesse, 2002). Moreover, infectivity experiments have shown that the *Symbiodinium* types recovered are a subset of the total number of types capable of infecting a given host and that this subset can vary under different environmental conditions (LaJeunesse and Trench, 2000; Coffroth et al., 2001). With respect to foraminiferal hosts, Pochon et al. (2001, 2004, 2006) sequenced their symbionts rDNA belonging to clades C, D, F, G and H. Only the clade H *Symbiodinium*, however, has been recovered exclusively from foraminiferal host taxa (Pochon et al., 2006).

Symbiodinum clades also exhibit variable biogeographic patterns of distribution. The relative frequency of some *Symbiodinium* clades has been shown to shift along latitudinal gradients (e.g. clades A and B are recovered more frequently from higher latitudes, while clade C is more commonly found at lower latitudes closer to the equator (reviewed in Baker, 2003)). Differential clade frequency also has been demonstrated between ocean basins wherein clade B dominates the Caribbean while clade C occurs with greater frequency in the Indo-Pacific (Rowan and Powers, 1991). These broad biogeograhic patterns, however, are underlain by smaller scale patterns in the distribution of *Symbiodinium* that correlate to environmental parameters such as irradiance and temperature (Rowan and Knowlton, 1995). For example, an increase has been reported in recent surveys in the frequency of "thermally tolerant" clade D

Symbiodinium detected in hosts from Indo-Pacific reefs damaged by bleaching episodes (Baker et al., 2004; Rowan, 2004).

The biogeographic distribution of soritine symbionts was examined by Pochon et al. (2004) using restriction fragment length polymorphism (RFLP) data collected from Carribbean and Eastern Pacific populations. Pochon et al. (2004) showed a biogeographic break between the two ocean basins in *Symbiodinium* clade frequencies and detected the presence of foraminifera specific clade (H), which dominates Caribbean soritine symbionts. The existence of a *Symbiodinium* clade that associates specifically with soritine hosts suggests the participation of foraminfera in the evolution of zooxanthellae (Pochon and Pawlowski, 2006).

Although considerable molecular (rDNA and cpDNA) diversity has been reported for the *Symbiodinium* types harbored within soritine foraminifera (Pochon et al., 2004; Pochon and Pawlowski, 2006), none of these symbionts have been cultured or characterized morphologically or physiologically. This may be in part due to the challenges posed by isolating and culturing *Symbiodinium* from host tissue. For example, it has been reported that *Symbiodinium* cultures exhibit phenotypic plasticity in cell and plastid size based on their nutrient exposure and irradiance *in hospite* (Rowan and Powers, 1991, and LaJeunesse, 2001). Moreover, it has been shown that culturing may select rare *Symbiodinium* types over types that are dominant *in vivo* (Santos et al., 2001). Nevertheless, isolating and characterizing the *Symbiodinium* types

inhabiting foraminifera remains a critical component to further understanding patterns of diversity indicated by molecular studies.

4.2 Specimen Collection

Symbiodinium specimens analyzed in this research were obtained from ten different culture lines maintained at the Marine Microbial Ecology Laboratory at CCNY, six culture lines obtained from the Provasoli-Guillard National Center for the Culture of Marine Protists (CCMP), and sequences directly amplified from ten foraminiferal hosts species. Eight of the culture lines used from the CCNY collection were comprised of isolates from soritine foraminifera (*Amphisorus*, *Marginopora*, and *Sorites*) collected from selected Caribbean, Pacific, and Red Sea near-shore reef habitats using SCUBA at ≤ 25 meters depth from sea grass beds or sandy substrates located adjacent to coral reefs. Table 8 provides specimen collection information. Two CCNY isolates from upside-down jellyfish—*Cassiopeia andromeda* (Eilat, Israel) and *Cassiopeia frondosa* (Key West, Florida)—were also analyzed. Additional sequence data included in analyses was downloaded from NCBI GenBank.

Table 8. *Symbiodinium* taxa analyzed

Symbiodinium	**Host genus**	**Source**	**Locality**
Ingroup:			
S. goreaui	*Discosoma*	CCMP2466	Jamaica
S. kawagutii	*Montipora*	CCMP2468	Hawaii (US)
S. microadriaticum	*Cassiopeia*	CCMP2458	Eilat (IS)
S. microadriaticum	*Cassiopeia*	CCMP2464	Florida (US)
S. pilosum	*Zoanthus*	CCMP2461	Jamaica
Symbodinium sp.	*Aiptasia*	CCMP 2460	Florida (US)
Symbodinium sp.	*Marginopora*	CCNY Culture	Guam (US)
Symbodinium sp.	*Amphisorus*	CCNY Culture	Eilat (IS)
Symbodinium sp.	*Cassiopeia*	CCNY Culture	Eilat (IS)
Symbodinium sp.	*Cassiopeia*	CCNY Culture	Florida (US)
Symbodinium sp.	*Marginopora*	CCNY Culture	Polynesia
Symbodinium sp.	*Sorites*	CCNY Culture	Florida (US)
Symbodinium sp.	*Amphisorus*	CCNY Culture	Hawaii (US)
Symbodinium sp.	*Amphisorus*	CCNY Culture	GBR (Australia)
Symbodinium sp.	*Amphisorus*	CCNY Culture	Okinawa (Japan)
Symbodinium sp.	*Marginopora*	DirectAmp.	Hawaii (US)
Symbodinium sp.	*Amphisorus*	DirectAmp.	GBR (Australia)
Symbodinium sp.	*Amphisorus*	DirectAmp.	Okinawa (Japan)
Symbodinium sp.	*Sorites*	DirectAmp.	Florida (US)
Symbodinium sp.	*Amphisorus*	DirectAmp.	Eilat (IS)
Symbodinium sp.	*Amphisorus*	DirectAmp.	Hawaii (US)
Symbodinium sp.	*Sorites*	DirectAmp.	Puerto Rico (US)
Symbodinium sp.	*Sorites*	DirectAmp.	Antigua
Symbodinium sp.	*Amphisorus*	DirectAmp.	Okinawa (Japan)
Symbodinium sp.	*Marginopora*	DirectAmp.	Guam (US)
Symbodinium sp.	*Sorites*	DirectAmp.	Guam (US)
Symbodinium sp.	*Amphisorus*	DirectAmp.	Guam (US)
Outgroup:			
Gymnodinium Simplex	*NA*	GenBank: DQ388466,	AY289695, AJ872114
Amphidinium operculatum	*NA*	GenBank: EF036578,	Aj582640
Gonyaulax polyedra	*NA*	GenBank: AJ415511,	DQ264867
Heterocapsa triquetra	*NA*	GenBank: AF022198,	AF130033, EF036578
Protoceratium reticulatum	*NA*	GenBank: DQ217789,	AF206711, AF260386

4.3 Methods of Isolation and Culture Conditions

Isolation of *Symbiodinium* algal cells from their soritine hosts required vigorous brushing and washing of the foraminiferal tests to remove surface contaminants. The cleaning of foraminfera was performed under a dissecting microscope with alcohol sterilized #00 sable brushes. During this procedure the foraminiferal specimens remained submerged in sterilized seawater in the wells of sterilized Pyrex® 9-hole spot plates. After transferring the symbiotic foraminfera through multiple serial washes, they then were aseptically divided into pieces whereby one piece was used for direct amplification of *Symbiodinium* sequences, one part was saved for morphological identification of the host in the SEM, and the remaining portion was used for isolation of the symbionts. This last piece was transferred aseptically into a fresh sterile well of a 9-hole spot plate containing 1mM Na EDTA in seawater. It was transferred every five minutes from one well to the next until the specimen was completely decalcified.

Following decalcification, the endosymbionts bound within intact symbiosome membranes were removed from the foraminferal protoplasm using sterilized glass needles. With the aid of sterile capillary pipettes, the symbionts were picked and transferred to test tubes containing F/2 medium. After incubation in the light (18hL/6hD) for 7-10 days, the isolates were aseptically streaked on F/2 agar Petri plates. After another week of growth, single axenic cloned colonies of *Symbiodinium* were transferred back into sterile liquid F/2 media for culture.

Because culturing *Symbiodinium* can alter the phenotype of these dinoflagellates and suppress the *in symbio* dominant algal type (LaJeunesse, 2001, Santos et al., 2001), protocols were designed to confirm the identity the CCNY cultures by comparison with CCMP cultures and symbiont phylotypes directly amplified from each host. To mitigate the potential effect of culture conditions on the observed morphology of *Symbiodinium* cells, cultures of previously characterized CCMP isolates maintained were reestablished at CCNY under conditions identical to those of the uncharacterized *Symbiodinium* cultures. This protocol enabled all isolates to be observed under identical conditions. To address the problem of rare or non-dominant *Symiodinium* strains being favored in culture, the molecular identity of each cultured strain was compared with sequences directly amplified from each holobiont (host/symbiont complex). This approach recognized correspondence between sequences between cultured and directly amplified as evidence corroborating each isolates identity; whereas the absence of such correspondence indicated the need for further measures to explore the *Symbiodinium* diversity harbored within a given host population.

4.4 Methods of Plastid Examination

Ten-day (log-phase) cultures and 30-day (stationary phase) cultures grown in medium F/2 were used to study the gross architecture of the plastids of each isolate. Differences in plastid appearance were observed under both an epifluorescent microscope with an FITC exciter filter using the auto-

fluorescence of these organelles and a confocal microscope at 40X with a 1.4 NA oil objective. The scan zoom was 4-8x, and argon laser power varied from 2-8%. Excitation was at 480 nm, and the barrier filter was a long pass at 585 nm. The pinhole setting was generally ~66 µm. Gain also varied with the autofluorescence and excitation power used for each individual strain studied. The numbers of individual cells studied in detail depended on the variance observed in each strain, but the minimum number of cells scanned was ten.

4.5 Methods of Molecular Examination

To prepare *Symbiodinium* cultures for molecular examination, 1ml of media and cells was removed from a culture in log-phase growth. The removed samples were then centrifuged for 5 min at 10,000 rpm until a visible pellet of cells formed. The supernatant was then removed and replaced with sterile seawater. This process was repeated 5 times to wash and concentrate the cells. After completing the last iteration of washing, extraction buffer was added to the *Symbiodinium* pellet to begin the process of DNA extraction.

Qiagen DNeasy® Plant kits were used to extract symbiont DNA from each *Symbiodinium* pellet and from each foraminiferal specimen. The extracted DNA was then subjected to PCR amplification using 2 µl of template and 0.5 µl of each 10 µM primer in 25 µl reaction tubes of PuReTaq Ready-To-Go™ PCR Beads (GE Healthcare). Although the PCR profile varied depending on the primer set used and the population being amplified, in general the conditions that proved the most successful in amplifying the dinoflagellate template

required 90 seconds at 94°C, followed by at least 35 cycles of 94°C for 45 seconds, 52°C annealing for 45 seconds and a 72°C extension for 120 seconds, and a final extension of 72°C for seven minutes. Successful amplification products were sequenced in both directions with 1 µl of ABI BigDye™ Terminator (v1.1 or v3.1), 1 µl of ABI BigDye™ Extender Buffer, 1 µl of 1 µM primer, and 3 µl of cleaned PCR template. Sequences were electrophoresed in ABI PRISM® 3730 sequencer (Applied Biosystems). PCR amplification and cycle sequence products were cleaned using the solutions AMPure™ and CleanSeq™ (Agencourt Bioscience Corporation), respectively.

4.6 Observations on Gross Plastid Morphology

While in the symbiotic condition, the general morphology of taxa within the genus *Symbiodinium* is characterized by coccoid cells possessing continuous cell walls that are underlain by a series of membranes (Van den Hoek et al., 1995). In contrast, cultured *Symbiodinium* exhibit a gymnodinoid motile stage with the hypocone being somewhat smaller than or of equal size to the epicone, a longitudinal flagellum without flagellar hairs, and a ribbon-like transverse flagellum (Fensome et al., 1993). One to several plastids without invasive thylakoids and a typically "mesokaryotic" dinoflagellate nucleus also have been observed (Fensome et al., 1993).

As most features of *Symbiodinium* taxa are obscured in the symbiotic state, morphological characterization of these algal cells requires isolation from host taxa and growth in axenic culture. However, culturing *Symbiodinium* can both

alter the expressed phenotype of these dinoflagellates and suppress the dominant algal type detected molecularly *in symbio* (LaJeunesse, 2001, Santos et al., 2001). This challenge requires finding characters possessing variation that can be observed without requiring the gymnodinoid life phase. To this end, this study provides an initial investigation in using plastid gross morphology as a potential character that may bring to bear information useful to the understanding of diversity contained within this genus.

Dinoflagellate plastids are bound by three membranes and are believed to be the product of tertiary endosymbiosis established by the engulfment of an alga containing a secondary plastid (Bhattacharya et al., 2004). Like a majority of dinoflagellates, *Symbiodinium* taxa have plastids that are surrounded by three membranes and contain chlorophylls *a*, *c*, and peridinin as the major photosynthetic pigments (Van den Hoek et al., 1995). Under UV excitation, the plastids auto-fluoresce to reveal their ultra-structural architecture.

The initial description of the plastid of the type species, *Symbiodinium microadriaticum*, reported the presence of multiple plastids that appeared as "irregular to disc-shaped bodies located on the periphery of the cell" (Freudenthal, 1962). Freudenthal's description of plastid morphology did not consider the previous work of Doyle and Doye (1940) that described a reticulate plastid structure. Fluorescent observation of plastids in cultured CCNY *Symbiodinium*, however, show single plastids occupying a large surface area beneath the cell wall (amphiaema) of two general morphological types: petal-like and reticulate as depicted in Figure 25.

The petal-like plastid morphology was characteristic among the CCNY cultures isolated from Australian and Guam *Marginopora*, and Red Sea *Amphisorus* specimens (Figure 25A-C). Lee and colleagues also recognized petal-like architecture among CCNY *Symbiodinium* isolates from Hawaiian and Japanese *Amphisorus* specimens. Aside from minor variability noted among isolates, the general petal-like morphology consisted of plastids with a broad base and finger-like projections. Thus far, the observation of the petal-like plastid morphology has been restricted to *Symbiodnium* isolates from soritine foraminiferal hosts.

The reticulate plastids found in both the CCNY *Symbiodinium* cultured from *Cassiopeia* sp. and from the *S. microadriaticum* cultures (CCMP 2458 and 2464) appear as a thin reticulate network consisting of autofluorescent strips (Figure 25D). The CCNY culture from an Australian *Amphisorus* specimen also exhibited a reticulate plastid morphology, however, the plastid network was characterized by large open areas between thread-like projections (Figure 25F). The CCNY culture isolated from a Polynesian *Marginopora* specimen was observed to have a reticulate plastid morphology intermediate to those found in the *Cassiopeia* and *Amphisorus* isolates in terms of the density of connections within the plastid network (Figure 25E). Additional observations by Dr. John Lee and students indicate that the *S. kawagutii* symbiont (CCMP 2468) also is characterized by a thick "net-like" reticulate plastid, the *S. pilosum* culture (CCMP 2461) had thicker reticular elements such that the spaces between the elements were slot-like, and the CCMP 2466 had 2 ribbon-like plastids which

occupied a very small fraction (~10%) of the surface area of the cortex (Lee et al., in prep).

Figure 25. Auto-fluorescent micrographs (40x) showing the petal-like (A-C) and reticulate (D-F) gross plastid morphologies of *Symbiodinium* cultures isolated from the following hosts: (A) *Amphisorus hemprichii* , Eilat, IS., (B) *Marginopora vertebralis*, Guam, (C) *Marginopora vertebralis*, GBR, AU., (D) *Cassiopeia andromeda*, Eilat, IS., (E) *Marginopora vertebralis*, Polynesia, (F) *Amphisorus* sp. GBR, AU.

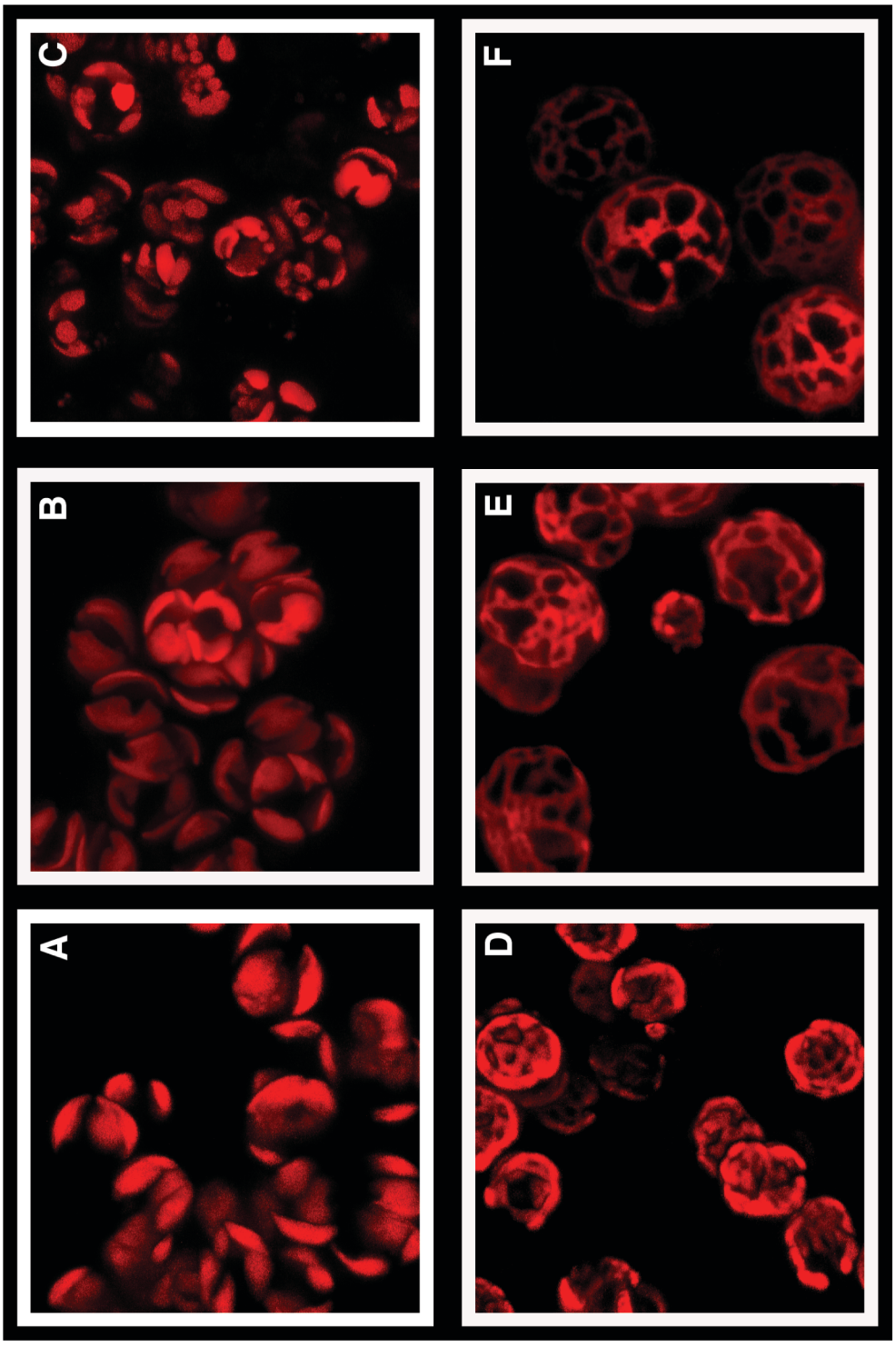
A
B
C
D
E
F

4.7 Exploration of Molecular Characters

The primary aim of this work was to contribute to the identification of *Symbiodinium* isolates cultured from soritine foraminiferal hosts by expanding the extant molecular data set and generating hypotheses of their phylogenetic relationships using all available molecular markers. *Symbiodinium* DNA sequences spanning 6822 nucleotides from ribosomal, plastid, and mitochondrial genes from eight CCNY cultures, six CCMP cultures, as well as 14 directly amplified from foraminiferal hosts were used in this effort. Sequence data from five dinoflagellate outgroup taxa also were included in analyses. Table 8, provided in section 4.2, contains the collection information and GenBank accession numbers, where applicable, for taxa included in this study.

The most commonly and often exclusively used molecular markers of *Symbiodinium* isolates are the nuclear encoded ribosomal (rDNA) genes (Coffroth and Santos, 2005; Stat et al., 2006). Generally, eukaryotic rDNA is organized in tandem repeated transcription units each containing small (18S), and large (5.8S, and 28S) subunit genes separated by internal transcribed spacers, ITS1 and ITS2. Both the large and small subunits are divided into domains of varying evolutionary rates due to secondary structure constraints (Hillis and Dixon, 1991).

In the genus *Symbiodinium*, molecular typing efforts have focused on the hyper-variable ITS2 region of rDNA to resolve within-clade relationships (e.g. LaJeunesse and Trench, 2000; LaJeunesse, 2001; Pochon et al., 2004). This

study included rDNA sequence data (2559 nt) that spans both conserved and variable domains of the large and small subunits as well as both ITS regions.

The small subunit rDNA primers of Rowan and Powers (1991) were used to amplify the 5' end of the 18S gene. The hyper-variable ITS regions of the small subunit, as well as part of the large subunit were recovered with the dinoflagellate-specific primer SDINO from Pawlowski et al. (2001) which is situated at the 3'-end of the small subunit gene, and the universal primer L0 situated approximately 800 nucleotides downstream from the 5'-end of the lsu rDNA. Additionally, the 28S primer pair of Wilcox (1998) was used to ensure that the complete D1 and D2 regions were sequenced from each culture.

The central paradigm for rDNA in metazoans is that of a single homologous sequence maintained through concerted evolution driven by unequal crossing over and gene conversion (Hillis and Dixon, 1991). In dinoflagellate taxa (e.g. *Alexandrium miniutm* and *Gymnodinium catenatum*), however, there is evidence of non-concerted sequence evolution in ribosomal genes where the rate of fixation is less than the rate of mutational divergence which results in rDNA heterogeneity (Zardoya et al., 1995). In *Symbiodinium*, heterogeneity within the rDNA tandem repeat has been recognized in recent studies (Toller et al., 2001 and Santos et al., 2003) and may contribute to an over-estimation of diversity within the genus (Stat et al., 2006). To avoid this potential bias, additional regions of the dinoflagellate genome (plastid and mitochondria) were sequenced and analyzed in addition to the ribosomal genes.

Table 9 provides a list of the primers used to amplify and sequence the genes used in this study.

Table 9 Sequence primers for *Symbiodinium* used in this work

Primer	Sequence 5'→3'	Reference
RDNA		
SS5Z(F)	GATCCTTCCGCAGGTTCACCTACGAAACC	Rowan & Powers (1991)
SDINO(F)	CGCTCCTACCGATTGAGTGA	Pawlowski et al., 2001
LSUFor	CCCGCTGAATTTAAGCATATAAGTAAGC	Wilcox, 1998
SS3Z(R)	AGCACTGCGTCAGTCCGAATAATTCACC	Rowan & Powers (1991)
L0(R)	GCTATCCTGAGRGAAACTTCG	Pawlowski et al., 2001
LSURev	GTTAGACTCCTTGGTCCGTGTTCAAGA	Wilcox, 1998
cp rDNA		
PSBA2F	ATGATGGWATAAGAGARCCGTAGC	Lee et al., in prep
PSBA2R	TCAGCACGATTMASATATCTGCCA	Lee et al., in prep
23SF	GACGGCTGTAACTATAACGG	Santos et al., 2002
23SR	CCATCGTATTGAACCCAGC	Santos et al., 2002
mtDNA		
DCOXF	AAAAATGTAATCATAAACGCTTAGG	Takabayashi et al., 2002
DCOXR	TGTTGAGCCACCTATAGTAAACATTA	Takabayashi et al., 2002

In contrast to other plant and algal plastids that generally contain a circular genome with between 130-250 genes, the dinoflagellate plastid genome is highly reduced and encodes for approximately 14 photosystem proteins and plastid ribosomal large and small subunits on minicircles (2-3 kbp) of double-stranded DNA (Zhang, et al., 2002, Bhattacharya et al., 2004). The minicircle

containing the photosystem II gene, *psbA* (1035 bp), encodes the D1 protein that acts to bind quinone and regulate photosynthetic flux (Takishita et al., 2003). In their study of the structure of the *psbA* minicircle Moore et al. (2003) found *psbA* to contain highly variable regions able to distinguish between closely related clade C *Symbiodinium* isolates from corals that were unable to be resolved using the D1/D2 region of the LSU rDNA gene. Based on these findings, *psbA* primers for this study were designed using sequences from a cDNA library of *Symbiodinium* cultured from the foraminifera *Amphisorus hemprichii* (Eilat, Israel). A detailed account of the protocols used to construct and screen the cDNA is provided in section 3.4, and Cevasco et al., (in review).

A second plastid gene used in this study was the 730 bp region of the plastid ribosomal large subunit (cp23S-rDNA). This gene was PCR amplified and sequenced from the *Symbiodinium* cultures using the primers of Santos et al. (2002). This region of the 23S gene includes the V1 domain that has been shown to be equivalent to the rDNA ITS regions in the amount of sequence variability (Coffroth and Santos, 2005). A recent comparison of *Symbiodinium* phylogenies recovered from foraminiferal hosts recovered largely congruent topologies among the phylogenetic trees generated using 28S rDNA and those constructed using 23S cpDNA sequences (Pochon and Pawlowski, 2006).

Mitochondrial *cox1* sequences also were included in the analyses. Cytochrome c oxidase (*cox1*) is the final protein complex in the electron transport chain and is composed of subunits encoded by both nuclear and mitochondrial genes. Although *cox1* is more conserved than either the rDNA

ITS or the cpDNA 23S V region, the *Symbiodinium* clades (A-F) were recovered in phylogenetic analyses of this mitochondrial gene (Takabayashi et al., 2004). Figure 26 modified from Pochon and Pawlowski (2006), Santos et al. (2002), and Takabayashi et al. (2004) shows generalized cladograms depicting the phylogenetic relationship among *Symbiodinium* clades recovered using different molecular markers (ITS rDNA, 23S cpDNA, and *cox1* mtDNA). Using the primer set of Takabayashi, et al. (2002) this study includes the first *cox1* sequences of *Symbiodinium* isolates recovered from foraminiferal hosts.

Figure 26. A schematic of the phylogenetic relationships among the major clades of Symbiodinium inferred from A: ribosomal (Pochon et al., 2004), B: plastid (Santos et al., 2002), and C: mitochondrial (Takabayashi et al., 2004) sequences.

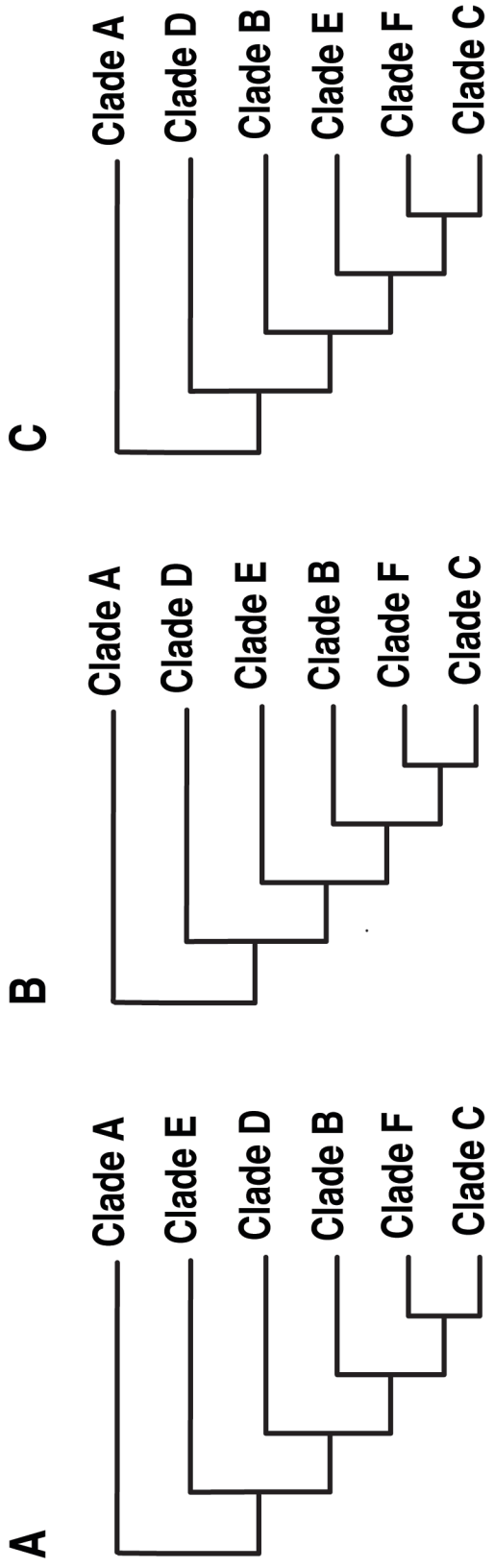
A
Clade A
Clade E
Clade D
Clade B
Clade F
Clade C
B
Clade A
Clade D
Clade E
Clade B
Clade F
Clade C
C
Clade A
Clade D
Clade B
Clade E
Clade F
Clade C

4.8 Phylogenetic analyses

Phylogenetic analyses were performed using the software packages, general search strategies, and support measures described in Chapter 3 section 5. One deviation from the described methodology is that the parsimony ratchet was not used in the analyses of *Symbiodinium* sequences as this heuristic tool is more effectively used with larger datasets (>50 taxa) (Goloboff, 1999).

4.9 Results

Nucleotide sequences recovered from four CCNY *Symbiodinium* cultures corresponded to either to directly amplified *Symbiodinium* sequences from host specimen or to CCMP cultures. The CCNY culture isolated from a *Marginopora* sp. specimen collected from Ritidian Bay (Guam) consistently grouped with *Symbiodinium* sequences directly amplified from the host taxa in both the separate analyses of mitochondrial, ribosomal, and plastid sequences, as well as the combined analysis employing the entire sequence data set. A similar pattern was evident between *Symbiodinium* sequences directly amplified from a Florida Keys *Sorites* sp. host, and its corresponding CCNY culture. Likewise, the two CCNY cultures isolated from *Cassiopeia* sp. specimens collected from the Caribbean and Red Seas consistently grouped with the CCMP cultures 2458 and 2464 (*S. microadriaticum*) also isolated from *Cassiopeia* sp. hosts from corresponding collection locations.

The CCNY *Symbiodinium* culture isolated from an *Amphisorus* sp. specimen collected in Okinawa, Japan grouped with the directly amplified

Symbiodinium sequence from the same host specimen in the tree resulting from the analysis of ribosomal sequences (Figure 30). This (sister taxa) relationship, however, was not recovered in the trees generated using plastid sequences (Figure 28) or combined data sets (Figure 29). In this instance, and in the case of two other CCNY cultures isolated from *Amphisorus* sp. hosts (Hawaii and Australia), the cultured and directly amplified *Symbiodinium* sequences, were not recovered as sister taxa but did co-occur consistently within the same clade.

Sequences recovered from two CCNY cultures, one isolated from a Polynesian *Marginopora* sp. host and the other from an *Amphisorus* sp, host from the Red Sea, were not found in association with any other directly amplified *Symbiodinium* sequences from soritine hosts. These two cultures, however, were recovered as sister taxa to each other.

The correspondence of clades to the existing *Symbiodinium* clade nomenclature was indicated by the relationships recovered in analysis of a 790 nt lsu rDNA fragment. Analysis of static homology characters using the program TNT generated the most parsimonious solution given the data (22 trees of 724 steps). The strict consensus of the TNT trees is provided in Figure 27. In addition to the CCMP type cultures this analysis also included five directly amplified *Symbiodinum* sequences from soritine host taxa reported in Pochon et al. (2004). Similar to the more inclusive ribosomal analysis, this analysis recovered an A clade which included *S. microadriaticum* (CCMP 2464 and 2458) and *S. pilosum* (CCMP 2461) along with the CCNY *Symbiodinium* cultures isolated from *Cassiopeia*, Polynesian *Marginopora*, and Red Sea

Amphisorus taxa. The CCMP culture 2460 was the only clade B *Symbiodinium* sequence analyzed. The F clade was divided into two subclades, one of which was characterized by Pacific *Amphisorus* sp. host taxa which included two Guam specimens (AJ308897 and AJ308896) from Pochon et al. (2004), a host specimen from Kudaka Island, Japan, and a specimen from Bird Island, Australia. The other F sub-clade contained *S. kawagutii* (CCMP 2468), as well as the CCNY culture isolated from a Hawaiian *Amphisorus* specimen, and *Symbiodinium* sequences directly amplified from a Florida Keys *Sorites* specimen and from Red Sea and Indian Ocean (Pochon, AJ308898) *Amphisorus* specimens. A third major clade was characterized as the *Symbiodinium* C clade based on the inclusion of *S. goreaui* (CCMP 2466) and two (clade C) sequences identified by Pochon et al. (2004) which were directly amplified from a Australian *Marginopora* specimen (AJ291515) and an Indian Ocean *Amphisorus* (AJ308894) specimen.

A single parsimonious solution (tree) resulted from each analysis (TNT and POY) using 1573 nucleotides of the plastid genes (23S and *psbA*). The dynamic homology (POY) tree with length 1962 (Figure 28), however, was 210 steps shorter than the TNT tree (Appendix B). Analysis of the plastid sequence data recovered a well-supported (jac = 100) clade (A) containing the two CCMP (2464 and 2458) *S. microadriaticum* cultures and the two CCNY cultures isolated from *Cassiopeia* hosts. In this analysis, the position of one A clade type culture *S. pilosum* (CCMP 2461) relative to the A clade *S. microadriaticum*

type cultures CCMP (2464) and CCMP (2458) rendered the A clade paraphyletic.

The cpDNA tree splits the F clade into two sub-clades. The *Symbiodinium* F sub-clade possessing the *S. kawagutii* (CCMP 2468) culture also contained the CCNY cultures from both Hawaiian, Australian, and Red Sea *Amphisorus* specimens. Unlike the high (jac = 99) support for the F clade recovered in the rDNA tree (Figure 30), support for the *S. kawagutii* (CCMP 2468) F sub-clade in the cpDNA tree was low (jac < 50). The other putative F sub-clade contained the CCNY culture isolated from a Japanese *Amphisorus* host, as well as, multiple directly amplified *Symbiodinium* from Pacific *Amphisorus* and Caribbean *Sorities* hosts. Support for this clade was high (jac = 92) relative to the *S. kawagutii* sub-clade. Interleaved between the two F sub-clades was a *Symbiodinium* B clade as identified by the presence of the CCMP culture 2460. In this analysis, the directly amplified *Symbiodinium* cpDNA from a Hawaiian *Marginopora vertebralis* host placed as the sister taxon to CCMP culture 2460 with moderate support (jac = 60).

The cpDNA tree recovered the *Symbiodinium* clade C as indicated by the placement of *S. goreaui* (CCMP 2466). This poorly supported (jac < 50) clade contained both the CCNY culture and directly amplified *Symbiodinium* sequences from a Guam *Marginopora vertebralis* specimen. Directly amplified *Symbiodinium* sequences from an Australian *Marginopora* and two Japanese *Amphisorus* specimens also placed within in this clade.

Analyses of 983 nucleotides of the *cox1* of mtDNA yielded 50 equally parsimonious trees of 627 steps using dynamic homology and five equally parsimonious trees 594 steps in length using static homology characters. The strict consensus of the static homology parsimony analysis (as implemented in TNT) divides the taxa into two major clades (A and B/C/F) (Figure 29). Clade A contains both *S. microadriaticum* and *S. pilosum* type cultures, as well as the CCNY cultures isolated from *Cassiopiea* sp., a Polynesian *Marginopora*, and Red Sea *Amphisorus* specimens. This clade is well supported (jac =100), although little resolution is found within the clade. Relationships within the clade containing the B (CCMP 2460), C (*S. goreaui*—CCMP 2466), F (*S. kawagutii*—CCMP 2468) type cultures were largely unresolved. The grouping of *S. kawagutii* with the directly amplified *Symbiodinium* sequences from Japanese, Hawaiian, and Red Sea *Amphisorus* specimens, however, had high jackknife support (jac = 94).

Analysis of 4316 rDNA nucleotides spanning both small and large ribosomal subunits resulted in two static homology parsimony trees of 4130 steps and a topologically similar dynamic homology tree of 4176 steps (Appendix B). The strict consensus (Figure 30) of the static homology trees showed a well supported (jac = 96) clade A containing the CCMP type cultures *S. microadriaticum* (CCMP 2461 and 2458), and *S. pilosum* (CCMP 2461), in addition to the CCNY cultures isolated from *Cassiopeia* sp., a Polynesian *Marginopora* specimen, and a Red Sea *Amphisorus* specimen. The F clade was recovered containing the *S. kawagutii* (CCMP 2458) sequence, as well as, the

CCNY cultures isolated from a Florida Keys *Sorites* specimen and a Hawaiian *Amphisorus* specimen (jac = 99). The clade C containing the *S. goreaui* (CCMP 2466) sequence also held two CCNY cultures isolated from Guam *Marginopora* and Japanese *Amphisorus* specimens. Support values for relationships resolved within C clade were poor (jac < 50) except for the branches indicating the close relationship between the CCNY cultured *Symbiodinium* isolates and their directly amplified compliments (jac > 95).

The phylogenetic analyses of the combined dataset included 6872 nucleotides from two nuclear genes (18S rDNA, 28S rDNA), two plastid genes (*psbA*, 23S rDNA), and one mitochondrial gene (*cox1*) for 29 *Symbiodinium* isolates and five outgroup dinoflagellate taxa (*Amphidinium operculatum, Gonyaulax polyedra, Heterocapsa triquetra*, *Protoceratium reticulatum*, and *Gymnodinium simplex*). The most parsimonious solution was generated using a dynamic homology approach and yielded two equally parsimonious trees of 7077 in length. The strict consensus of these trees (Figure 31) yielded a topology similar to that recovered in the rDNA consensus tree. One noticeable difference between the topologies occurs within the C clade wherein the CCNY culture isolated from a Guam *Marginopora* specimen forms a highly supported sister relationship (jac =100) with the directly amplified *Symbiodinium* sequence recovered from that specimen. The overall jackknife support for nodes of the combined data set tree was greater than the support values determined for each partitioned analysis (i.e. mtDNA, rDNA, or cpDNA). The plastid morphologies mapped on the tree appear to be homoplastic as both the petal-like and reticulate

morphologies characterize both the A and F clades. In the *Symbiodinium* C clade, however, only the petal-like plastid morphology was observed.

Figure 27. Strict consensus cladogram (724 steps) from 22 equally parsimonious trees. The tree was generated in the TNT program using static homology nucleotide characters from a 790 nt segment of lsu rDNA containing the variable D1 and D2 loops from *Symbiodinium*. Jackknife support values >50 are indicated at nodes. Correspondence to established *Symbiodinium* Clades noted in colored circles.

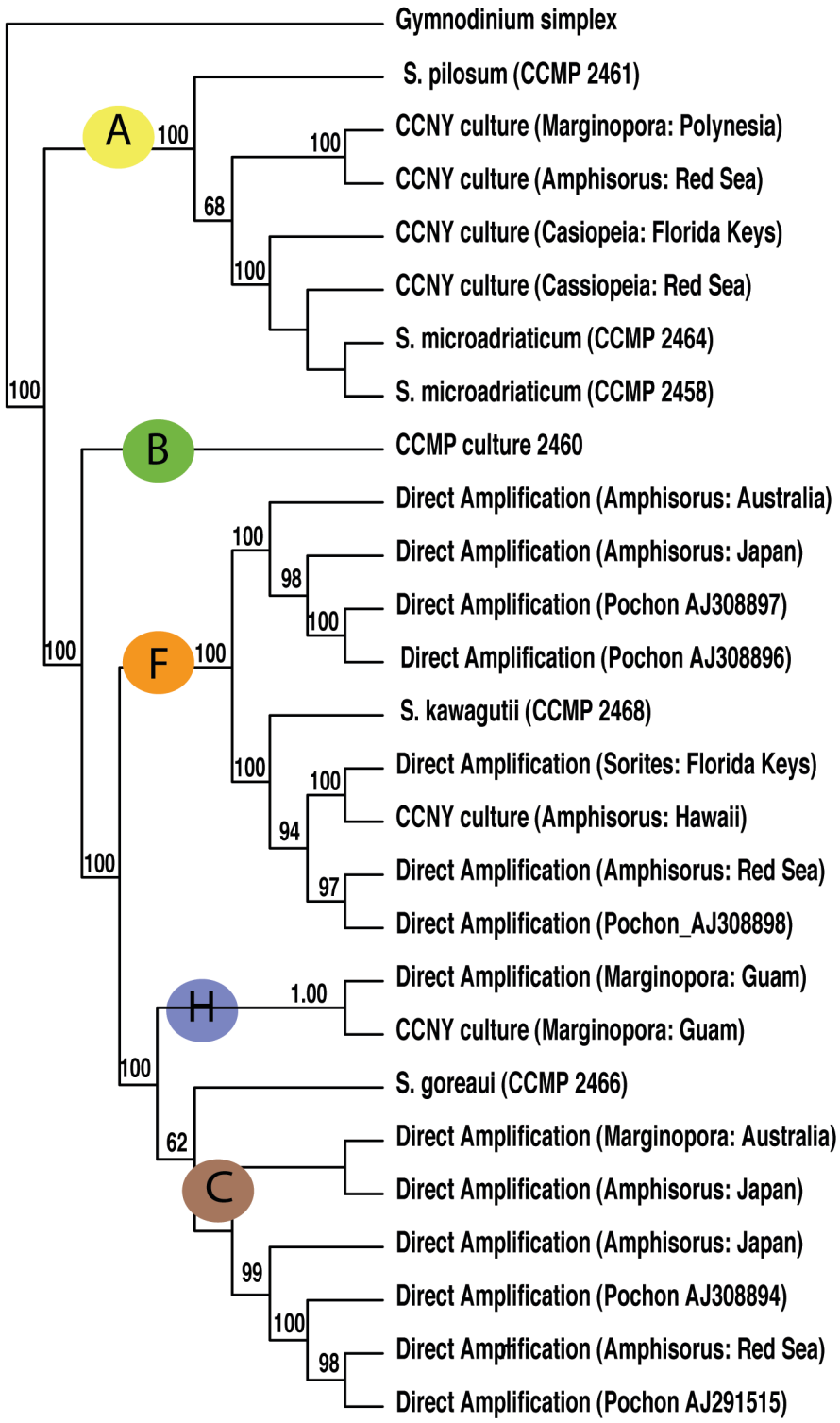
Gymnodinium simplex
S. pilosum (CCMP 2461)
A
CCNY culture (Marginopora: Polynesia)
CCNY culture (Amphisorus: Red Sea)
CCNY culture (Casiopeia: Florida Keys)
CCNY culture (Cassiopeia: Red Sea)
S. microadriaticum (CCMP 2464)
S. microadriaticum (CCMP 2458)
B
CCMP culture 2460
Direct Amplification (Amphisorus: Australia)
Direct Amplification (Amphisorus: Japan)
Direct Amplification (Pochon AJ308897)
F
Direct Amplification (Pochon AJ308896)
S. kawagutii (CCMP 2468)
Direct Amplification (Sorites: Florida Keys)
CCNY culture (Amphisorus: Hawaii)
Direct Amplification (Amphisorus: Red Sea)
Direct Amplification (Pochon_AJ308898)
H
Direct Amplification (Marginopora: Guam)
CCNY culture (Marginopora: Guam)
S. goreaui (CCMP 2466)
C
Direct Amplification (Marginopora: Australia)
Direct Amplification (Amphisorus: Japan)
Direct Amplification (Amphisorus: Japan)
Direct Amplification (Pochon AJ308894)
Direct Amplification (Amphisorus: Red Sea)
Direct Amplification (Pochon AJ291515)

Figure 28. Lowest cost cladogram (1962 steps) of 1573 nucleotides of cpDNA (23S and *psbA*) generated using direct optimization in POY. Jackknife support values >50 indicated at nodes.

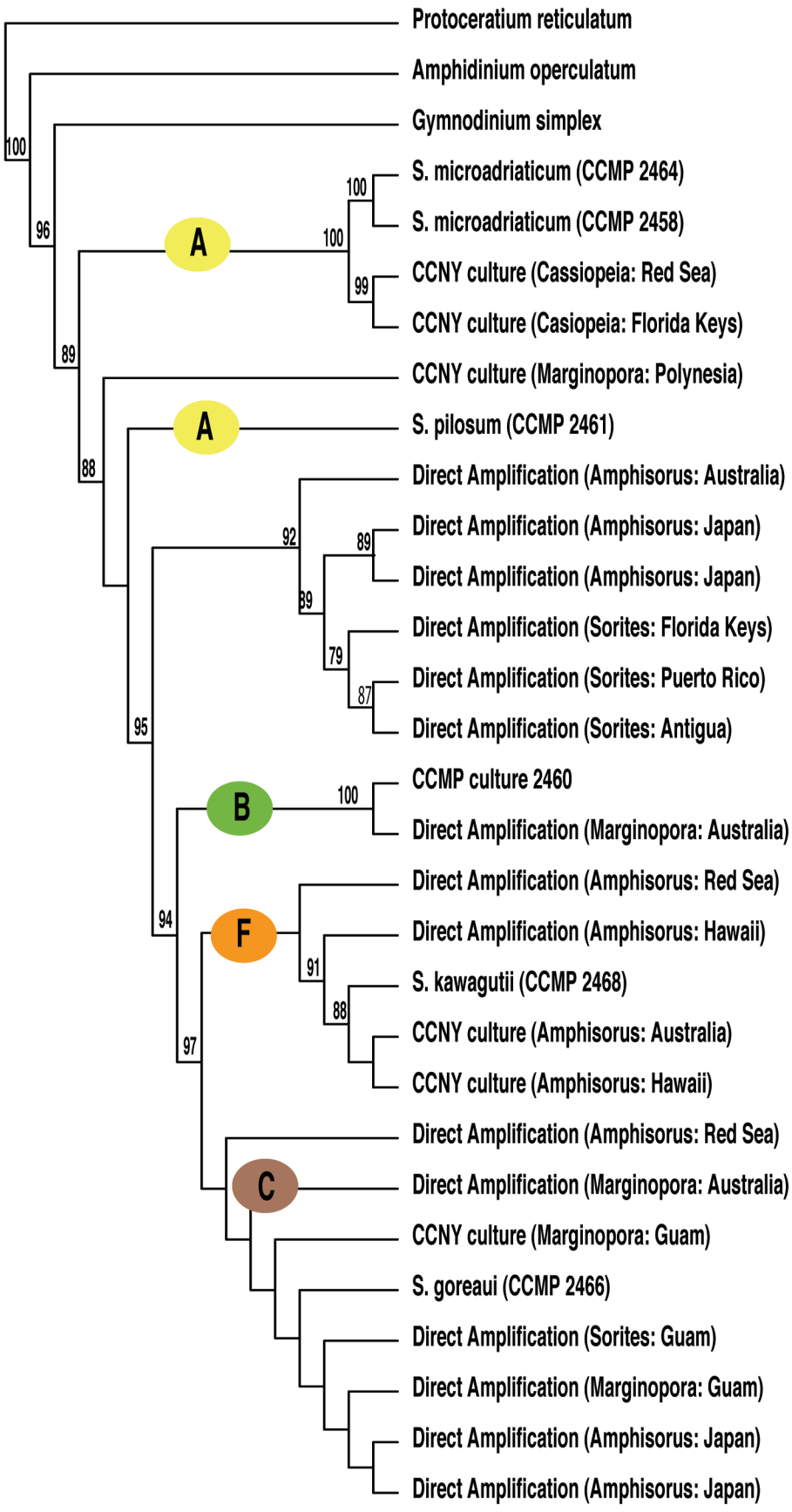
Protoceratium reticulatum
Amphidinium operculatum
Gymnodinium simplex
S. microadriaticum (CCMP 2464)
S. microadriaticum (CCMP 2458)
CCNY culture (Cassiopeia: Red Sea)
CCNY culture (Casiopeia: Florida Keys)
CCNY culture (Marginopora: Polynesia)
S. pilosum (CCMP 2461)
Direct Amplification (Amphisorus: Australia)
Direct Amplification (Amphisorus: Japan)
Direct Amplification (Amphisorus: Japan)
Direct Amplification (Sorites: Florida Keys)
Direct Amplification (Sorites: Puerto Rico)
Direct Amplification (Sorites: Antigua)
CCMP culture 2460
Direct Amplification (Marginopora: Australia)
Direct Amplification (Amphisorus: Red Sea)
Direct Amplification (Amphisorus: Hawaii)
S. kawagutii (CCMP 2468)
CCNY culture (Amphisorus: Australia)
CCNY culture (Amphisorus: Hawaii)
Direct Amplification (Amphisorus: Red Sea)
Direct Amplification (Marginopora: Australia)
CCNY culture (Marginopora: Guam)
S. goreaui (CCMP 2466)
Direct Amplification (Sorites: Guam)
Direct Amplification (Marginopora: Guam)
Direct Amplification (Amphisorus: Japan)
Direct Amplification (Amphisorus: Japan)
A
A
B
F
C
100
96
100
100
99
89
88
92
89
89
79
87
95
100
94
91
88
97

Figure 29. Strict consensus cladogram (594 steps) of 50 equally parsimonious trees based on a 983 nt sequence of mtDNA (*cox1*) and analyzed using static homology characters in TNT. Jackknife support values >50 indicated at nodes.

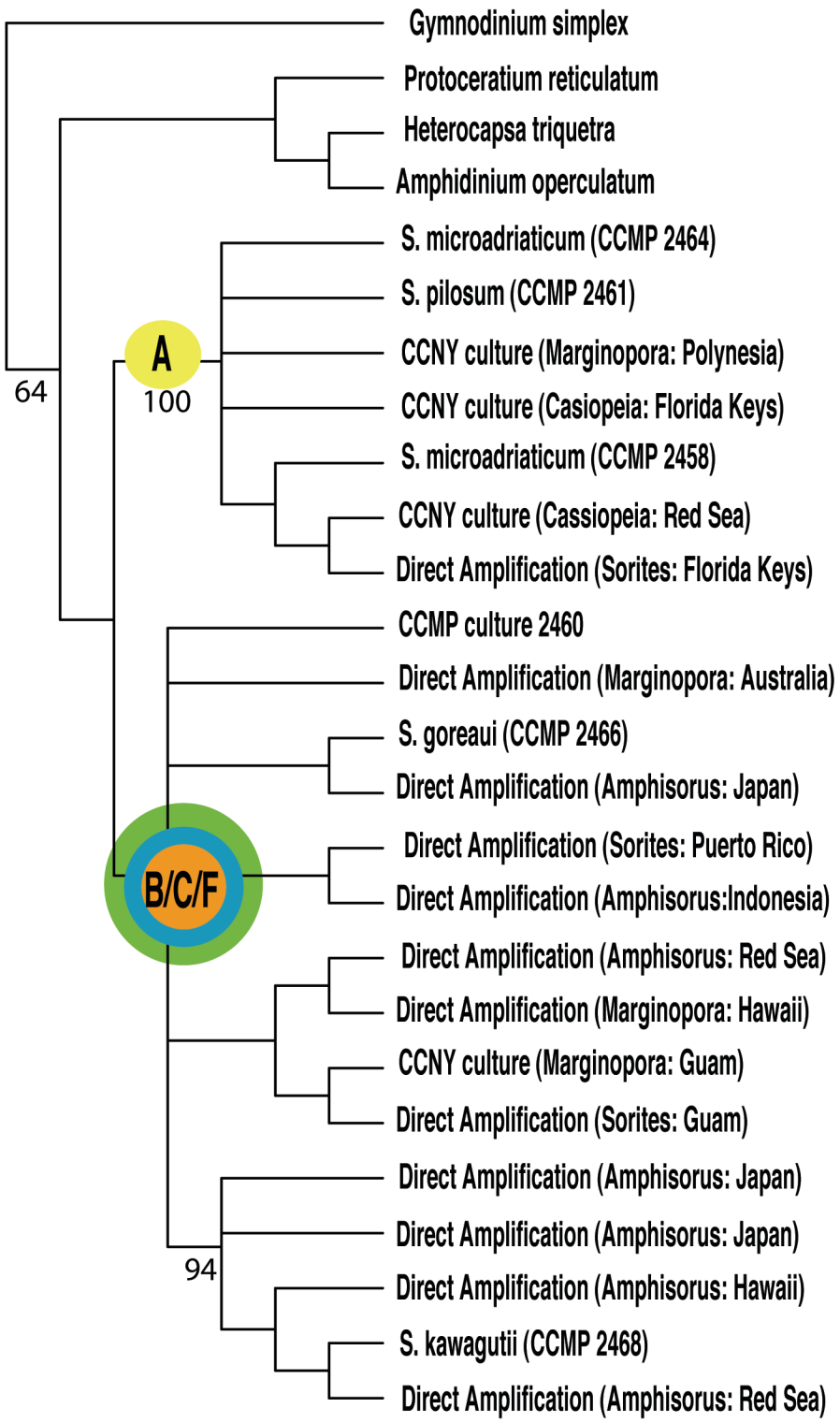
Gymnodinium simplex
Protoceratium reticulatum
Heterocapsa triquetra
Amphidinium operculatum
S. microadriaticum (CCMP 2464)
S. pilosum (CCMP 2461)
A
CCNY culture (Marginopora: Polynesia)
64
100
CCNY culture (Casiopeia: Florida Keys)
S. microadriaticum (CCMP 2458)
CCNY culture (Cassiopeia: Red Sea)
Direct Amplification (Sorites: Florida Keys)
CCMP culture 2460
Direct Amplification (Marginopora: Australia)
S. goreaui (CCMP 2466)
Direct Amplification (Amphisorus: Japan)
B/C/F
Direct Amplification (Sorites: Puerto Rico)
Direct Amplification (Amphisorus:Indonesia)
Direct Amplification (Amphisorus: Red Sea)
Direct Amplification (Marginopora: Hawaii)
CCNY culture (Marginopora: Guam)
Direct Amplification (Sorites: Guam)
Direct Amplification (Amphisorus: Japan)
Direct Amplification (Amphisorus: Japan)
94
Direct Amplification (Amphisorus: Hawaii)
S. kawagutii (CCMP 2468)
Direct Amplification (Amphisorus: Red Sea)

Figure 30. Strict consensus cladogram (4130 steps) of two equally parsimonious trees built with the combined dataset (6822 nucleotides of rDNA (18S, ITS, 28S) generated using static homology characters in TNT. Jackknife support values >50 indicated at nodes.

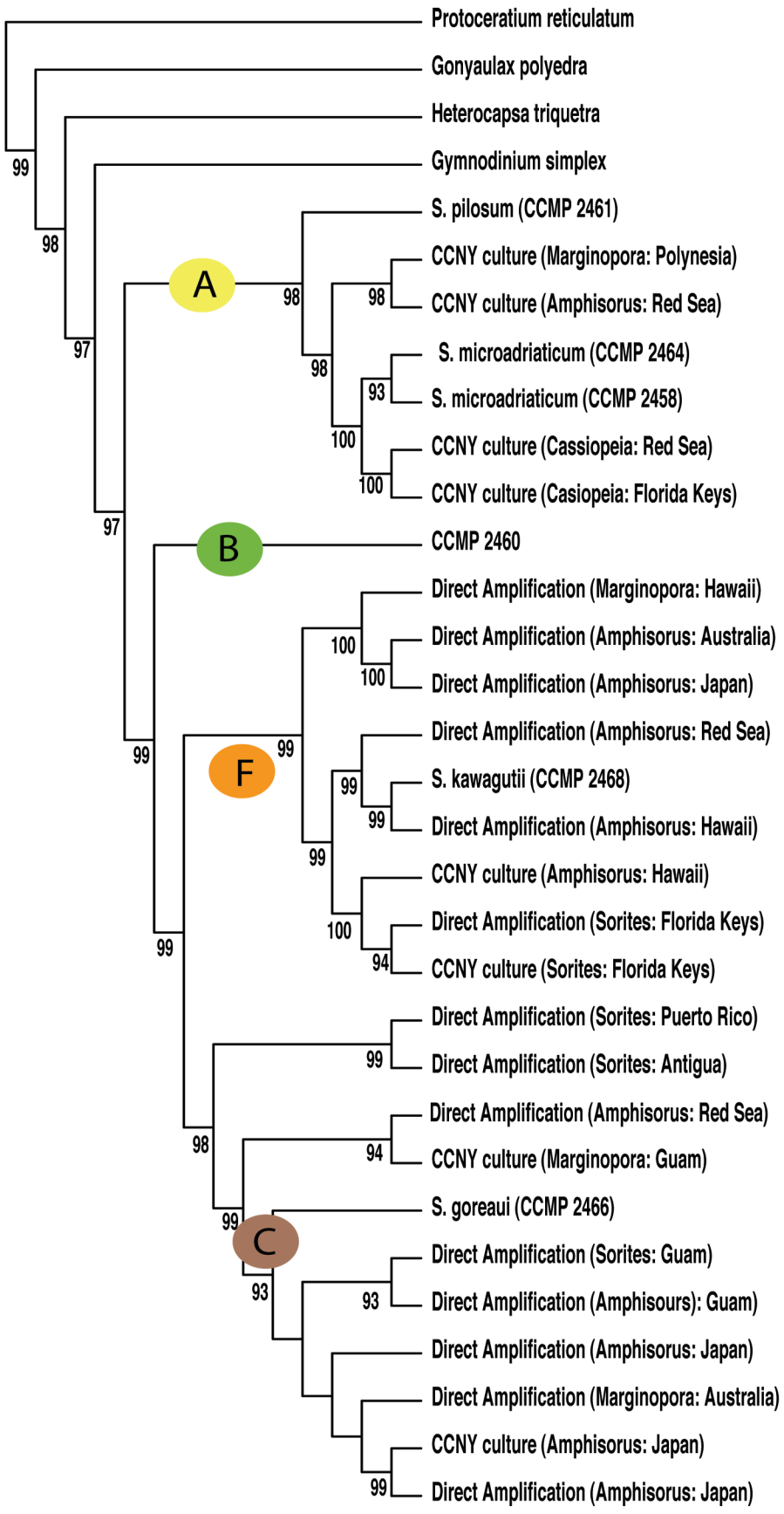
Protoceratium reticulatum
Gonyaulax polyedra
Heterocapsa triquetra
Gymnodinium simplex
S. pilosum (CCMP 2461)
CCNY culture (Marginopora: Polynesia)
CCNY culture (Amphisorus: Red Sea)
S. microadriaticum (CCMP 2464)
S. microadriaticum (CCMP 2458)
CCNY culture (Cassiopeia: Red Sea)
CCNY culture (Casiopeia: Florida Keys)
CCMP 2460
Direct Amplification (Marginopora: Hawaii)
Direct Amplification (Amphisorus: Australia)
Direct Amplification (Amphisorus: Japan)
Direct Amplification (Amphisorus: Red Sea)
S. kawagutii (CCMP 2468)
Direct Amplification (Amphisorus: Hawaii)
CCNY culture (Amphisorus: Hawaii)
Direct Amplification (Sorites: Florida Keys)
CCNY culture (Sorites: Florida Keys)
Direct Amplification (Sorites: Puerto Rico)
Direct Amplification (Sorites: Antigua)
Direct Amplification (Amphisorus: Red Sea)
CCNY culture (Marginopora: Guam)
S. goreaui (CCMP 2466)
Direct Amplification (Sorites: Guam)
Direct Amplification (Amphisours): Guam)
Direct Amplification (Amphisorus: Japan)
Direct Amplification (Marginopora: Australia)
CCNY culture (Amphisorus: Japan)
Direct Amplification (Amphisorus: Japan)
A
B
C
F
99
98
97
98
98
93
100
100
97
99
99
100
100
99
99
99
99
100
94
98
99
94
99
93
93
99

Figure 31. Strict consensus cladogram of two equally parsimonious trees (7077 steps) constructed using 5 gene loci (6872 nucleotides of cpDNA, rDNA, and mtDNA) analyzed using direct optimization in POY. Jackknife support values >50 indicated at nodes.

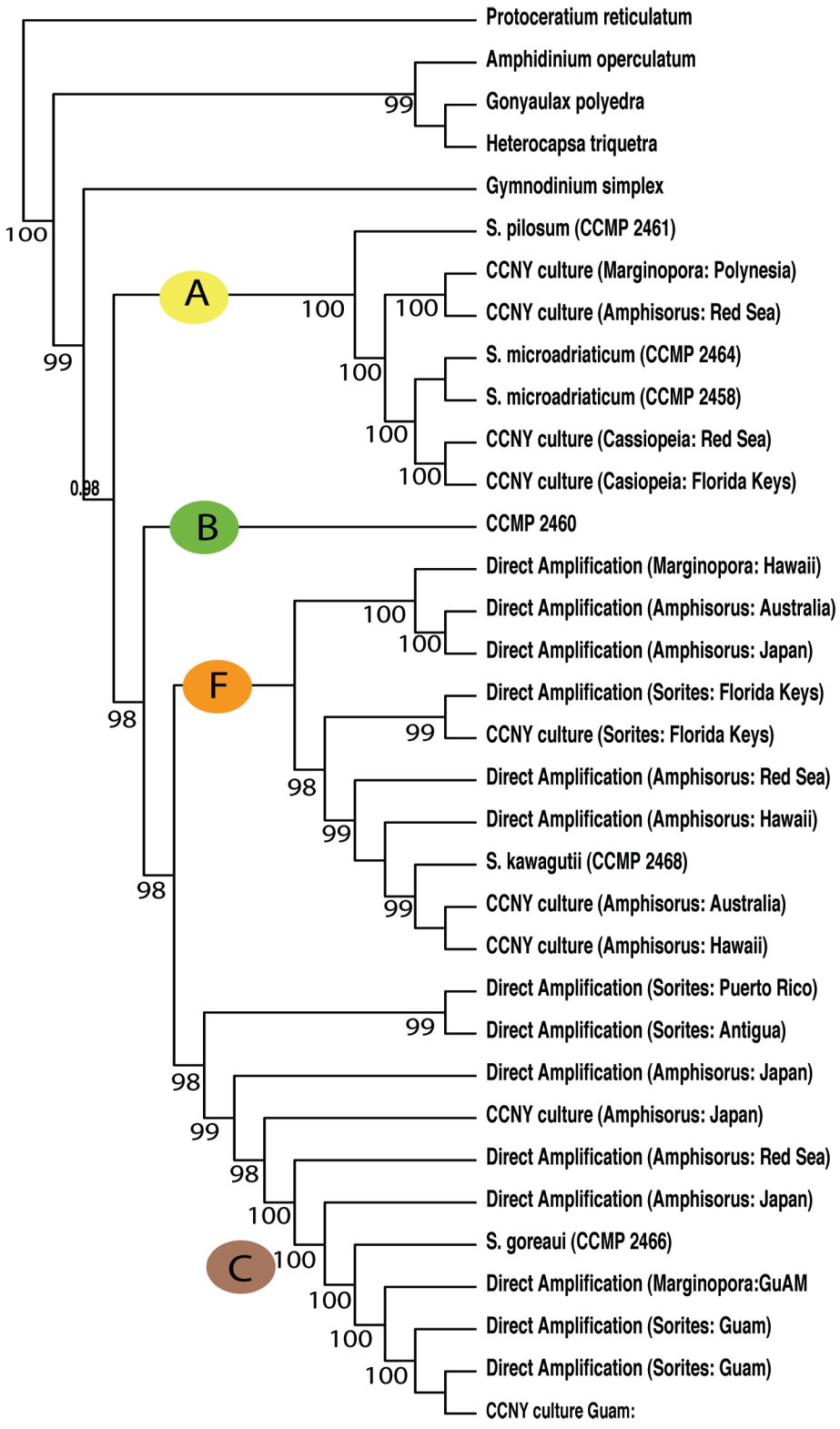
Protoceratium reticulatum
Amphidinium operculatum
Gonyaulax polyedra
Heterocapsa triquetra
Gymnodinium simplex
S. pilosum (CCMP 2461)
CCNY culture (Marginopora: Polynesia)
CCNY culture (Amphisorus: Red Sea)
S. microadriaticum (CCMP 2464)
S. microadriaticum (CCMP 2458)
CCNY culture (Cassiopeia: Red Sea)
CCNY culture (Casiopeia: Florida Keys)
CCMP 2460
Direct Amplification (Marginopora: Hawaii)
Direct Amplification (Amphisorus: Australia)
Direct Amplification (Amphisorus: Japan)
Direct Amplification (Sorites: Florida Keys)
CCNY culture (Sorites: Florida Keys)
Direct Amplification (Amphisorus: Red Sea)
Direct Amplification (Amphisorus: Hawaii)
S. kawagutii (CCMP 2468)
CCNY culture (Amphisorus: Australia)
CCNY culture (Amphisorus: Hawaii)
Direct Amplification (Sorites: Puerto Rico)
Direct Amplification (Sorites: Antigua)
Direct Amplification (Amphisorus: Japan)
CCNY culture (Amphisorus: Japan)
Direct Amplification (Amphisorus: Red Sea)
Direct Amplification (Amphisorus: Japan)
S. goreaui (CCMP 2466)
Direct Amplification (Marginopora:GuAM
Direct Amplification (Sorites: Guam)
Direct Amplification (Sorites: Guam)
CCNY culture Guam:
A
B
C
F
100
99
0.98
98

4.10 Discussion

This study provides the first molecular characterization of cultured *Symbiodinium* taxa isolated from soritine foraminifera. As part of an ongoing effort to investigate foraminiferal endosymbionts (Lee et al., in prep), the results generated herein provide a critical link between the current molecular systematic framework for directly amplified sequence data and *Symbiodinum* taxa maintained in culture. Moreover, in contrast to using a single molecular marker to resolve relationships among taxa (e.g. LaJeunesse, 2001, Pochon et al., 2004, Santos et al., 2003), this work presents the first phylogenetic treatment to simultaneously analyze all available genetic markers for the *Symbiodinium* genus.

As this work constitutes an initial investigation into the biology of *Symbiodinium* isolates cultured from soritine foraminifera, it is important to recognize the limitations associated with the methods employed. The primary limitation arises from the multiple *Symbiodinium* strains housed within any given foraminiferal host. Pochon and Pawlowski (2006) report the presence of multiple *Symbidinium* strains (from multiple clades) within individual soritine specimens and that the dominant strain can shift coincident with seasonal or other environmental cures. This source of ambiguity compounded with a paucity of species level descriptions significantly limits the ability to culture and assess the total *Symbiodinium* diveristy contained within soritine specimens,

The molecular phylogenetic analyses revealed the distribution of the CCNY cultures to be among three *Symbiodinium* clades: (A/C/F). The

placement of *Symbiodinium* isolated from *Cassiopeia* sp. in the A clade adjacent to the *S. microadriaticum* CCMP cultures (2464 and 2458) provides a necessary link between the molecular characterization of this taxon and the morphological and physiological investigations ongoing in the Marine Microbial Ecology lab of Dr. John Lee.

Due to a lack of directly amplified material available, a confirmed host correspondence could not be generated for the CCNY culture isolated from a Polynesian *Marginopora* specimen. The placement of this CCNY culture within the A clade is at odds with Pochon et al.'s (2004 and 2006) directly amplified sequence determination that *Symbiodinium* harbored within soritine hosts is absent from this clade.

A host correspondence also could not be established for the CCNY culture isolated from a Red Sea, *Amphisorus* specimen. In this case, however, the directly amplified *Symbiodinium* sequence from that specimen conflicted with the cultured sequence and was found within the F clade. This discrepancy may be due to a non-dominant *Symbiodinium* type being favored in culture over the type that is dominant *in symbio*. Additional culture lines established from multiple Red Sea hosts are required to corroborate this result.

Three CCNY culture isolates placed within the *Symbiodinium* F clade: (Hawaiian and Australian *Amphisorus* hosts and Florida Keys *Sorites* host). Although the only described *Symbiodinium* species for this clade, *S. kawagutii*, was isolated from a Hawaiian coral (*Montipora* sp.), the F clade was expanded by Pochon et al, (2001) based upon directly amplified *Symbiodinium* sequences

from soritine hosts across a broad geographic range. As such, it is not surprising to identify CCNY cultures isolated from different soritine genera and ocean basins within this clade. Despite the close molecular relationship between the CCNY cultures isolated from Hawaiian and Australian *Amphisorus* specimens, the differences noted between their plastid morphologies indicates the need for further morphological investigation.

Symbiodinium sequences directly amplified from foraminiferal hosts have also been reported by Pochon et al. (2001, 2004, 2006) in the C clade. The two CCNY cultures found within this clade were isolated from Guam and Japanese soritine hosts which is concordant with the characterization of the C clade as being the most diverse and commonly recovered among Indo-Pacific hosts (Baker, 2004). Both the Guam and Japanese CCNY cultures exhibit similar petal-like plastid morphologies.

CHAPTER 5

Significance and Future Directions

5.1 Significance

The endosymbiosis between foraminifera and their photosynthetic zooxanthellae provides a model system to study the establishment and maintenance of the symbiotic condition between two unicellular eukaryotic organisms. Moreover, since the recognition of the symbiosis between phototrophic dinoflagellates and foraminifera, researchers have postulated this relationship to be a driving force in the evolution and diversification of the host taxa (Lee and McEnery, 1983; Lee and Hallock, 1987). As such assessing the phylogenetic diversity of both symbiotic partners is a critical component in such investigations. To this end, the research presented in this dissertation presents the first phylogenetic analyses of the hosts (foraminifera within the sub-family soritinae) to use combined datasets of both molecular and morphological characters. This research also provides the first molecular treatment of the endosymbiotic dinoflagellate partners (genus *Symbiodinium*) isolated and cultured from soritine foraminiferal hosts.

The taxonomic diversity observed within the soritinae reveals phylogenetic patterns discordant with the accepted paradigm of soritine evolution. Specifically, the long accepted idea —from Carpenter (1883) to Richardson (2001)—of relationships among the genera as defined by a progression from simple (*Sorites*) through intermediate (*Amphisorus*) to complex (*Marginopora*) test morphologies was not supported in this study. Rather, the most intricate (in terms of apertural density and endoskeletal complexity) genus morphologically (*Marginopora*) formed a clade together with

the genus (*Sorites*) possessing the least morphological complexity. This grouping based on the combined analysis of large and small subunit rDNA and morphology concurs with the small subunit rDNA analyses of Holzmann et al., (2001) and indicates the need to develop additional molecular markers for further corroboration.

A second significant pattern revealed through these analyses is the large amount of diversity found within the genus *Amphisorus* both morphologically and molecularly. Previous to this work, *Amphisorus* was generally regarded as a monotypic genus restricted to the Red Sea (Loblich and Tappan, 1987. Gudmundsson, 1994). The molecular work of Holzmann et al. (2001), that placed *Marginopora kudkajimaensis* -like specimens within the genus *Amphisorus*, opened the possibility that additional *Amphisorus* diversity existed within Pacific populations. Samples collected from eight Pacific sites and analyzed for this dissertation show a broad range of morphological and molecular variation contained within three well-supported clades. The taxonomic consequence of the phylogenetic analyses is to not only describe the new *Amphisorus* species (*A. saurensis*) and confirm that *A. kudkajimaensis* specimens unequivocally belong to the genus *Amphisorus*, but also to indicate that the "*kudakajimaensis*" specimen from Guam analyzed in Holzmann et al. (2001) belongs to a separate *Amphisorus* taxonomic grouping. This *Amphisorus* clade consisting of the Ritidian Bay (Guam) and Zampa Point (Japan) populations has yet to be described as a new species pending further

investigation into the presence of unique insertions within the large subunit sequences of the Japanese specimens.

The significance of the phylogenetic investigations of the *Symbiodinium* isolates cultured from soritine hosts lies in the correspondence of cultures to *Symbiodinium* sequences directly amplified from the holobiont (host/symbiont) complexes. The work presented in this dissertation identifies a positive correspondence between four CCNY culture lines and the directly amplified sequences recovered from the same specimens. These identifications provide a foundation for the morphological and physiological characterization of the cultures currently underway at the Marine Microbial Ecology Laboratory at CCNY. Moreover, the placement of these isolates within the existing molecular phylotype framework using all available molecular markers for *Symbiodinium* provides a molecular identification of these isolates essential for their use in further experimental approaches to characterize the endosymbiotic condition.

5.2 Future Directions

The previously unrecognized diversity within the Soritinae revealed in this work indicates the need both for additional taxonomic sampling and the development of additional molecular markers appropriate for phylogenetic resolution at the species level. The necessity for further taxon sampling is supported by the observation of a potentially new Australian *Marginopora* species recently acquired by Dr. John Lee (pers. comm.). Moreover, due to the poor preservation of Indonesian and Philippine *Amphisorus* specimens,

nucleotide sequence recovery was severely limited. Intensive Indo-Pacific sampling of soritines for molecular and morphological evaluation is required to resolve the placement of these taxa within their respective genera.

In conjunction with sampling efforts, additional species-level molecular markers must be developed for the Soritinae. Accomplishing this will require extensive cDNA library screening beyond the scope of that attempted for this study. Although such efforts have been unsuccessfully attempted multiple times by colleagues (Dr. Jan Pawlowski pers. comm.), the success (albeit limited) of generating primer sets from a small scale subtracted library constructed for this research indicates the potential in modifying subtractive hybridization techniques for the exploration of soritine genomes.

Subsequent to the characterization of soritine *Symbiodinium* cultures, one promising direction that research on the symbiotic condition can take is the attempt to understand the signaling between host and symbiont. Pilot studies conducted with Dr. John Lee using soritine surface proteins detected the presence of one (or more) *Symbiodinium*-specific surface markers. This result indicates the potential of an approach using monoclonal antibodies generated from different *Symbiodinium* cultures to determine fine-scale specificity between symbiotic partners. Comparison of expressed sequence tag (EST) libraries generated from *Symbiodinium* strains in culture and *in symbio* may also yield information on the impact of the symbiotic state on expression patterns.

APPENDIX A

Character List

1) *Biconvex Test: 0 = absent; 1 = present
2) Biconcave Test: 0 = absent; 1 =< 5° from proloculus to margin ; 2 = ≥ 5° proloculus to margin
3) *Biumbilicate Test: 0 = absent; 1 = present
4) *Keel: 0 = absent; 1 = present
5) Avg. Test Diameter: 0 = ≤ 5mm; 1 = > 5 ≤ 15mm; 2 = > 15mm
6) Creased Test Margin: 0 = absent; 1 = present
7) Common loss of Embryonic Chambers in Microspheric Test: 0 = absent; 1 = present
8) Dinoflagellate Symbionts: 0 = absent; 1 = present
9) *Planispiral Growth Stage: 0 = absent; 1 = present
10) *Annular Growth Stage: 0 = absent; 1 = present
11) *Flabelliform Chambers: 0 = absent; 1 = present
12) Vorhof: 0 = absent; 1 = < 1/2 whorl; 2 = > 1/2 whorl
13) *Advolute Coiling in Microspheric Test: 0 = absent; 1 = present
14) *Involute Coiling in Microspheric Test: 0 = absent; 1 = present
15) **Sutures between Chambers: 0 = straight; 1 = wavy
16) Endoskeleton: 0 = absent; 1 = present
17) Chamberlets: 0 = absent; 1 = present
18) Septula: 0 = absent; 1 = spanning chamber diameter; 2 = extending to chamber median; 3 = extending ≤ 1/4 chamber diameter
19) Annular Canal(s): 0 = absent; 1 = single; 2 = divided into 2 parallel channels; 3 = irregularly partitioned
20) Annular Canal(s) Area: 0 = absent; 1= constant; 2 = expanded in outer whorls
21) *Pillars: 0 = absent; 1 = present
22) Crosswise-oblique Stolon System: 0 = absent; 1 = present
23) **Double Row of Marginal Apertures: 0 = absent; 1 = present
24) **Medial Apertures: 0 = absent; 1 = present
25) *Lateral Row of Apertures: 0 = absent; 1 = present
26) *Longitudinal Aperture Furrow: 0 = absent; 1 = present
27) Aperture Shape: 0 = round/ovate; 1 = elongate; 2 = irregular; 3 = round & elongate; 4 = round & irregular; 5 = elongate & irregular; 6 = round, elongate & irregular
28) Relative Aperture Size: 0 = < 1/4 chamber height; 1 = 1/4 - 1/2 chamber height; 2 = >1/2 chamber height
29) Aperture Density: 0 = N/A; 1=1-2 per chamberlet; 2 = 2-3 per chamberlet; 3 = 4+ per chamberlet
30) Aperture lips: 0 = absent; 1 = present

* = character from Richardson (2001); ** = character from Gudmundsson (1994)

Distribution of Characters

Sampled Populations

Laevipeneroplis proteus	1 0 0 1 0 0 0 0 1 0 1 0 1 1 0 0 0 0 0 0 0 0 0 0 0 1 0 0 0 1
Parasorites orbitolitoides	0 0 0 1 0 0 0 0 1 1 1 0 0 0 0 1 1 0 0 0 0 0 0 0 0 1 0 2 0 1
Peneroplis pertusus	0 0 1 1 0 0 0 0 1 0 1 0 0 1 0 0 0 0 0 0 0 0 0 0 0 0 0 0 0 1
Antigua (Made Island.)	0 0 0 0 0 0 0 0 1 1 1 1 0 1 0 1 1 1 1 1 1 0 1 0 0 1 0 0 2 1 1
Australia (Bird Island:1)	0 1 0 0 2 0 0 1 1 1 1 1 1 0 1 1 1 2 1 2 0 1 1 1 0 0 2 1 2 0
Australia (Bird Island:2)	0 2 0 0 2 0 1 1 0 1 0 2 1 0 1 1 1 3 3 2 1 1 1 1 0 0 0 0 3 1
Australia (Lizard Island)	0 2 0 0 1 1 0 1 0 1 0 2 1 0 1 1 1 3 3 2 1 1 1 1 0 0 0 0 3 1
Australia (Pigeon Point)	0 2 0 0 1 1 0 1 0 1 0 2 1 0 1 1 1 3 3 2 1 1 1 1 0 0 0 0 3 1
Florida (Sand Key)	0 0 0 0 0 0 0 0 1 1 1 1 0 1 0 1 1 1 1 1 1 0 1 0 0 1 0 0 2 1 1
Florida (Key West)	0 0 0 0 0 0 0 0 1 1 1 1 0 1 0 1 1 1 1 1 1 0 1 0 0 1 0 0 2 1 1
Florida (Key Largo)	0 0 0 0 0 0 0 0 1 1 1 1 0 1 0 1 1 1 1 1 1 0 1 0 0 1 0 0 2 1 1
Guam (Ritidian Bay:1)	0 2 0 0 1 0 0 1 1 1 1 1 1 0 1 1 1 3 2 1 1 1 1 1 0 0 3 1 1 1
Guam (Ritidian Bay:2)	0 0 0 0 0 0 0 0 1 1 1 1 0 1 0 1 1 1 1 1 1 0 1 0 0 1 0 0 2 1 1

Guam (Ritidian Bay:3)	0 2 0 0 2 0 0 1 0 1 0 2 1 0 1 1 1 3 3 2 1 1 1 1 0 0 0 0 3 1
Hawaii (Kailua, Oahu:1)	0 1 0 0 1 0 0 1 1 1 1 1 1 0 1 1 1 3 2 1 1 1 1 1 0 0 3 1 2 1
Hawaii (Kailua, Oahu:2)	0 2 0 0 1 0 0 1 0 1 0 2 1 0 1 1 1 3 3 2 1 1 1 1 0 0 0 0 3 1
Hawaii (Poipu, Kauai)	0 1 0 0 1 0 0 1 1 1 1 1 1 0 1 1 1 3 2 1 1 1 1 1 0 0 3 1 2 1
Indonesia (E. Kalimantan)	0 1 0 0 2 0 0 ? 1 1 1 1 1 0 1 1 1 3 2 2 1 1 1 1 0 0 5 0 3 1
Japan (Kudaka Island)	0 2 0 0 2 0 0 1 1 1 1 2 1 0 1 1 1 3 3 2 1 1 1 1 0 0 5 0 3 1
Japan (Zampa Beach, OK)	0 2 0 0 2 0 0 1 1 1 1 1 1 0 1 1 1 3 2 1 1 1 1 1 0 0 4 0 2 0
Philippines (Cebu)	0 1 0 0 2 0 0 ? 1 1 1 1 1 0 1 1 1 3 2 2 1 1 1 1 0 0 5 0 3 1
Puerto Rico (La Parguera)	0 0 0 0 0 0 0 1 1 1 1 0 1 0 1 1 1 1 1 1 0 1 0 0 1 0 0 2 1 1
Red Sea (Eilat:*Halophyla*)	0 1 0 0 1 0 0 1 1 1 1 1 1 0 1 1 1 2 1 1 0 1 1 1 0 0 3 1 2 1
Red Sea (Eilat:stones)	0 1 0 0 1 0 0 1 1 1 1 1 1 0 1 1 1 2 1 1 0 1 1 1 0 0 3 1 2 1

APPENDIX B

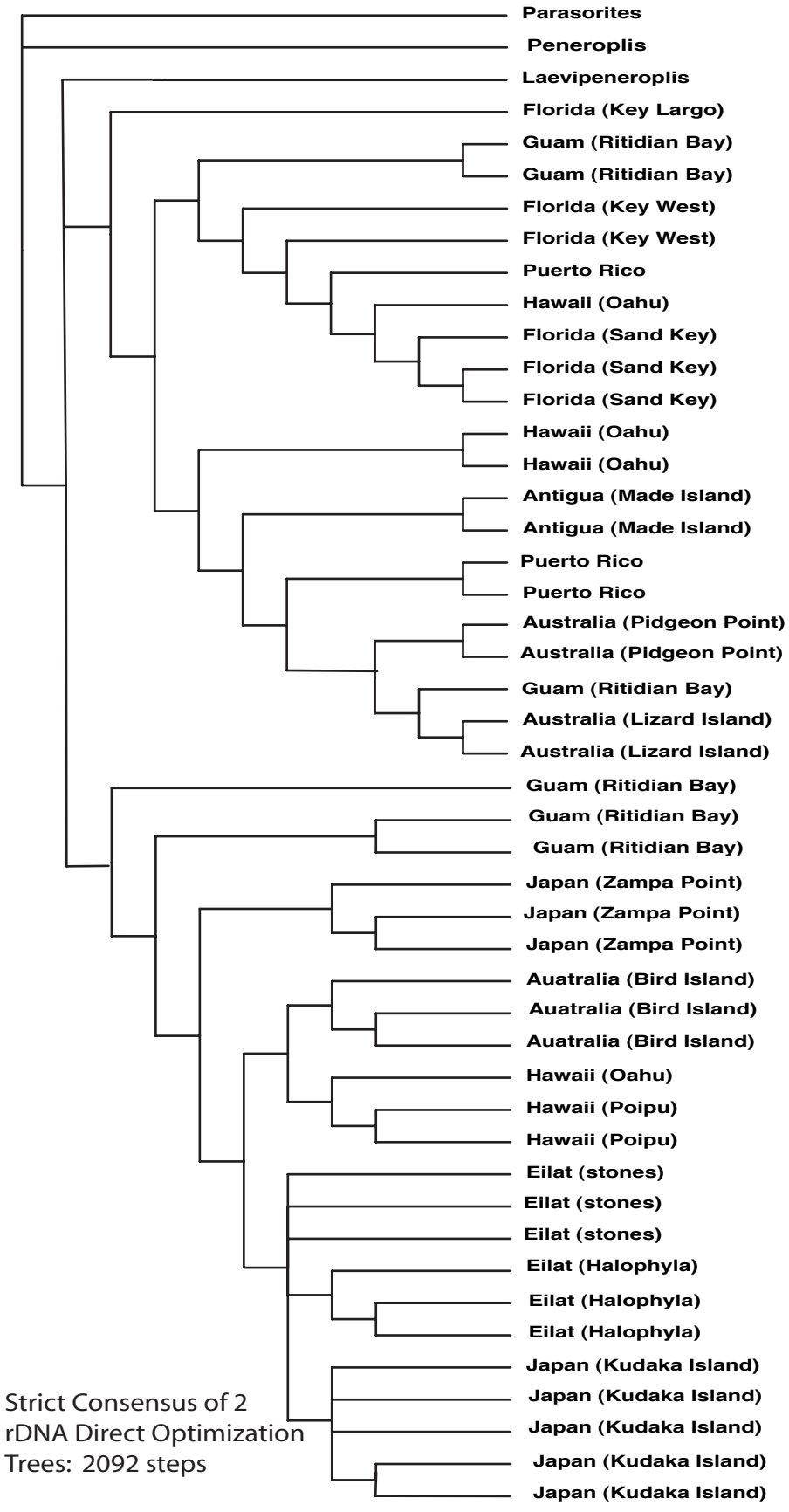

Strict Consensus of 2
rDNA Direct Optimization
Trees: 2092 steps

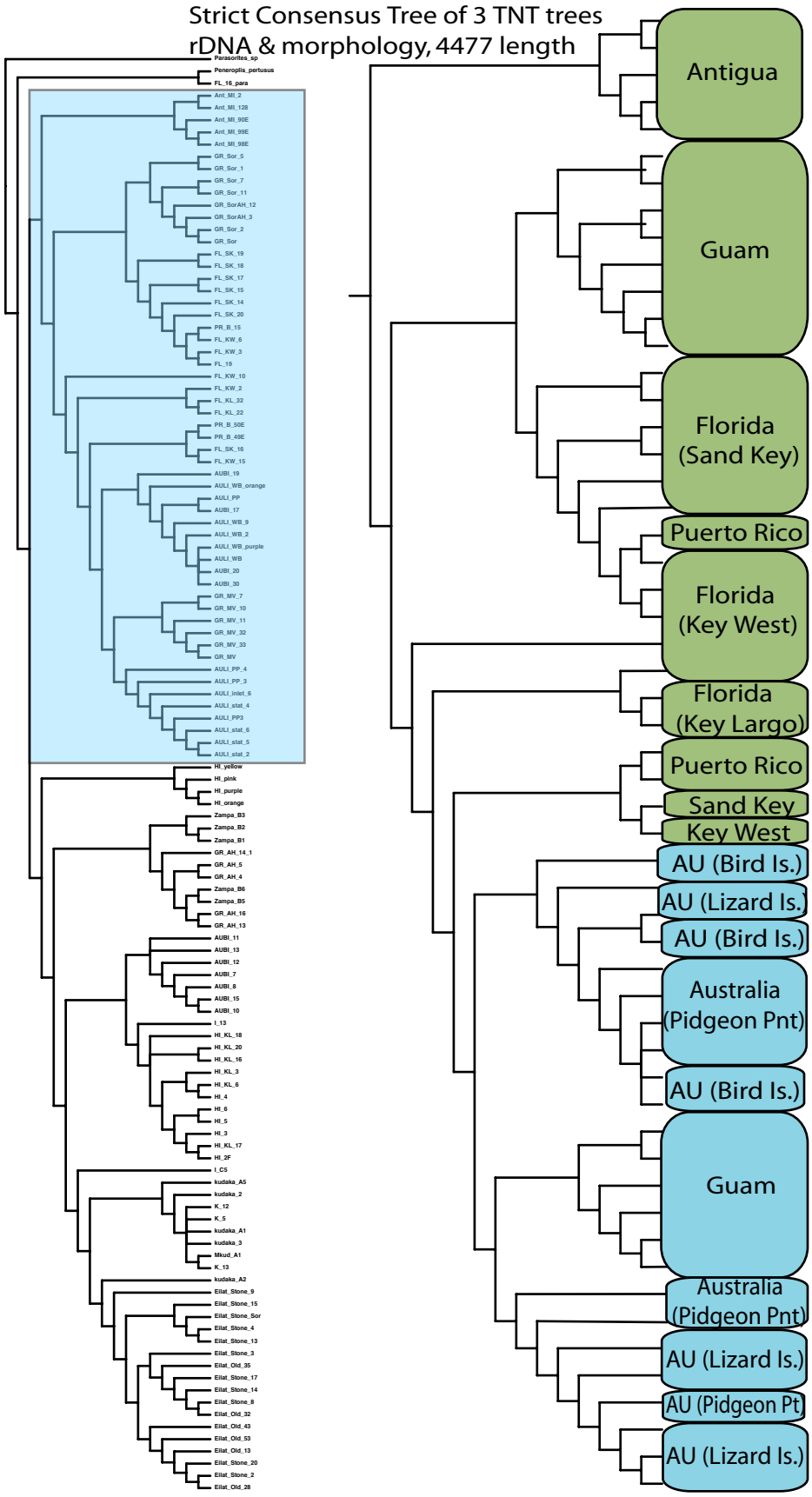
Strict Consensus Tree of 3 TNT trees
rDNA & morphology, 4477 length
Parasorites_sp
Peneroplis_pertusus
FL_16_para
Ant_MI_2
Ant_MI_128
Ant_MI_90E
Ant_MI_99E
Ant_MI_98E
GR_Sor_5
GR_Sor_1
GR_Sor_7
GR_Sor_11
GR_SorAH_12
GR_SorAH_3
GR_Sor_2
GR_Sor
FL_SK_19
FL_SK_18
FL_SK_17
FL_SK_15
FL_SK_14
FL_SK_20
PR_B_15
FL_KW_6
FL_KW_3
FL_19
FL_KW_10
FL_KW_2
FL_KL_32
FL_KL_22
PR_B_50E
PR_B_49E
FL_SK_16
FL_KW_15
AUBI_19
AULI_WB_orange
AULI_PP
AUBI_17
AULI_WB_9
AULI_WB_2
AULI_WB_purple
AULI_WB
AUBI_20
AUBI_30
GR_MV_7
GR_MV_10
GR_MV_11
GR_MV_32
GR_MV_33
GR_MV
AULI_PP_4
AULI_PP_3
AULI_inlet_6
AULI_stat_4
AULI_PP3
AULI_stat_6
AULI_stat_5
AULI_stat_2
HI_yellow
HI_pink
HI_purple
HI_orange
Zampa_B3
Zampa_B2
Zampa_B1
GR_AH_14_1
GR_AH_5
GR_AH_4
Zampa_B6
Zampa_B5
GR_AH_16
GR_AH_13
AUBI_11
AUBI_13
AUBI_12
AUBI_7
AUBI_8
AUBI_15
AUBI_10
I_13
HI_KL_18
HI_KL_20
HI_KL_16
HI_KL_3
HI_KL_6
HI_4
HI_6
HI_5
HI_3
HI_KL_17
HI_2F
I_C5
kudaka_A5
kudaka_2
K_12
K_5
kudaka_A1
kudaka_3
Mkud_A1
K_13
kudaka_A2
Eilat_Stone_9
Eilat_Stone_15
Eilat_Stone_Sor
Eilat_Stone_4
Eilat_Stone_13
Eilat_Stone_3
Eilat_Old_35
Eilat_Stone_17
Eilat_Stone_14
Eilat_Stone_8
Eilat_Old_32
Eilat_Old_43
Eilat_Old_53
Eilat_Old_13
Eilat_Stone_20
Eilat_Stone_2
Eilat_Old_28
Antigua
Guam
Florida
(Sand Key)
Puerto Rico
Florida
(Key West)
Florida
(Key Largo)
Puerto Rico
Sand Key
Key West
AU (Bird Is.)
AU (Lizard Is.)
AU (Bird Is.)
Australia
(Pidgeon Pnt)
AU (Bird Is.)
Guam
Australia
(Pidgeon Pnt)
AU (Lizard Is.)
AU (Pidgeon Pt)
AU (Lizard Is.)

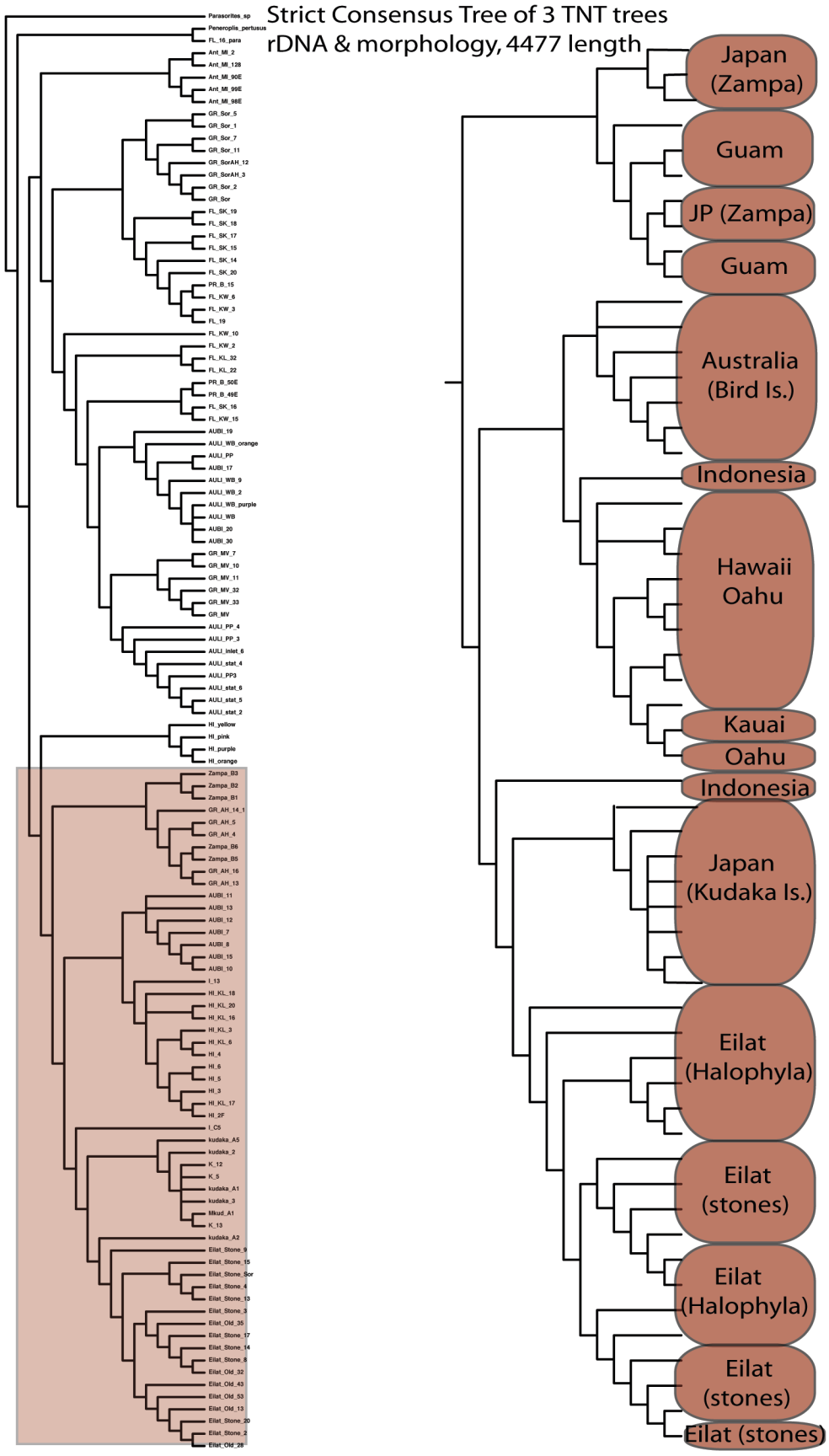
Strict Consensus Tree of 3 TNT trees
rDNA & morphology, 4477 length
Parasorites_sp
Peneroplis_pertusus
FL_16_para
Ant_MI_2
Ant_MI_128
Ant_MI_90E
Ant_MI_99E
Ant_MI_98E
GR_Sor_5
GR_Sor_1
GR_Sor_7
GR_Sor_11
GR_SorAH_12
GR_SorAH_3
GR_Sor_2
GR_Sor
FL_SK_19
FL_SK_18
FL_SK_17
FL_SK_15
FL_SK_14
FL_SK_20
PR_B_15
FL_KW_6
FL_KW_3
FL_19
FL_KW_10
FL_KW_2
FL_KL_32
FL_KL_22
PR_B_50E
PR_B_49E
FL_SK_16
FL_KW_15
AUBI_19
AULI_WB_orange
AULI_PP
AUBI_17
AULI_WB_9
AULI_WB_2
AULI_WB_purple
AULI_WB
AUBI_20
AUBI_30
GR_MV_7
GR_MV_10
GR_MV_11
GR_MV_32
GR_MV_33
GR_MV
AULI_PP_4
AULI_PP_3
AULI_Inlet_6
AULI_stat_4
AULI_PP3
AULI_stat_6
AULI_stat_5
AULI_stat_2
HI_yellow
HI_pink
HI_purple
HI_orange
Zampa_B3
Zampa_B2
Zampa_B1
GR_AH_14_1
GR_AH_5
GR_AH_4
Zampa_B6
Zampa_B5
GR_AH_16
GR_AH_13
AUBI_11
AUBI_13
AUBI_12
AUBI_7
AUBI_8
AUBI_15
AUBI_10
I_13
HI_KL_18
HI_KL_20
HI_KL_16
HI_KL_3
HI_KL_6
HI_4
HI_6
HI_5
HI_3
HI_KL_17
HI_2F
I_C5
kudaka_A5
kudaka_2
K_12
K_5
kudaka_A1
kudaka_3
Mkud_A1
K_13
kudaka_A2
Eilat_Stone_9
Eilat_Stone_15
Eilat_Stone_Sor
Eilat_Stone_4
Eilat_Stone_13
Eilat_Stone_3
Eilat_Old_35
Eilat_Stone_17
Eilat_Stone_14
Eilat_Stone_8
Eilat_Old_32
Eilat_Old_43
Eilat_Old_53
Eilat_Old_13
Eilat_Stone_20
Eilat_Stone_2
Eilat_Old_28
Japan (Zampa)
Guam
JP (Zampa)
Guam
Australia (Bird Is.)
Indonesia
Hawaii Oahu
Kauai
Oahu
Indonesia
Japan (Kudaka Is.)
Eilat (Halophyla)
Eilat (stones)
Eilat (Halophyla)
Eilat (stones)
Eilat (stones)

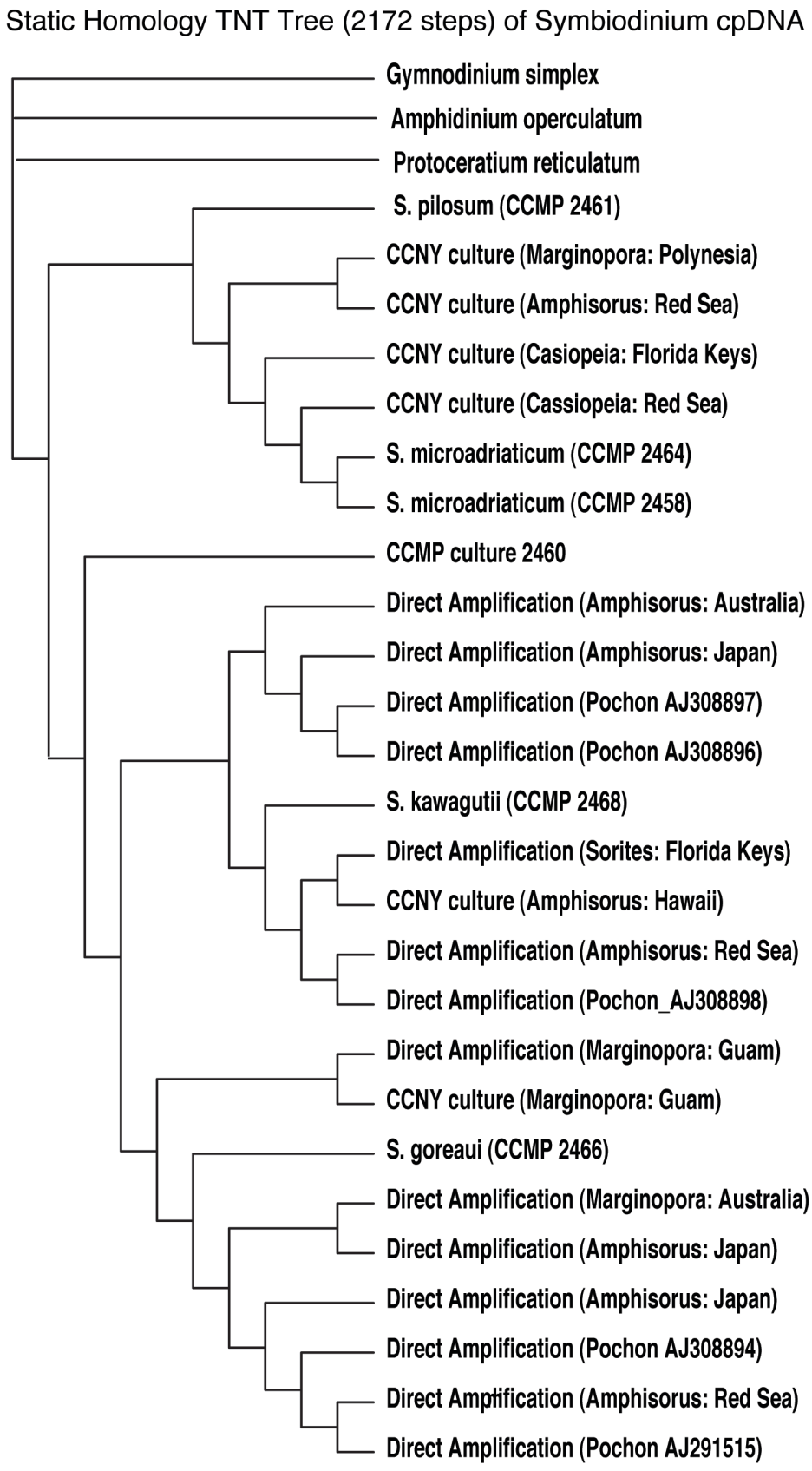
Static Homology TNT Tree (2172 steps) of Symbiodinium cpDNA
Gymnodinium simplex
Amphidinium operculatum
Protoceratium reticulatum
S. pilosum (CCMP 2461)
CCNY culture (Marginopora: Polynesia)
CCNY culture (Amphisorus: Red Sea)
CCNY culture (Casiopeia: Florida Keys)
CCNY culture (Cassiopeia: Red Sea)
S. microadriaticum (CCMP 2464)
S. microadriaticum (CCMP 2458)
CCMP culture 2460
Direct Amplification (Amphisorus: Australia)
Direct Amplification (Amphisorus: Japan)
Direct Amplification (Pochon AJ308897)
Direct Amplification (Pochon AJ308896)
S. kawagutii (CCMP 2468)
Direct Amplification (Sorites: Florida Keys)
CCNY culture (Amphisorus: Hawaii)
Direct Amplification (Amphisorus: Red Sea)
Direct Amplification (Pochon_AJ308898)
Direct Amplification (Marginopora: Guam)
CCNY culture (Marginopora: Guam)
S. goreaui (CCMP 2466)
Direct Amplification (Marginopora: Australia)
Direct Amplification (Amphisorus: Japan)
Direct Amplification (Amphisorus: Japan)
Direct Amplification (Pochon AJ308894)
Direct Amplification (Amphisorus: Red Sea)
Direct Amplification (Pochon AJ291515)

Dynamic Homology Tree of Symbiodinium rDNA (4176 steps)

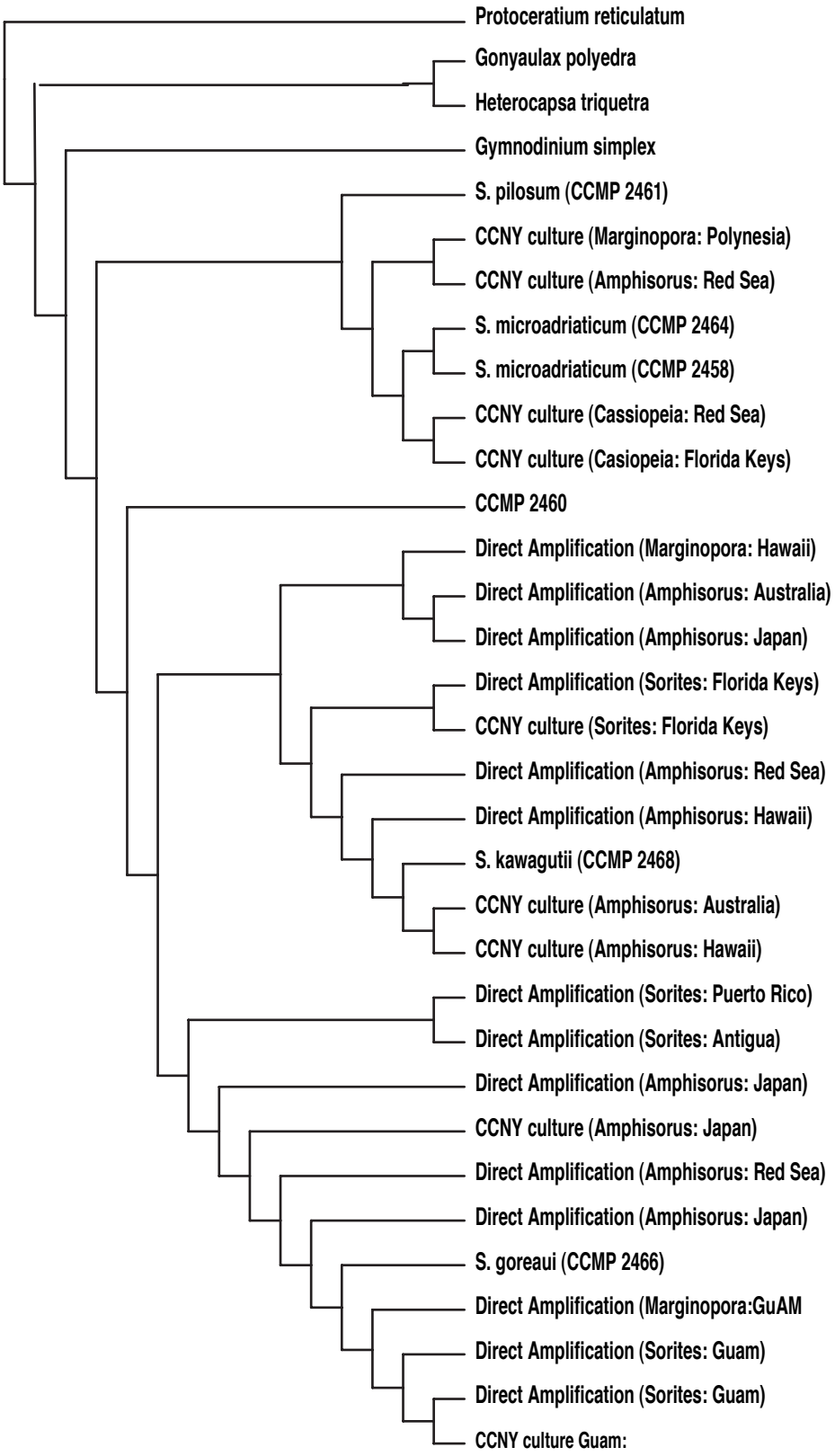

BIBLIOGRAPHY:

Altschul, S.F., Gish, W., Miller, W., Myers, E.W., and Lipman, D. 1990. Basic local alignment search tool. *Journal of Molecular Biology*. 215: 403-10.

Baker, A.C. 2003. Flexibility and specificity in coral—algal symbiosis: diversity, ecology, and biogeography of Symbiodinium. *Annual Review of Ecology, Evolution, and Systematics*. 34: 661-689.

Baker, A.C., Starger, C.J., McClanahan, T.M., and Glynn, P.W. 2004. Corals' adaptative response to climate change. Nature. 430: 741.

Baker, A.C., and Rowan, R. 1997. Diversity of symbiotic dinoflagellates (zooxanthellae) in scleractinian corals of the Caribbean and Eastern Pacific. *Proc 8th International Coral Reef Symbiodinium*. 2: 1301-1306.

Banaszak, A.T., LaJeunesse, T.C., and Trench, R.K., 2000. The synthesis of mycosporine-like amino acid (MAAs) by cultured, symbiotic dinoflagellates. *Journal of Experimental Marine Biology and Ecology*. 249:219-233.

Banaszak, A.T., Igelsias-Prieto R., and Trench, R.K. 1993. *Scrippsiella velellae* sp. nov. (Peridiniales) and *Gloedinium viscum* sp. nove. (Phytodiniales), dinoflagellate symbiont of two hyrozoans (Cnidaria). *Journal of Phycology*. 29: 517-528.

Bhattacharya, D., Yoon, H.S. and Hackett, J.D. 2004. Photosynthetic eukaryotes unite; endosymbiosis connects the dots. BioEssays 26: 50 -60.

Bacus, S. 1997. Contributions to our knowledge of the larger foraminifera *Marginopora vertebralis*. Thesis, City College of New York, City University of New York, New York.

Blank, R.J., and Trench, R.K.1985a. *Symbiodinium microadriaticum*: a single species? In: Proceedings of the Fifth International Coral Reef Conference. 6: 113-117.

Blank, R.J., and Trench, R.K.1985b. Speciation in symbiotic dinoflagellates. *Science*. 229: 656-658.

Brady, H.B. 1881. Notes on some of the reticularian rhizopoda of the Challenger expedition. *Quarterly Journal Of Microscopical Science*. 21. 31-71.

Brady, H.B. 1884. Report on the foraminifera dredged by H. M. S. Challenger, during the years 1873-1876 in Report on the Scientific Results of the H. M.S. Challenger during the years 1873-1876. Zoology 9.

Cantino, P.D., and de Queiroz, K. 2000. PhyloCode: a phylogenetic code of Biological nomenclature (revision dated: April 8, 2000): http //www.ohio.edu/phylocode/.

Carlos, A.A., Baillie, B.K., Masanobu, K., and Maruyama, T. 1999. Phylogenetic position of *Symbiodinium* (Dinophyceae) isolates from tridacnids (Bivalvia), cardiids (Bivalvia), a sponge (Porifera), a soft coral (Anthozoa), and a free-living strain. *Journal of Phycology*. 35: 1054-1062.

Carpenter, W., Parker, W. and Jones T. R. 1862. *Introduction to the study of the Foraminifera*. R. Hardwicke, London. 1-319.

Carpenter, W.B. 1883. Researches on the foraminifera, Supplemental memoire. On the abyssal type of the genus Orbitolites; a study in the theory of decent. *Philosophical Transactions of the Royal Society*. 174. 551-573.

Cevasco, M.E, Lee, J.J., Siddall, M. Observations of variable test morphologies within the symbiotic foramnifera (genus *Amphisorus*). 2007. *Symbiosis*. in review)

Coffroth, M.A., Santos, S.R., and Goulet, T.L. 2001. Early ontogenetic expression of specificity in a cnidarian—algal symbiosis. Marine Ecology Progress Series. 222: 85-96.

Coffroth, M.A., and Santos, S.R. 2005 Genetic diversity of Symbiotic Dinoflagellates in the Genus *Symbiodinium*. *Protist*. 156:19-34.

Cushman, J.A. 1930. Foraminifera of the Atlantic Ocean. *Bulletin of the U.S. NationalMuseum*. 104(7):1-79.

Cushman, J.A. 1933. Foraminfera, Their Classification and Economic Use. Second Edition. Revised and Enlarged. *Cushman Lab. Foram Res. Special Publication* 4. 1-349.

D'Orbigny, A. 1826. "Tableau Methodique de la Classe des Cephalopodes." *Annales des Sciences Naturelles, Paris* Serie 1(7). 245-314.

Delage, Y. and Hérouard, E. 1896. *Traité de zoologie concrète. Tome I: La cellule et Les Protozoaires*. Reinwald/Schleicher Bros. Paris. 1-584.

Doyle, W.L., and Doyle, M.M. I940 The structure of zooxanthellae. Paper. Tortugas Lab. 32:127-142.

Dujardin, F. 1835. Observations novelles sur les Cephalopodes microscopiques. *Annale des Sciences Naturelles Zoologie*. Serie 2(3). 108-109.

Eherenberg, C. 1839. Uber die Bildung der Kreidefelsen und des Kreidemergels durch unsichtbare Organismen. *Physikalishe Abhandlungen der Könglichen Akedemie der Wissenschaften zu Berlin*. 1838 Berlin, (Jahrgang 1839). 59-147.

Farris, J.S. 1999. XAC program and documentation. Swedish Natural History Museum. Stockholm, Sweden.

Fensome, R.A., Taylor, F.J.R., Norris, G., Sarjeant, W.A.S., Wharton, D.I., and Williams, G.L. 1993. *A Classification of Living and Fossil Dinoflagellates*. American Museum of Natural History, Micropaleontology, Special Publication Number 7. 1-351.

Forskål, P. 1775. *Descriptiones animalium, avium, amphibiorum, piscium, insectorum, vermium; quae in itinere orientali observavit Petrus Forskål. Post mortem auctoris edidit Carsten Niebuhr. Adjuncta est materia medica kahirina atque tabula maris Rubri geographica*. Hauniæ, ex officina Mölleri, Copenhagen. 1-164.

Freundenthal, H. 1962. *Symbiodinium* gen. nov. and *Symbiodinium microadriaticum* sp. nov., a zooxanthella: taxonomy, life cycle, morphology. *Journal of Protozoology*. 9. 45-52.

Garcia-Cuetos, L. Pochon, X., and Pawlowski, J. 2005. Molecular evidence for Host symbiont specificity in soritid foraminifera. *Protist*. 156. 399-412.

Goloboff, P. 1999. Analyzing large data sets in reasonable times: solutions for composite optima. *Cladistics*. 15: 415-428.

Goloboff, P., Farris, J.S., Nixon, K. 2001. TNT (Tree analysis using New Technology) Version1.1. Published by the authors, Tucamán, Argentina.

Gudmundsson, G. 1994. Phylogeny, ontgeny and systematics of recent Soritacea Ehrenberg 1839 (Foraminiferida). *Micropaleontology*. 40(2). 101-155.

Haynes, J. R. 1990. The classification of the Foraminifera: A review of historical and philosophical perspectives. *Palaeontology*. 33. 503-528.

Hallock, P. 1987. Fluctations of the trophic resource continuum: a factor of global diversity cycles. Paleobiology. 11: 195-208.

Hallock, P. 2000. Symbiont-bearing forminifera: harbingers of global change. In: Lee, J. J.and Hallock, P. (eds.): *Advances in biology of Foraminifera. Micropaleontology*. New York. 46(suppl. 1). 95-104.

Hillis, D., and Dixon, M. 1991. Ribosomal DNA: molecular evolution and phylogenetic inference. Quart. Rev. Biol. 66: 411-453.

Hofker, J. 1930. The Foraminfera of the Siboga Expedition. Part 2. *Monography IV Siboga Expedtion*: 79-170.

Holzmann, M., Hohenegger, J., Hallock, P., Piller, W.E., and Pawlowski, J. 2001. Molecular phylogeny of large miliolid foraminfera (Soritacea, Eherenberg, 1839). *Marine Micropaleontology*. 43. 57-74.

Hottinger, L. 1979. Araldit als Helfer der Mirkopaläontologie. Ciba-Geigy Aspekte. 3. 1-10.

Hottinger, L. 2000a. Archaiasinids and related porcelaneous larger foraminifera from The late Miocene of the Dominican Republic. *Journal of Paleontology*. 75(3). 475-512.

Hottinger, L. 2000b. Functional morphology of benthic foraminiferal shells, envelopes of cells beyond measure. In: Lee, J. J. and Hallock, P. (eds.): *Advances in biology of Foraminifera. Micropaleontology*. New York. 46(suppl. 1). 57-86.

Hottinger, L., Halicz, E., Reiss, Z. 1993. Recent Foraminifera from the Gulf of Aqaba, Red Sea. Slovenska Akademiga Znanosti in Umetnosti, Acadenia Scientiarium et atrium Slovenica.

Kazuhiko, F., Hiroshi, N., and Tsunemasa, S. 2000. Population dynamics of *Marginopora kudakajimaensis* Gudmundsson (Foraminifera: soritidae) in the Ryuku Islands, the subtropical northwest Pacific. *Marine Micropaleontology*. 38: 267-284.

Kawaguti, S. 1944. On the physiology of reef corals. VII. Zooxanthella of the reef corals is *Gymnodinium* sp., Dinoflagellata; its culture in vitro. *Palao Trop. Biol. Stat. Stud*. 2: 675-679.

Kevin, M.J., Hall, W.T., McLaughlin, J.J.A., and Zahl, P.A. 1969. *Symbiodinium microadriaticum* Freudenthal, a revised taxonomic description - ultrastructure. *Journal of Phycology*. 53: 341-350.

Klebs, G.1892. Flaellatenstudien. *Z. Wiss. Zool*. 55: 265-445.

Kluge, A.G., and Farris, J.S. 1969. Quantitative phyletics and the evolution of anurans. *Systematic Zoology*. 18:1-32.

LaJeunesse, T.C. 2001. Investigating the biodiversity, ecology, and phylogeny of endosymbiotic dinoflagellates in the genus Symbiodinium using the ITS region: in search of a "species" level marker. *Journal of Phycology*. 37: 866-880.

LaJeunesse, T.C. 2002. Diversity and community structure of symbiotic Dinoflagellates from Carribbean coral reefs, *Marine Biology*. 141: 387-400.

LaJeunesse, T.C., Loh, W.K., van Woesik, R., Hoegh-Guldberg, O., and Fitt, W.K., 2003. Low symbiont diversity in southern Great Barrier Reef corals, relative to those of the Caribbean. *Limnology and Ocean ography*. 48: 2046-2054.

LaJeunesse, T.C., and Trench, R.K. 2000. Biogeography of two species of *Symbiodinium* (Freudenthal inhabiting the intertidal sea anemone *Anthopleura elegantissima* (Brandt). *Biological Bulletin*. 199: 126-134.

Lamarck, J.B. 1801. *Systême des aminaux sans vertèbres*. Paris: L'auteur. 1-432.

Lalli, C., and Parson, T. 1993. Biological Oceanography: an Introduction, Open Univeristy, Oxford, Butterworth and Heinemann.

Lee, J.J., and Anderson, O.R. 1991. Symbiosis in Foraminifera. In: Lee, J. and Anderson, O.R., (eds.). Biology of the Foraminifera. New York. Academic Press. 157-220.

Lee, J.J., Burnham, B., and Cevasco, M. 2004. A new modern soritid foraminifer from the Lizard Island Group (Great Barrier Reef, Australia). *Micropaleontolgy* 50(4): 357-368.

Lee, J.J. 1995. Living Sands. *Bioscience*. 45(4):252-261.

Lee, J.J., Faber, W.W., Anderson, O.R., and Pawlowski, J. 1991. Life cycle in Foraminfera. In: Lee, J.J. and Anderson, O.R. (eds.): *Biology of Foraminifera*. Academic Press. London. 285-343.

Lee, J.J. and Hallock, P. 1987. Algal symbiosis as the driven force in the evolution of larger foraminifera. *Annals of NY Academy of Science*. 503. 330-347.

Lee, J.J. and McEnery, M.E. 1983. Symbiosis in foraminifera. In: Goff, L.J. (ed.): *Algal Symbiosis*. Cambridge University Press. New York. 34-68.

Lee, J.J., Morales, J., Bacus, S., Diamont, A., Hallock, P., Pawlowski, J., and Thorpe, J. 1997. Progress in characterizing the endosymbiotic dinoflagellates of soritid foraminifera and related studies on some stages in the life cycle of *Marginopora vertebralis*. *Journal of Foraminiferal Research*. 27. 254-263.

Lee, J. and Pawlowski, J. 1992. Feulgen staining the nuclei of foraminifera. *Society of Protozoologists*, C 12.1-12.2.

Linnaeus, C. 1766. *Systema naturae per regna tria naturae secundum classes, ordines, genera, species, cum characteribus, differentiis, synonymis, locis. I. Pars. I. Editio duodecima, reformata [12th edition]*. Laurentii Salvii, Holmiae. 1- 532.

Lobban, C.S., Schefter, M., Simpson, A.G.B., Pochon, X., Pawlowski, J., and Foissner, W. 2002. *Maristentor dinoferus* n. gen., n. sp., a giant heterotrich ciliate (Spirotrichea: Heterotrichida) with zooxanthellae, from coral reefs on Guam, Mariana Islands. *Marine Biology*. 141: 411-423.

Loeblich, A. and Tappan, H. 1987. *Foraminiferal genera and their classification.* Van Nostrand Reinhold. New York. 1-970.

Just, L. 1884. Botanischer Jahresbericht, 1881. Borntrager. Berlin.

McEnery, M. and Lee, J.J. 1981. Cytological and fine structural studies of three species of symbiont-bearing larger foraminifera from the Red Sea. *Micropaleontology*. 27(1): 71-83.

Moore, R.B., Ferguson, K.M., Loh, W.K., Hoegh-Guldberg, O., Carter, D.A. 2003. Highly organized structure in the non-coding region of the *psbA* minicircle from clade C *Symbiodinium*. *International Journal of Systematic and Evolutionary Microbiology*. 53:1725-1734.

Muller-Merz, E., and Lee, J. 1976. Symbiosis in the larger foraminiferan *Sorites marginalis*. Journal of Protozoology, 23(3): 390-396.

Munier-Chalmas, E. 1902. Un genre nouveau de Foraminifères. Bull. Soc. géol. France, (4)2, 353.

Pawlowski, J., Holzmann, M., Fahrni, J., Pochon, X., and Lee, J.J. 2001. Molecular identification of algal endosymbionts in large miliolid foraminifera: 2. Dinoflagellates. *Journal Eukaryotic Microbiology*. 48: 368-373.

Pascher, A. 1911. Uber die Beziehungen der Cryptomonaden zu den Algen. Ber Dtsch Bot Ges. 29: 193-203.

Pochon, X., Pawlowski, J., Zaninetti, L., Rowan, R. 2001. High genetic diversity and relative specificity among *Symbiodinium*-like endosymbiotic dinoflagellates in soritid foramiiferans. *Marine Biology*. 139: 1069-1078.

Pochon, X., LaJeunesse, T.C., and Pawlowski, J. 2004. Biogeographic partitioning and host specialization among foraminfieran dinoflagellate symbiont (*Symbiodinium*; Dinophyta) *Marine Biology* 146: 17-27.

Pochon, X. and Pawlowski, J. 2006. Evolution of the soritids-Symbiodinium symbiosis. *Symbiosis*. 42: 77-88.

Quoi, J.R. and Gaimard, P. 1830. Mollsques, vers et Zoophytes. In: Blainville, H. (ed.): *Dictionnaire des Sciences Naturelles*. Levrault, F. Paris.

Richardson, S. 2001. Endosymbiont change as a key innovation in the adaptive radiation of Soritida (Foraminifera). Paleobiology. 27(2). 262-289.

Ross, C.A. 1972. Biology and ecology of *Marginopora vertebralis* (Foraminiferida), Great Barrier Reef. *Journal of Protozoology*, 25:5-12.

Ross, C.A., and Ross, J.R., 1978. Adaptive evolution in the soritids *Marginopora* and *Amphisorus* (Foraminiferida). Scanning Electron Microscopy. II:53-60.

Rowan, R. 2004. Thermal adaptation in reef coral symbionts. *Nature*. 430:742.

Rowan, R., and Powers, D. A. 1991. Molecular genetic identification of symbiotic dinoflagellates (zooxanthellae). *Marine Ecology Progress Series*. 71: 65-73.

Rowan, R., and Knowlton, N. 1995. Intraspecific diversity and ecological zonation in coral-algal symbiosis. *Proc. Natl. Acad. Sci.* USA. 92: 2850-2853.

Santos, S.R., Taylor, D.J., Coffroth, M.A., 2001. Genetic comparisons of freshly isolated vs. cultured symbiotic dinoflagellates: Implications for extrapolating to the intact symbiosis. *J. Phycol*. 37: 866–880.

Santos, S.R, Gutierrez-Rodriguez, C., and Coffroth, M.A. 2003. Phylogenetic identification of symbiotic dinoflagellates via length heteroplasmy in domain V of chloroplst large subunit (cp23S)-ribosomal DNA sequenes. *Marine Biotechnology* (NY). 5: 130-140

Santos, S.R, Taylor, D., Kinzie, R.A, Hidaka, M., Sakai, K, and Coffroth, M.A. 2002. Molecular phylogeny of symbiotic dinoflagellates inferred from partial chloroplast large subunit (23S)rDNA sequences. *Molecular Phylogenetics and Evolution*. 23: 97-111.

Schoenberg, D., and Trench, R. K. 1980a. Genetic variation in *Symbiodinium* (= *Gymnodinium*) microadriaticum freudenthal, and specificity in its symbiosis with marine invertebrates I. Isoenzyme and sluble protein patterns of axenic cultures of *Symbiodinium microadriaticum*. *Proc R Soc Lond B*. 207: 405-427.

Schoenberg, D., and Trench, R. K. 1980b. Genetic variation in *Symbiodinium* (= *Gymnodinium*) microadriaticum freudenthal, and specificity in its symbiosis with marine invertebrates.II. Morphological variation in *Symbiodinium microadriaticum*. *Proc R Soc Lond B*. 207: 429-444.

Schoenberg, D., and Trench, R. K. 1980c. Genetic variation in *Symbiodinium* (= *Gymnodinium*) microadriaticum freudenthal, and specificity in its symbiosis with marine invertebrates III. Specificity and infectivity *Symbiodinium microadriaticum*. *Proc R Soc Lond B*. 207: 405-427.

Seiglie, G.A., Grove, K., and Rivera, J.A. 1977. Revision of some Caribbean Archaiasinae,new genera, species and subspecies. *Eclogae Geologicae Helvetiae*. 70: 855-883.

Smout, A. 1963. The genus *Pseudedomia* and its phyletic relationships, with remarks on *Orbitolites* and other complex foraminifera. In: Koensingswald GH, Emeis J, Bunig W, Wagner C (eds) *Evolutionary Trends in Foraminifera*. Elsevier Publishing Company, London, p 224-281.

Stat, M., Carter, D., and Hoegh-Guldberg, O. 2006. The evolutionary history of *Symbiodinium* and scleractinian hosts —Symbiosis, diversity, and the effect of climate change. *Perspectives in Plant Ecology, Evolution, and Systematics*. 8: 23-43.

Stein, F.R. 1878. Der Organismus der Infusionsthiere. III. Der Organismus der Flagellaten I. Wilhelm Engelmann, Leipzig.

Swofford, D.L. 2000. PAUP*. Phylogenetic Analysis Using Parsimony (*and Other Methods). Version 4.' Sinauer Associates, Sunderland, Massachusetts.

Taylor, D.L. 1968. In situ studies of the cytochemistry and ultrastructure of a symbiotic dinoflagellate. *J. Mar. Biol. Assoc.* UK. 48: 349-366.

Takabayashi, M., Santos, S.R, and Cook, C. B. 2004. Mitochondrial DNA Phylogeny of the Symbiotic Dinoflagellates (*Symbiodinium*, Dinophyta). *Journal of Phycology* . 40: 160-164.

Takishita, K., Ishikura, M., Kioke, K., and Maruyama, T. 2003. Comparison of phylogenies based on nuclear-encoded SSU rDNA and plastid-encoded psbA in the symbiotic dinoflagellate genus Symbiodinium. *Phycologia*. 42: 285-291.

Ter Kuile, B.H. and Erez, J. 1991. Carbon Budgets for 2 species of benthonic Symbiont bearing foraminifera. *Biological Bulletin*. 180(3): 489-495.

Trench, R.K. 1997. Diversity of symbiotic dinoflagellates and the evoution of microalgal-invvertebrate symbioses. *Proc. 8th Coral Reef Sym.* 2: 1275-1286.

Trench, R.K., and Thinh, L. 1995. *Gynodinium linucheae* sp. nov.: They dinofalgellate symbiont of the jellyfish *Linuche unguiculata*. *Eur. Journal of Phycology*. 30: 149-154.

Trench, R.K., and Blank, R. J., 1987. *Symbiodiniium microadriaticum* Freudenthal. *S. Goreauii* sp. nov,, *S. Kawagutii* sp nov., and *S. pilosum* sp. nov.: gymnodinioid dinoflagellate symbionts of marine invertebrates. *Journal of Phycology*. 23:469-481.

Toller, W.W., Rowan, R., and Knowlton, N. 2001. Zooxanthellae of the Montastrea annularis species complex; patterns of distribution of four taxa of Symbiodinium on different reefs and across depths. *Biological Bulletin*. 201: 348 -359.

Van den Hoek, C., Mann, D.G., and Jahns, H.M. 1995. Algae : An introduction to phycology. Cambridge, UK: Cambridge University Press, XIV, 623 p.

Varón, A., Vinh, L.S., Bomash, I., and Wheeler, W. 2007. POY 4 Beta. American Museum of Natural History http://research.amnh.org/scicomp/projects/poy.php.

Van Oppen, M.J., Palstra, F.P., Piquet, M.T., Muller, D.J. 2001. Patterns of coral-dinoflagellate associations in *Acropora*. Significance of local availability and physiology of *Symbiodinium* strans and host-symbiont selectivity. *Proc. R. Soc. Lond. B* 268. 1759-1767.

Vaughan,, T.W. 1928. *Yaberinella jamaicensis*, a new genus and species of arenaceous foraminifera. *Journal of Palenotology* 2: 7-12.

Wheeler, W.C. 1996. Optimization Alignment: the end of multiple sequence alignment in phylogenetics?. *Cladistics*. 12: 1-9.

Wilcox, T.P. 1998. Large-subunit ribosomal RNA systematics of symbiotic dinoflagellates: morphology does not recapitulate phylogeny. *Molecular Phylogenetics and Evolution.* 10: 436-448.

Zardoya, R., Costas, E., Lopez-Rodas, V., Garrido-Pertierra, A., and Bautista, J.M. 1995. Revised dinoflagellate phylogeny inferred from molecular analysis of large-subunit ribosomal RNA gene sequences. *Journal of Molecular Evolution*. 41: 637-645.

Zhang, Z., T. Cavalier-Smith, and B. R. Green. 2002. Evolution of dinoflagellate unigenic minicircles and the partially concerted divergence of their putative replicon origins. *Molecular Biology and Evolution* 19: 489-500.